

Issue 3

2014 | Volume 10

The Journal on Advanced Studies in Theoretical and Experimental Physics,
including Related Themes from Mathematics

PROGRESS IN PHYSICS



“All scientists shall have the right to present their scientific research results, in whole or in part, at relevant scientific conferences, and to publish the same in printed scientific journals, electronic archives, and any other media.” — Declaration of Academic Freedom, Article 8

ISSN 1555-5534

PROGRESS IN PHYSICS

A quarterly issue scientific journal, registered with the Library of Congress (DC, USA). This journal is peer reviewed and included in the abstracting and indexing coverage of: Mathematical Reviews and MathSciNet (AMS, USA), DOAJ of Lund University (Sweden), Zentralblatt MATH (Germany), Scientific Commons of the University of St. Gallen (Switzerland), Open-J-Gate (India), Referativnyi Zhurnal VINITI (Russia), etc.

Electronic version of this journal:
<http://www.ptep-online.com>

Editorial Board

Dmitri Rabounski, Editor-in-Chief
rabounski@ptep-online.com
Florentin Smarandache, Assoc. Editor
smarand@unm.edu
Larissa Borissova, Assoc. Editor
borissova@ptep-online.com

Editorial Team

Gunn Quznetsov
quznetsov@ptep-online.com
Andreas Ries
ries@ptep-online.com
Ebenezer Chifu
ndikilar@ptep-online.com
Felix Scholkmann
scholkmann@ptep-online.com
Pierre Millette
millette@ptep-online.com

Postal Address

Department of Mathematics and Science,
University of New Mexico,
705 Gurley Ave., Gallup, NM 87301, USA

Copyright © *Progress in Physics*, 2014

All rights reserved. The authors of the articles do hereby grant *Progress in Physics* non-exclusive, worldwide, royalty-free license to publish and distribute the articles in accordance with the Budapest Open Initiative: this means that electronic copying, distribution and printing of both full-size version of the journal and the individual papers published therein for non-commercial, academic or individual use can be made by any user without permission or charge. The authors of the articles published in *Progress in Physics* retain their rights to use this journal as a whole or any part of it in any other publications and in any way they see fit. Any part of *Progress in Physics* howsoever used in other publications must include an appropriate citation of this journal.

This journal is powered by \LaTeX

A variety of books can be downloaded free from the Digital Library of Science:
<http://www.gallup.unm.edu/~smarandache>

ISSN: 1555-5534 (print)

ISSN: 1555-5615 (online)

Standard Address Number: 297-5092

Printed in the United States of America

July 2014

Vol. 10, Issue 3

CONTENTS

| | |
|---|-----|
| Cahill R. T. Gravitational Wave Experiments with Zener Diode Quantum Detectors: Fractal Dynamical Space and Universe Expansion with Inflation Epoch | 131 |
| Quznetsov G. Chrome of Baryons | 139 |
| Potter F. CKM and PMNS Mixing Matrices from Discrete Subgroups of $SU(2)$ | 146 |
| Medvedev S. Yu. Superluminal Velocities in the Synchronized Space-Time | 151 |
| Robitaille P.-M. On the Equation which Governs Cavity Radiation II | 157 |
| Nyibule S., Henry E., Töoke J., Skulski W., Schröder W.-U. Digital Gamma-Neutron Discrimination with Organic Plastic Scintillator EJ 299-33 | 163 |
| Robitaille P.-M. Blackbody Radiation in Optically Thick Gases? | 166 |
| Proffitt D. Black Hole Structure in Schwarzschild Coordinates | 169 |
| Silva P. R. Drude-Schwarzschild Metric and the Electrical Conductivity of Metals | 171 |
| Daywitt W. C. Why the Proton is Smaller and Heavier than the Electron | 175 |
| Heymann Y. The Dichotomous Cosmology with a Static Material World and Expanding Luminous World | 178 |
| Suhendro I. Tractatus Logico-Realismus: Surjective Monism and the Meta-Differential Logic of the Whole, the Word, and the World | 182 |
| Silva N. P. A Closed Universe Expanding Forever | 191 |
| Dumitru S. New Possible Physical Evidence of the Homogeneous Electromagnetic Vector Potential for Quantum Theory. Idea of a Test Based on a G. P. Thomson-like Arrangement | 196 |

Information for Authors and Subscribers

Progress in Physics has been created for publications on advanced studies in theoretical and experimental physics, including related themes from mathematics and astronomy. All submitted papers should be professional, in good English, containing a brief review of a problem and obtained results.

All submissions should be designed in L^AT_EX format using *Progress in Physics* template. This template can be downloaded from *Progress in Physics* home page <http://www.ptep-online.com>. Abstract and the necessary information about author(s) should be included into the papers. To submit a paper, mail the file(s) to the Editor-in-Chief.

All submitted papers should be as brief as possible. We accept brief papers, no larger than 8 typeset journal pages. Short articles are preferable. Large papers can be considered in exceptional cases to the section *Special Reports* intended for such publications in the journal. Letters related to the publications in the journal or to the events among the science community can be applied to the section *Letters to Progress in Physics*.

All that has been accepted for the online issue of *Progress in Physics* is printed in the paper version of the journal. To order printed issues, contact the Editors.

This journal is non-commercial, academic edition. It is printed from private donations. (Look for the current author fee in the online version of the journal.)

Gravitational Wave Experiments with Zener Diode Quantum Detectors: Fractal Dynamical Space and Universe Expansion with Inflation Epoch

Reginald T. Cahill

School of Chemical and Physical Sciences, Flinders University, Adelaide 5001, Australia.

The discovery that the electron current fluctuations through Zener diode *pn* junctions in reverse bias mode, which arise via quantum barrier tunnelling, are completely driven by space fluctuations, has revolutionized the detection and characterization of gravitational waves, which are space fluctuations, and also has revolutionized the interpretation of probabilities in the quantum theory. Here we report new data from the very simple and cheap table-top gravitational wave experiment using Zener diode detectors, and reveal the implications for the nature of space and time, and for the quantum theory of “matter”, and the emergence of the “classical world” as space-induced wave function localization. The dynamical space possesses an intrinsic inflation epoch with associated fractal turbulence: gravitational waves, perhaps as observed by the BICEP2 experiment in the Antarctica.

1 Introduction

Physics, from the earliest days, has missed the existence of space as a dynamical and structured process, and instead took the path of assuming space to be a geometrical entity. This failure was reinforced by the supposed failure of the earliest experiment designed to detect such structure by means of light speed anisotropy: the 1887 Michelson-Morley experiment [1]. Based upon this so-called “null” experiment the geometrical modelling of space was extended to the spacetime geometrical model. However in 2002 [2, 3] it was discovered that this experiment was never “null”: Michelson had assumed Newtonian physics in calibrating the interferometer, and a re-analysis of that calibration using neo-Lorentz relativity [4] revealed that the Newtonian calibration overestimated the sensitivity of the detector by nearly a factor of 2000, and the observational data actually indicated an anisotropy speed up to ± 550 km/s, depending of direction. The spacetime model of course required that there be no anisotropy [4]. The key result of the neo-Lorentz relativity analysis was the discovery that the Michelson interferometer had a design flaw that had gone unrecognized until 2002, namely that the detector had zero sensitivity to light speed anisotropy, unless operated with a dielectric present in the light paths. Most of the more recent “confirmations” of the putative null effect employed versions of the Michelson interferometer in vacuum mode: vacuum resonant cavities, such as [5].

The experimental detections of light speed anisotropy, via a variety of experimental techniques over 125 years, shows that light speed anisotropy detections were always associated with significant turbulence/fluctuation wave effects [6, 7]. Repeated experiments and observations are the hallmark of science. These techniques included: gas-mode Michelson interferometers, RF EM Speeds in Coaxial Cable, Optical Fiber Michelson Interferometer, Optical Fiber / RF Coaxial Cables, Earth Spacecraft Flyby RF Doppler Shifts and 1st Order Dual RF Coaxial Cables. These all use classical phenomena.

However in 2013 the first direct detection of flowing space was made possible by the discovery of the Nanotechnology Zener Diode Quantum Detector effect [8]. This uses waveform correlations between electron barrier quantum tunnelling current fluctuations in spatially separated reverse-biased Zener diodes: gravitational waves. The first experiments discovered this effect in correlations between detectors in Australia and the UK, which revealed the average anisotropy vector to be 512 km/s, RA=5.3 hrs, Dec=81°S (direction of Earth through space) on January 1, 2013, in excellent agreement with earlier experiments, particularly the Spacecraft Earth-Flyby RF Doppler Shifts [9].

Here we elaborate the very simple and cheap table-top gravitational wave experiments using Zener diode detectors, and reveal the implications for the nature of space and time, and for the quantum theory of “matter”, and the emergence of the “classical world” as space-induced wave function localization. As well we note the intrinsic inflation epoch of the dynamical 3-space theory, which arises from the same dynamical term responsible for bore hole *g* anomalies, flat spiral galaxy rotation plots, black holes and cosmic filaments. This reveals the emerging physics of a unified theory of space, gravity and the quantum [10].

2 Quantum gravitational wave detectors

The Zener diode quantum detector for gravitational waves is shown in Fig. 1. Experiments reveal that the electron current fluctuations are solely caused by space fluctuations [8]. Fig. 5, top, shows the highly correlated currents of two almost collocated Zener diodes. The usual interpretations of quantum theory, see below, claim that these current fluctuations should be completely random, and so uncorrelated, with the randomness intrinsic to each diode. Hence the Zener diode experiments falsifies that claim. With these correlations the detector S/N ratio is then easily increased by using diodes in parallel, as shown in Fig. 1. The source of the “noise” is,

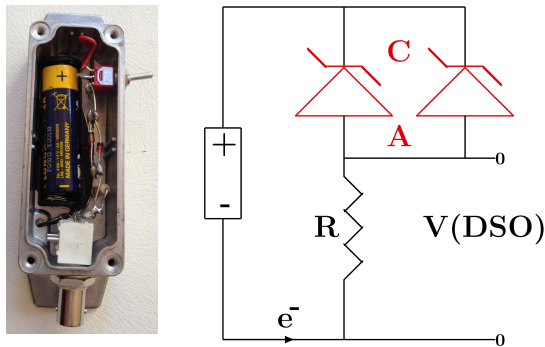


Fig. 1: Right: Circuit of Zener Diode Gravitational Wave Detector, showing 1.5V AA battery, two 1N4728A Zener diodes operating in reverse bias mode, and having a Zener voltage of 3.3V, and resistor $R = 10\text{K}\Omega$. Voltage V across resistor is measured and used to determine the space driven fluctuating tunnelling current through the Zener diodes. Correlated currents from two collocated detectors are shown in Fig. 5. Left: Photo of detector with 5 Zener diodes in parallel. Increasing the number of diodes increases the S/N ratio, as the V measuring device will produce some noise. Doing so demonstrates that collocated diodes produce in-phase current fluctuations, as shown in Fig. 5, top, contrary to the usual interpretation of probabilities in quantum theory.

in part, space induced fluctuations in the DSO that measures the very small voltages. When the two detectors are separated by 25 cm, and with the detector axis aligned with the South Celestial Pole, as shown in Fig. 4, the resulting current fluctuations are shown in Fig. 5, bottom, revealing that the N detector current fluctuations are delayed by $\sim 0.5 \mu\text{s}$ relative to the S detector.

The travel time delay $\tau(t)$ was determined by computing the correlation function between the two detector voltages

$$C(\tau, t) = \int_{t-T}^{t+T} dt' S_1(t' - \tau/2) S_2(t' + \tau/2) e^{-a(t'-t)^2}. \quad (1)$$

The fluctuations in Fig. 5 show considerable structure at the μs time scale (higher frequencies have been filtered out by the DSO). Such fluctuations are seen at all time scales, see [11], and suggest that the passing space has a fractal structure, illustrated in Fig. 7. The measurement of the speed of passing space is now elegantly and simply measured by this very simple and cheap table-top experiment. As discussed below those fluctuations in velocity are gravitational waves, but not with the characteristics usually assumed, and not detected despite enormous effects. At very low frequencies the data from Zener diode detectors and from resonant bar detectors reveal sharp resonant frequencies known from seismology to be the same as the Earth vibration frequencies [12–14]. We shall now explore the implications for quantum and space theories.

3 Zener diodes detect dynamical space

The generalized Schrödinger equation [15]

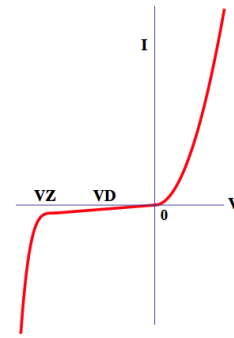


Fig. 2: Current-Voltage (IV) characteristics for a Zener Diode. $VZ = -3.3\text{V}$ is the Zener voltage, and $VD \approx -1.5\text{V}$ is the operating voltage for the diode in Fig. 1. $V > 0$ is the forward bias region, and $V < 0$ is the reverse bias region. The current near VD is very small and occurs only because of wave function quantum tunnelling through the potential barrier, as shown in Fig. 3.

$$i\hbar \frac{\partial \psi(\mathbf{r}, t)}{\partial t} = -\frac{\hbar^2}{2m} \nabla^2 \psi(\mathbf{r}, t) + V(\mathbf{r}, t) \psi(\mathbf{r}, t) - i\hbar \left(\mathbf{v}(\mathbf{r}, t) \cdot \nabla + \frac{1}{2} \nabla \cdot \mathbf{v}(\mathbf{r}, t) \right) \psi(\mathbf{r}, t) \quad (2)$$

models “quantum matter” as a purely wave phenomenon. Here $\mathbf{v}(\mathbf{r}, t)$ is the velocity field describing the dynamical space at a classical field level, and the coordinates \mathbf{r} give the relative location of $\psi(\mathbf{r}, t)$ and $\mathbf{v}(\mathbf{r}, t)$, relative to a Euclidean embedding space, also used by an observer to locate structures. At sufficiently small distance scales that embedding and the velocity description is conjectured to be not possible, as then the dynamical space requires an indeterminate dimension embedding space, being possibly a quantum foam [10]. This minimal generalization of the original Schrödinger equation arises from the replacement $\partial/\partial t \rightarrow \partial/\partial t + \mathbf{v} \cdot \nabla$, which ensures that the quantum system properties are determined by the dynamical space, and not by the embedding coordinate system, which is arbitrary. The same replacement is also to be implemented in the original Maxwell equations, yielding that the speed of light is constant only with respect to the local dynamical space, as observed, and which results in lensing from stars and black holes. The extra $\nabla \cdot \mathbf{v}$ term in (2) is required to make the hamiltonian in (2) hermitian. Essentially the existence of the dynamical space in all theories has been missing. The dynamical theory of space itself is briefly reviewed below.

A significant effect follows from (2), namely the emergence of gravity as a quantum effect: a wave packet analysis shows that the acceleration of a wave packet, due to the space terms alone (when $V(\mathbf{r}, t) = 0$), given by $\mathbf{g} = d^2 \langle \mathbf{r} \rangle / dt^2$ [15]

$$\mathbf{g}(\mathbf{r}, t) = \frac{\partial \mathbf{v}}{\partial t} + (\mathbf{v} \cdot \nabla) \mathbf{v}. \quad (3)$$

That derivation showed that the acceleration is independent

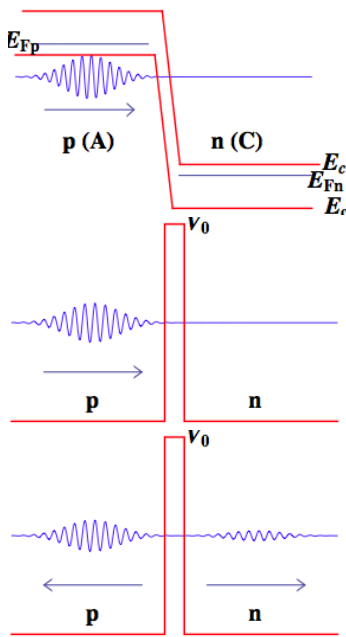


Fig. 3: Top: Electron before tunnelling, in reverse biased Zener diode, from valence band in doped p semiconductor, with hole states available, to conduction band of doped n semiconductor. A and C refer to anode and cathode labelling in Fig. 1. E_c is bottom of conduction bands, and E_v is top of valence bands. E_{Fp} and E_{Fn} are Fermi levels. There are no states available in the depletion region. Middle: Schematic for electron wave packet incident on idealized effective interband barrier in a pn junction, with electrons tunnelling A to C , appropriate to reverse bias operation. Bottom: Reflected and transmitted wave packets after interaction with barrier. Energy of wave packet is less than potential barrier height V_0 . The wave function transmission fluctuations and collapse to one side or the other after barrier tunnelling is now experimentally demonstrated to be caused by passing space fluctuations.

of the mass m : whence we have the first derivation of the Weak Equivalence Principle, discovered experimentally by Galileo. The necessary coupling of quantum systems to the fractal dynamical space also implies the generation of masses, as now the waves are not propagating through a structureless Euclidean geometrical space: this may provide a dynamical mechanism for the Higgs phenomenology.

4 Quantum tunnelling fluctuations

It is possible to understand the space driven Zener diode reverse-bias-mode current fluctuations. The operating voltage and energy levels for the electrons at the pn junction are shown schematically in Figs.2 and 3. For simplicity consider wave packet solutions to (2) applicable to the situation in Fig. 3, using a complete set of plane waves,

$$\psi(\mathbf{r}, t) = \int d^3\mathbf{k} d\omega \psi(\mathbf{k}, \omega) \exp(i\mathbf{k}\cdot\mathbf{r} - i\omega t). \quad (4)$$

Then the space term contributes the term $\hbar\mathbf{v}\cdot\mathbf{k}$ to the equa-

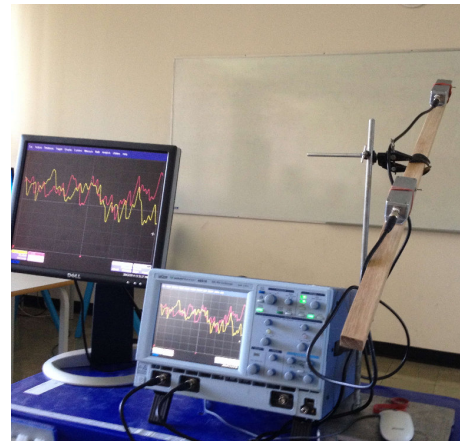


Fig. 4: Zener diode gravitational wave detector, showing the two detectors orientated towards south celestial pole, with a separation of 50cm. The data reported herein used a 25cm separation. The DSO is a LeCroy Waverunner 6000A. The monitor is for lecture demonstrations of gravitational wave measurements of speed and direction, from time delay of waveforms from S to N detectors.

tions for $\psi(\mathbf{k}, \omega)$, assuming we can approximate $\mathbf{v}(\mathbf{r}, t)$ by a constant over a short distance and interval of time. Here \mathbf{k} are wave numbers appropriate to the electrons. However the same analysis should also be applied to the diode, considered as a single massive quantum system, giving an energy shift $\hbar\mathbf{v}\cdot\mathbf{K}$, where \mathbf{K} is the much larger wavenumber for the diode. Effectively then the major effect of space is that the barrier potential energy is shifted: $V_0 \rightarrow V_0 + \hbar\mathbf{v}\cdot\mathbf{K}$. This then changes the barrier quantum tunnelling amplitude, $T(V_0 - E) \rightarrow T(V_0 + \hbar\mathbf{v}\cdot\mathbf{K} - E)$, where E is the energy of the electron, and this amplitude will then be very sensitive to fluctuations in \mathbf{v} .

Quantum theory accurately predicts the transition amplitude $T(V_0 - E)$, with $|T|^2 i$ giving the average electron current, where i is the incident current at the pn junction. However quantum theory contains no randomness or probabilities: the original Schrödinger equation is purely deterministic: probabilities arise solely from *ad hoc* interpretations, and these assert that the actual current fluctuations are purely random, and intrinsic to each quantum system, here each diode. However the experimental data shows that these current fluctuations are completely determined by the fluctuations in the passing space, as demonstrated by the time delay effect, herein at the μs time scale and in [8] at the 10-20 sec scale. Hence the Zener diode effect represents a major discovery regarding the so called interpretations of quantum theory.

5 Alpha decay rate fluctuations

Shnoll [16] discovered that the α decay rate of ^{239}Pu is not completely random, as it has discrete preferred values. The same effect is seen in the histogram analysis of Zener diode tunnelling rates [18]. This α decay process is another exam-

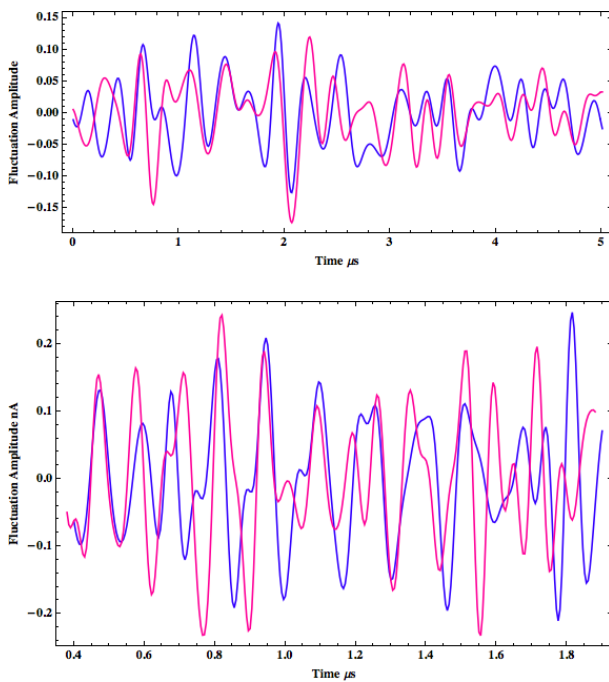


Fig. 5: Top: Current fluctuations from two collocated Zener diode detectors, as shown in Fig. 1, separated by 3-4 cm in EW direction due to box size, revealing strong correlations. The small separation may explain slight differences, revealing a structure to space at very small distances. Bottom: Example of Zener diode current fluctuations (nA), about a mean of $\sim 3.5 \mu\text{A}$, when detectors separated by 25cm, and aligned in direction RA=5hrs, Dec=-80°, with southerly detector signal delayed in DSO by $0.48 \mu\text{s}$, and then showing strong correlations with northerly detector signal. This time delay effect reveals space traveling from S to N at a speed of approximately 476km/s, from maximum of correlation function $C(\tau, t)$, with time delay τ expressed as a speed. Data has been smoothed by FFT filtering to remove high and low frequency components. Fig. 6, top, shows fluctuations in measured speed over a 15 sec interval.

ple of quantum tunnelling: here the tunnelling of the α wave packet through the potential energy barrier arising from the Coulomb repulsion between the α “particle” and the residual nucleus, as first explained by Gamow in 1928 [17]. The analysis above for the Zener diode also applies to this decay process: the major effect is the changing barrier height produced by space velocity fluctuations that affect the nucleus energy more than it affects the α energy. Shnoll also reported correlations between decay rate fluctuations measured at different locations. However the time resolution was ~ 60 sec, and so no speed and direction for the underlying space velocity was determined. It is predicted that α decay fluctuation rates with a time resolution of ~ 1 sec would show the time delay effect for experiments well separated geographically.

6 Reinterpretation of quantum theory

The experimental data herein clearly implies a need for a reinterpretation of quantum theory, as it has always lacked the

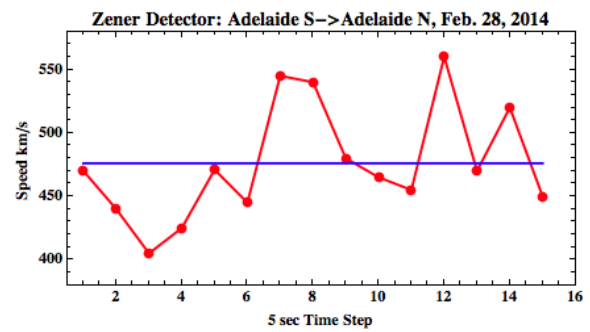


Fig. 6: Average projected speed, and projected speed every 5 sec, on February 28, 2014 at 12:20 hrs UTC, giving average speed = 476 ± 44 (RMS) km/s, from approximately S \rightarrow N. The speeds are effective projected speeds, and so do not distinguish between actual speed and direction effect changes. The projected speed = (actual speed)/ $\cos[a]$, where a is the angle between the space velocity and the direction defined by the two detectors, and cannot be immediately determined with only two detectors. However by varying direction of detector axis, and searching for maximum time delay, the average direction (RA and Dec) may be determined. As in previous experiments there are considerable fluctuations at all time scales, indicating a fractal structure to space.

dynamical effects of the fractal space: it only ever referred to the Euclidean static embedding space, which merely provides a position labelling. However the interpretation of the quantum theory has always been problematic and varied. The main problem is that the original Schrödinger equation does not describe the localization of quantum matter when measured, e.g. the formation of spots on photographic films in double slit experiments. From the beginning of quantum theory a metaphysical addendum was created, as in the Born interpretation, namely that there exists an almost point-like “particle”, and that $|\psi(\mathbf{r}, t)|^2$ gives the probability density for the location of that particle, whether or not a measurement of position has taken place. This is a dualistic interpretation of the quantum theory: there exists a “wave function” as well as a “particle”, and that the probability of a detection event is completely internal to a particular quantum system. So there should be no correlations between detection events for different systems, contrary to the experiments reported here. To see the failure of the Born and other interpretations consider the situation shown in Fig. 3. In the top figure the electron state is a wave packet $\psi_1(\mathbf{r}, t)$, partially localized to the left of a potential barrier. After the barrier tunnelling the wave function has evolved to the superposition $\psi_2(\mathbf{r}, t) + \psi_3(\mathbf{r}, t)$: a reflected and transmitted component. The probability of the electron being detected to the LHS is $\|\psi_2(\mathbf{r}, t)\|^2$, and to the RHS is $\|\psi_3(\mathbf{r}, t)\|^2$, the respective squared norms. These values do indeed predict the observed average reflected and transmitted electron currents, but make no prediction about the fluctuations that lead to these observed averages. As well, in the Born interpretation there is no mention of a collapse of the wave function to one of the states in the linear combina-

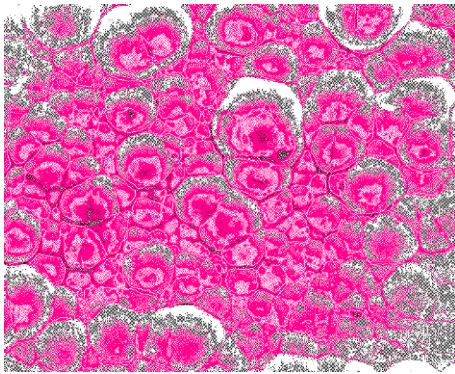


Fig. 7: Representation of the fractal wave data as revealing the fractal textured structure of the 3-space, with cells of space having slightly different velocities and continually changing, and moving wrt the Earth with a speed of ~ 500 km/s.

tion, as a single location outcome is in the metaphysics of the interpretation, and not in any physical process.

This localization process has never been satisfactorily explained, namely that when a quantum system, such as an electron, in a de-localized state, interacts with a detector, i.e. a system in a metastable state, the electron would put the combined system into a de-localized state, which is then observed to localize: the detector responds with an event at one location, but for which the quantum theory can only provide the expected average distribution, $|\psi(\mathbf{r}, t)|^2$, and is unable to predict fluctuation details. In [10] it was conjectured that the de-localized electron-detector state is localized by the interaction with the dynamical space, and that the fluctuation details are produced by the space fluctuations, as we see in Zener diode electron tunnelling and α decay tunnelling. Percival [19] has produced detailed models of this wave function collapse process, which involved an intrinsic randomness, and which involves yet another dynamical term being added to the original Schrödinger equation. It is possible that this randomness may also be the consequence of space fluctuations.

The space driven localization of quantum states could give rise to our experienced classical world, in which macroscopic “matter” is not seen in de-localized states. It was the inability to explain this localization process that gave rise to the Copenhagen and numerous other interpretations of the original quantum theory, and in particular the dualistic model of wave functions and almost point-like localized “particles”.

7 Dynamical 3-space

If Michelson and Morley had more carefully presented their pioneering data, physics would have developed in a very different direction. Even by 1925/26 Miller, a junior colleague of Michelson, was repeating the gas-mode interferometer experiment, and by not using Newtonian mechanics to attempt a calibration of the device, rather by using the Earth aberration effect which utilized the Earth orbital speed of 30 km/s to set

the calibration constant, although that also entailed false assumptions. The experimental data reveals the existence of a dynamical space. It is a simple matter to arrive at the dynamical theory of space, and the emergence of gravity as a quantum matter effect as noted above. The key insight is to note that the emergent matter acceleration in (3), $\partial\mathbf{v}/\partial t + (\mathbf{v}\cdot\nabla)\mathbf{v}$, is the constituent Euler acceleration $\mathbf{a}(\mathbf{r}, t)$ of space

$$\begin{aligned}\mathbf{a}(\mathbf{r}, t) &= \lim_{\Delta t \rightarrow 0} \frac{\mathbf{v}(\mathbf{r} + \mathbf{v}(\mathbf{r}, t)\Delta t, t + \Delta t) - \mathbf{v}(\mathbf{r}, t)}{\Delta t} \\ &= \frac{\partial\mathbf{v}}{\partial t} + (\mathbf{v}\cdot\nabla)\mathbf{v}\end{aligned}\quad (5)$$

which describes the acceleration of a constituent element of space by tracking its change in velocity. This means that space has a structure that permits its velocity to be defined and detected, which experimentally has been done. This then suggests that the simplest dynamical equation for $\mathbf{v}(\mathbf{r}, t)$ is

$$\begin{aligned}\nabla \cdot \left(\frac{\partial\mathbf{v}}{\partial t} + (\mathbf{v}\cdot\nabla)\mathbf{v} \right) &= -4\pi G\rho(\mathbf{r}, t); \\ \nabla \times \mathbf{v} &= 0\end{aligned}\quad (6)$$

because it then gives $\nabla \cdot \mathbf{g} = -4\pi G\rho(\mathbf{r}, t)$; $\nabla \times \mathbf{g} = 0$, which is Newton’s inverse square law of gravity in differential form. Hence the fundamental insight is that Newton’s gravitational acceleration field $\mathbf{g}(\mathbf{r}, t)$ is really the acceleration field $\mathbf{a}(\mathbf{r}, t)$ of the structured dynamical space*, and that quantum matter acquires that acceleration because it is fundamentally a wave effect, and the wave is refracted by the accelerations of space.

While the above lead to the simplest 3-space dynamical equation this derivation is not complete yet. One can add additional terms with the same order in speed spatial derivatives, and which cannot be *a priori* neglected. There are two such terms, as in

$$\nabla \cdot \left(\frac{\partial\mathbf{v}}{\partial t} + (\mathbf{v}\cdot\nabla)\mathbf{v} \right) + \frac{5\alpha}{4} \left((trD)^2 - tr(D^2) \right) + \dots = -4\pi G\rho \quad (7)$$

where $D_{ij} = \partial v_i / \partial x_j$. However to preserve the inverse square law external to a sphere of matter the two terms must have coefficients α and $-\alpha$, as shown. Here α is a dimensionless space self-interaction coupling constant, which experimental data reveals to be, approximately, the fine structure constant, $\alpha = e^2/\hbar c$ [21]. The ellipsis denotes higher order derivative terms with dimensioned coupling constants, which come into play when the flow speed changes rapidly with respect to distance. The observed dynamics of stars and gas clouds near the centre of the Milky Way galaxy has revealed the need for such a term [22], and we find that the space dynamics then requires an extra term:

$$\nabla \cdot \left(\frac{\partial\mathbf{v}}{\partial t} + (\mathbf{v}\cdot\nabla)\mathbf{v} \right) + \frac{5\alpha}{4} \left((trD)^2 - tr(D^2) \right) +$$

*With vorticity $\nabla \times \mathbf{v} \neq 0$ and relativistic effects, the acceleration of matter becomes different from the acceleration of space [10].

$$+ \delta^2 \nabla^2 ((trD)^2 - tr(D^2)) + \dots = -4\pi G \rho \quad (8)$$

where δ has the dimensions of length, and appears to be a very small Planck-like length, [22]. This then gives us the dynamical theory of 3-space. It can be thought of as arising via a derivative expansion from a deeper theory, such as a quantum foam theory [10]. Note that the equation does not involve c , is non-linear and time-dependent, and involves non-local direct interactions. Its success implies that the universe is more connected than previously thought. Even in the absence of matter there can be time-dependent flows of space.

Note that the dynamical space equation, apart from the short distance effect - the δ term, there is no scale factor, and hence a scale free structure to space is to be expected, namely a fractal space. That dynamical equation has back hole and cosmic filament solutions [21,22], which are non-singular because of the effect of the δ term. At large distance scales it appears that a homogeneous space is dynamically unstable and undergoes dynamical breakdown of symmetry to form a spatial network of black holes and filaments [21], to which matter is attracted and coalesces into gas clouds, stars and galaxies.

We can write (8) in non-linear integral-differential form

$$\frac{\partial u}{\partial t} = -\frac{(\nabla u)^2}{2} + G \int d^3 r' \frac{\rho(r', t) + \rho_{DM}(v(r', t))}{|r - r'|} \quad (9)$$

on satisfying $\nabla \times v = 0$ by writing $v = \nabla u$. Effects on the Gravity Probe B (GPB) gyroscope precessions caused by a non-zero vorticity were considered in [24]. Here ρ_{DM} is an effective “dark density” induced by the 3-space dynamics, but which is not any form of actual matter,

$$\rho_{DM}(v(r, t)) = \frac{1}{4\pi G} \left(\frac{5\alpha}{4} ((trD)^2 - tr(D^2)) + \delta^2 \nabla^2 ((trD)^2 - tr(D^2)) \right) \quad (10)$$

8 Universe expansion and inflation epoch

Even in the absence of matter (6) has an expanding universe solution. Substituting the Hubble form $v(r, t) = H(t)r$, and then using $H(t) = \dot{a}(t)/a(t)$, where $a(t)$ is the scale factor of the universe for a homogeneous and isotropic expansion, we obtain the exact solution $a(t) = t/t_0$, where t_0 is the age of the universe, since by convention $a(t_0) = 1$. Then computing the magnitude-redshift function $\mu(z)$, we obtain excellent agreement with the supernova data, and without the need for ‘dark matter’ nor ‘dark energy’ [20]. However using the extended dynamics in (8) we obtain $a(t) = (t/t_0)^{1/(1+5\alpha/2)}$ for a homogeneous and isotropic expansion, which has a singularity at $t = 0$, giving rise to an inflationary epoch. Fig. 8 shows a plot of $da(t)/dt$, which more clearly shows the inflation. However in general this space expansion will be turbulent:

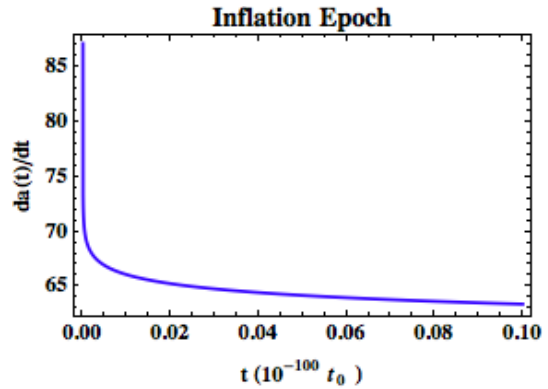


Fig. 8: Plot of $da(t)/dt$, the rate of expansion, showing the inflation epoch. Age of universe is $t_0 \approx 14 * 10^9$ years. On time axis $0.01 \times 10^{-100} t_0 = 4.4 \times 10^{-83}$ secs. This inflation epoch is intrinsic to the dynamical 3-space.

gravitational waves, perhaps as seen by the BICEP2 experiment in the Antarctica. Such turbulence will result in the creation of matter. This inflation epoch is an *ad hoc* addition to the standard model of cosmology [26]. Here it is intrinsic to the dynamics in (8) and is directly related to the bore hole g anomaly, black holes without matter infall, cosmic filaments, flat spiral galaxy rotation curves, light lensing by black holes, and other effects, all without the need for “dark matter”.

9 Zener diodes and REG devices

REGs, Random Event Generators, use current fluctuations in Zener diodes in reverse bias mode, to supposedly generate random numbers, and are used in the GCP network. However the outputs, as shown in [8], are not random. GCP data is available from <http://teillard.global-mind.org/>. This data extends back some 15 years and represents an invaluable resource for the study of gravitational waves, and their various effects, such as solar flares, coronal mass ejections, earthquakes, eclipse effects, moon phase effects, non-Poisson fluctuations in radioactivity [16], and variations in radioactive decay rates related to distance of the Earth from the Sun [23], as the 3-space fluctuations are enhanced by proximity to the Sun.

10 Earth scattering effect

In [8] correlated waveforms from Zener diode detectors in Perth and London were used to determine the speed and direction of gravitational waves, and detected an Earth scattering effect: the effective speed is larger when the 3-space path passes deeper into the Earth, Fig. 9. Eqn. (9) displays two kinds of waveform effects: disturbances from the first part, $\partial u/\partial t = -(\nabla u)^2/2$; and then matter density and the “dark matter” density effects when the second term is included. These later effects are instantaneous, indicating in this theory, that the universe (space) is highly non-locally

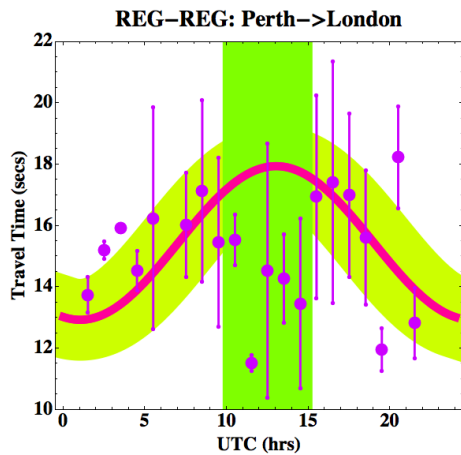


Fig. 9: Travel times from Zener Diode detectors (REG-REG) Perth-London from correlation delay time analysis, from [8]. The data in each 1 hr interval has been binned, and the average and rms shown. The thick (red line) shows best fit to data using plane wave travel time predictor, see [8], but after excluding those data points between 10 and 15hrs UTC, indicated by vertical band. Those data points are not consistent with the plane wave fixed average speed modelling, and suggest a scattering process when the waves pass deeper into the Earth, see [8]. This Perth-London data gives space velocity: 528 km/s, from direction RA = 5.3 hrs, Dec = 81°S. The broad band tracking the best fit line is for +/- 1 sec fluctuations, corresponding to speed fluctuation of +/- 17km/s. Actual fluctuations are larger than this, as 1st observed by Michelson-Morley in 1887 and by Miller in 1925/26.

connected, see [10], and combine in a non-linear manner with local disturbances that propagate at the speed of space. The matter density term is of course responsive for conventional Newtonian gravity theory.

However because these terms cross modulate the “dark matter” density space turbulence can manifest, in part, as a speed-up effect, as in the data in Fig. 9. Hence it is conjectured that the Earth scattering effect, manifest in the data, affords a means to study the dynamics arising from (10). That dynamics has already been confirmed in the non-singular space inflow black holes and the non-singular cosmic filaments effects, which are exact analytic solutions to (8) or (9). Indeed by using data from suitably located Zener diode detectors, for which the detected space flow passes through the centre of the Earth, we could be able to study the black hole located there, i.e. to perform black hole scattering experiments.

11 Gravitational waves as space flow turbulence

In the dynamical 3-space theory gravity is an emergent quantum effect, see (3), being the quantum wave response to time varying and inhomogeneous velocity fields. This has been confirmed by experiment. In [12] it was shown that Zener diodes detected the same signal as resonant bar gravitational wave detectors in Rome and Frascati in 1981. These detectors

respond to the induced $g(\mathbf{r}, t)$, via (3), while the Zener diode detectors respond directly to $\mathbf{v}(\mathbf{r}, t)$. As well the Zener diode data has revealed the detection of deep Earth core vibration resonances known from seismology, but requiring superconductor seismometers. The first publicized coincidence detection of gravitational waves by resonant bar detectors was by Weber in 1969, with detectors located in Argonne and Maryland. These results were criticized on a number of spurious grounds, all being along the lines that the data was inconsistent with the predictions of General Relativity, which indeed it is, see Collins [27]. However in [7] it was shown that Weber’s data is in agreement with the speed and direction of the measured space flow velocity. Data collected in the experiments reported in [8] revealed that significant fluctuations in the velocity field were followed some days later by solar flares, suggesting that these fluctuations, via the induced $g(\mathbf{r}, t)$, were causing solar dynamical instabilities. This suggests that the very simple Zener diode detection effect may be used to predict solar flares. As well Nelson and Baner [25] report that Zener diode detectors (REGs) have repeatedly detected earthquakes. The mechanism would appear to be explained by (9) in which fluctuations in the matter density $\rho(\mathbf{r}, t)$ induce fluctuations in $\mathbf{v}(\mathbf{r}, t)$, but with the important observation that this field decreases like $1/\sqrt{r}$, unlike the g field which decreases like $1/r^2$. So in all of the above examples we see the link between time dependent gravitational forces and the fluctuations of the 3-space velocity field. A possibility for future experiments is to determine if the incredibly sensitive Zener diode detector effect can directly detect primordial gravitational waves from the inflation epoch, 3-space turbulence, as a background to the local galactic 3-space flow effects.

12 Conclusions

We have reported refined direct quantum detection of 3-space turbulence: gravitational waves, using electron current fluctuations in reverse bias mode Zener diodes, separated by a mere 25cm, that permitted the absolute determination of the 3-space velocity of some 500 km/s, in agreement with the speed and direction from a number of previous analyzes that involved light speed anisotropy, including in particular the NASA spacecraft Earth-flyby Doppler shift effect, and the first such Zener diode direct detections of space flow using correlations between Perth and London detectors in 2013. The experimental results reveal the nature of the dominant gravitational wave effects; they are caused by turbulence / fluctuations in the passing dynamical space, a space missing from physics theories, until its recent discovery. This dynamical space explains bore hole anomalies, black holes without matter infall, cosmic filaments and the cosmic network, spiral galaxy flat rotation curves, universe expansion in agreement with supernova data, and all without dark matter nor dark energy, and a universe inflation epoch, accompanied

by gravitational waves. Quantum tunnelling fluctuations have been shown to be non-random, in the sense that they are completely induced by fluctuations in the passing space. It is also suggested that the localization of massive quantum systems is caused by fluctuations in space, and so generating our classical world of localized objects, but which are essentially wave phenomena at the microlevel. There is then no need to invoke any of the usual interpretations of the quantum theory, all of which failed to take account of the existence of the dynamical space. Present day physics employs an embedding space, whose sole function is to label positions in the dynamical space. This [3]-dimensional embedding in a geometrical space, while being non-dynamical, is nevertheless a property of the dynamical space at some scales. However the dynamical space at very small scales is conjectured not to be embeddable in a [3]-geometry, as discussed in [10].

Received on March 11, 2014 / Accepted on March 24, 2014

References

1. Michelson A. A., Morley E. W. On the relative motion of the earth and the luminiferous ether. *Am. J. Sci.*, 1887, v. 34, 333–345.
2. Cahill R. T., Kitto K. Michelson-Morley Experiments Revisited. *Apeiron*, 2003, v. 10 (2), 104–117.
3. Cahill R. T. The Michelson and Morley 1887 Experiment and the Discovery of Absolute Motion. *Progress in Physics*, 2005 v. 3, 25–29.
4. Cahill R. T. Dynamical 3-Space: Neo-Lorentz Relativity. *Physics International*, 2013, v. 4 (1), 60–72.
5. Braxmaier C., Müller H., Pradl O., Mlynek J., Peters O. Tests of Relativity Using a Cryogenic Optical Resonator. *Phys. Rev. Lett.*, 2001, v. 88, 010401.
6. Cahill R. T. Discovery of Dynamical 3-Space: Theory, Experiments and Observations - A Review. *American Journal of Space Science*, 2013, v. 1 (2), 77–93.
7. Cahill R. T. Review of Gravitational Wave Detections: Dynamical Space. *Physics International*, 2014, v. 5 (1), 49–86.
8. Cahill R. T. Nanotechnology Quantum Detectors for Gravitational Waves: Adelaide to London Correlations Observed. *Progress in Physics*, 2013, v. 4, 57–62.
9. Cahill R. T. Combining NASA/JPL One-Way Optical-Fiber Light-Speed Data with Spacecraft Earth-Flyby Doppler-Shift Data to Characterise 3-Space Flow. *Progress in Physics*, 2009, v. 4, 50–64.
10. Cahill R. T. Process Physics: From Information Theory to Quantum Space and Matter. Nova Science Pub., New York, 2005.
11. Cahill R. T. Characterisation of Low Frequency Gravitational Waves from Dual RF Coaxial-Cable Detector: Fractal Textured Dynamical 3-Space. *Progress in Physics*, 2012, v. 3, 3–10.
12. Cahill R. T. Observed Gravitational Wave Effects: Amaldi 1980 Frascati-Rome Classical Bar Detectors, 2013 Perth-London Zener-Diode Quantum Detectors, Earth Oscillation Mode Frequencies. *Progress in Physics*, 2014, v. 10 (1), 21–24.
13. Amaldi E., Coccia E., Frasca S., Modena I., Rapagnani P., Ricci F., Pallottino G. V., Pizzella G., Bonifazi P., Cosmelli C., Giovanardi U., Iafolla V., Ugazio S., Vannaroni G. Background of Gravitational-Wave Antennas of Possible Terrestrial Origin - I. *Il Nuovo Cimento*, 1981, v. 4C (3), 295–308.
14. Amaldi E., Frasca S., Pallottino G. V., Pizzella G., Bonifazi P. Background of Gravitational-Wave Antennas of Possible Terrestrial Origin - II. *Il Nuovo Cimento*, 1981, v. 4C (3), 309–323.
15. Cahill R. T., Dynamical Fractal 3-Space and the Generalised Schrödinger Equation: Equivalence Principle and Vorticity Effects. *Progress in Physics*, 2006, v. 1, 27–34.
16. Shnoll S. E. *Cosmophysical Factors in Stochastic Processes*. American Research Press, Rehoboth, NM, 2012.
17. Gamow G. Zur Quantentheorie des Atomkernes. *Z. Physik*, 1928, v. 51, 204.
18. Rothall D. P., Cahill R. T. Dynamical 3-Space: Observing Gravitational Wave Fluctuations with Zener Diode Quantum Detector: the Shnoll Effect. *Progress in Physics*, 2014, v. 10 (1), 16–18.
19. Percival I. *Quantum State Diffusion*. Cambridge University Press, Cambridge, 1998.
20. Cahill R. T., Rothall D. Discovery of Uniformly Expanding Universe. *Progress in Physics*, 2012, v. 1, 63–68.
21. Rothall D. P., Cahill R. T. Dynamical 3-Space: Black Holes in an Expanding Universe. *Progress in Physics*, 2013, v. 4, 25–31.
22. Cahill R. T., Kerrigan D. Dynamical Space: Supermassive Black Holes and Cosmic Filaments. *Progress in Physics*, 2011, v. 4, 79–82.
23. Jenkins J. H., Fischbach E., Buncher J. B., Gruenwald J. T., Krause, D. E., Mattes J. J. Evidence for Correlations Between Nuclear Decay Rates and Earth-Sun Distance. *Astropart. Phys.*, 2009, v. 32, 42.
24. Cahill R. T. Novel Gravity Probe B Frame Dragging Effect. *Progress in Physics*, 2005, v. 3 (1), 30–33.
25. Nelson R. D., Bancel P. A. Anomalous Anticipatory Responses in Networked Random Data, *Frontiers of Time: Retrocausation - Experiment and Theory. AIP Conference Proceedings*, 2006, v. 863, 260–272.
26. Guth A. H. The Inflationary Universe: A Possible Solution to the Horizon and Flatness Problems. *Phys. Rev.*, 1981, v. D23, 347. OCLC 4433735058.
27. Collins H. *Gravity's Shadow: The Search for Gravitational Waves*. University of Chicago Press, Chicago, 2004.

Chrome of Baryons

Gunn Quznetsov

gunn@mail.ru, quznets@yahoo.com

Chromes of quarks are changed under the Cartesian turns. And the Lorentz's transformations change chromes and grades of quarks. Baryons represent one of ways of elimination of these noninvariancy.

Introduction

According to the quark model [1], the properties of hadrons are primarily determined by their so-called valence quarks. For example, a proton is composed of two up quarks and one down quark. Although quarks also carry color charge, hadrons must have zero total color charge because of a phenomenon called color confinement. That is, hadrons must be "colorless" or "white". These are the simplest of the two ways: three quarks of different colors, or a quark of one color and an antiquark carrying the corresponding anticolor. Hadrons with the first arrangement are called baryons, and those with the second arrangement are mesons.

1 Cartesian rotation

Let α be any real number and

$$\begin{aligned} x'_0 &:= x_0, \\ x'_1 &:= x_1 \cos(\alpha) - x_2 \sin(\alpha); \\ x'_2 &:= x_1 \sin(\alpha) + x_2 \cos(\alpha); \\ x'_3 &:= x_3; \end{aligned} \quad (1)$$

Since j_A is a 3+1-vector then from [2, p. 59]:

$$\begin{aligned} j'_{A,0} &= -\varphi^\dagger \beta^{[0]} \varphi, \\ j'_{A,1} &= -\varphi^\dagger (\beta^{[1]} \cos(\alpha) - \beta^{[2]} \sin(\alpha)) \varphi; \\ j'_{A,2} &= -\varphi^\dagger (\beta^{[1]} \sin(\alpha) + \beta^{[2]} \cos(\alpha)) \varphi; \\ j'_{A,3} &= -\varphi^\dagger \beta^{[3]} \varphi. \end{aligned} \quad (2)$$

Hence if for φ' :

$$\begin{aligned} j'_{A,0} &= -\varphi'^\dagger \beta^{[0]} \varphi', \\ j'_{A,1} &= -\varphi'^\dagger \beta^{[1]} \varphi'; \\ j'_{A,2} &= -\varphi'^\dagger \beta^{[2]} \varphi'; \\ j'_{A,3} &= -\varphi'^\dagger \beta^{[3]} \varphi', \end{aligned}$$

and

$$\varphi' := U_{1,2}(\alpha) \varphi$$

then

$$\begin{aligned} U_{1,2}^\dagger(\alpha) \beta^{[0]} U_{1,2}(\alpha) &= \beta^{[0]}, \\ U_{1,2}^\dagger(\alpha) \beta^{[1]} U_{1,2}(\alpha) &= \beta^{[1]} \cos \alpha - \beta^{[2]} \sin \alpha; \\ U_{1,2}^\dagger(\alpha) \beta^{[2]} U_{1,2}(\alpha) &= \beta^{[2]} \cos \alpha + \beta^{[1]} \sin \alpha; \\ U_{1,2}^\dagger(\alpha) \beta^{[3]} U_{1,2}(\alpha) &= \beta^{[3]}; \end{aligned} \quad (3)$$

from [2, p. 62]: because

$$\rho_A = \varphi^\dagger \varphi = \varphi'^\dagger \varphi',$$

then

$$U_{1,2}^\dagger(\alpha) U_{1,2}(\alpha) = 1_4. \quad (4)$$

If

$$U_{1,2}(\alpha) := \cos \frac{\alpha}{2} \cdot 1_4 - \sin \frac{\alpha}{2} \cdot \beta^{[1]} \beta^{[2]}$$

i.e.:

$$U_{1,2}(\alpha) = \begin{bmatrix} e^{-i\frac{1}{2}\alpha} & 0 & 0 & 0 \\ 0 & e^{i\frac{1}{2}\alpha} & 0 & 0 \\ 0 & 0 & e^{-i\frac{1}{2}\alpha} & 0 \\ 0 & 0 & 0 & e^{i\frac{1}{2}\alpha} \end{bmatrix} \quad (5)$$

then $U_{1,2}(\alpha)$ fulfils to all these conditions (3), (4).

Then let

$$\begin{aligned} x'_0 &:= x_0, \\ x'_1 &:= x_1 \cos(\alpha) - x_3 \sin(\alpha), \\ x'_2 &:= x_2, \\ x'_3 &:= x_1 \sin(\alpha) + x_3 \cos(\alpha). \end{aligned} \quad (6)$$

Let

$$U_{1,3}(\alpha) := \cos \frac{\alpha}{2} \cdot 1_4 - \sin \frac{\alpha}{2} \cdot \beta^{[1]} \beta^{[3]}.$$

In this case:

$$U_{1,3}(\alpha) = \begin{bmatrix} \cos \frac{1}{2}\alpha & \sin \frac{1}{2}\alpha & 0 & 0 \\ -\sin \frac{1}{2}\alpha & \cos \frac{1}{2}\alpha & 0 & 0 \\ 0 & 0 & \cos \frac{1}{2}\alpha & \sin \frac{1}{2}\alpha \\ 0 & 0 & -\sin \frac{1}{2}\alpha & \cos \frac{1}{2}\alpha \end{bmatrix} \quad (7)$$

and

$$\begin{aligned} U_{1,3}^\dagger(\alpha) \beta^{[0]} U_{1,3}(\alpha) &= \beta^{[0]}, \\ U_{1,3}^\dagger(\alpha) \beta^{[1]} U_{1,3}(\alpha) &= \beta^{[1]} \cos \alpha - \beta^{[3]} \sin \alpha, \\ U_{1,3}^\dagger(\alpha) \beta^{[2]} U_{1,3}(\alpha) &= \beta^{[2]}, \\ U_{1,3}^\dagger(\alpha) \beta^{[3]} U_{1,3}(\alpha) &= \beta^{[3]} \cos \alpha + \beta^{[1]} \sin \alpha. \end{aligned} \quad (8)$$

If

$$\varphi' := U_{1,3}(\alpha) \varphi$$

and

$$j'_{A,k} := \varphi'^{\dagger} \beta^{[k]} \varphi'$$

where $(k \in \{0, 1, 2, 3\})$ then

$$j'_{A,0} = j_{A,0}, \tag{9}$$

$$j'_{A,1} = j_{A,1} \cos \alpha - j_{A,3} \sin \alpha, \tag{10}$$

$$j'_{A,2} = j_{A,2},$$

$$j'_{A,3} = j_{A,3} \cos \alpha + j_{A,1} \sin \alpha.$$

Then let

$$\begin{aligned} x'_0 &:= x_0, \\ x'_1 &:= x_1, \\ x'_2 &= \cos \alpha \cdot x_2 + \sin \alpha \cdot x_3, \\ x'_3 &= \cos \alpha \cdot x_3 - \sin \alpha \cdot x_2. \end{aligned} \tag{11}$$

Let

$$U_{3,2}(\alpha) = \cos \frac{\alpha}{2} \cdot 1_4 - \sin \frac{\alpha}{2} \cdot \beta^{[3]} \beta^{[2]}$$

In this case:

$$U_{3,2}(\alpha) = \begin{bmatrix} \cos \frac{1}{2}\alpha & i \sin \frac{1}{2}\alpha & 0 & 0 \\ i \sin \frac{1}{2}\alpha & \cos \frac{1}{2}\alpha & 0 & 0 \\ 0 & 0 & \cos \frac{1}{2}\alpha & i \sin \frac{1}{2}\alpha \\ 0 & 0 & i \sin \frac{1}{2}\alpha & \cos \frac{1}{2}\alpha \end{bmatrix}, \tag{12}$$

and

$$\begin{aligned} U_{3,2}^{\dagger}(\alpha) \beta^{[0]} U_{3,2}(\alpha) &= \beta^{[0]}, \\ U_{3,2}^{\dagger}(\alpha) \beta^{[1]} U_{3,2}(\alpha) &= \beta^{[1]}, \\ U_{3,2}^{\dagger}(\alpha) \beta^{[0]} U_{3,2}(\alpha) &= \beta^{[0]} \cos \alpha + \beta^{[3]} \sin \alpha, \\ U_{3,2}^{\dagger}(\alpha) \beta^{[3]} U_{3,2}(\alpha) &= \beta^{[3]} \cos \alpha - \beta^{[2]} \sin \alpha \end{aligned} \tag{13}$$

If

$$\varphi' := U_{3,2}(\alpha) \varphi$$

and

$$j'_{A,k} := \varphi'^{\dagger} \beta^{[k]} \varphi'$$

where $(k \in \{0, 1, 2, 3\})$ then

$$\begin{aligned} j'_{A,0} &= j_{A,0}, \\ j'_{A,1} &= j_{A,1}, \\ j'_{A,2} &= j_{A,2} \cos \alpha + j_{A,3} \sin \alpha, \\ j'_{A,3} &= j_{A,3} \cos \alpha - j_{A,1} \sin \alpha. \end{aligned} \tag{14}$$

2 Lorentzian rotation

Let v be any real number such that $-1 < v < 1$.

And let:

$$\alpha := \frac{1}{2} \ln \frac{1-v}{1+v}.$$

In this case:

$$\begin{aligned} \cosh \alpha &= \frac{1}{\sqrt{1-v^2}}, \\ \sinh \alpha &= -\frac{v}{\sqrt{1-v^2}}. \end{aligned} \tag{15}$$

Let

$$\begin{aligned} x'_0 &:= x_0 \cosh \alpha - x_1 \sinh \alpha, \\ x'_1 &:= x_1 \cosh \alpha - x_0 \sinh \alpha, \\ x'_2 &:= x_2, \\ x'_3 &:= x_3. \end{aligned} \tag{16}$$

Let

$$U_{1,0}(\alpha) = \cosh \frac{\alpha}{2} \cdot 1_4 - \sinh \frac{\alpha}{2} \cdot \beta^{[1]} \beta^{[0]}.$$

That is:

$$U_{1,0}(\alpha) := \begin{bmatrix} \cosh \frac{1}{2}\alpha & \sinh \frac{1}{2}\alpha & 0 & 0 \\ \sinh \frac{1}{2}\alpha & \cosh \frac{1}{2}\alpha & 0 & 0 \\ 0 & 0 & \cosh \frac{1}{2}\alpha & -\sinh \frac{1}{2}\alpha \\ 0 & 0 & -\sinh \frac{1}{2}\alpha & \cosh \frac{1}{2}\alpha \end{bmatrix}. \tag{17}$$

In this case:

$$\begin{aligned} U_{1,0}^{\dagger}(\alpha) \beta^{[0]} U_{1,0}(\alpha) &= \beta^{[0]} \cosh \alpha - \beta^{[1]} \sinh \alpha, \\ U_{1,0}^{\dagger}(\alpha) \beta^{[1]} U_{1,0}(\alpha) &= \beta^{[1]} \cosh \alpha - \beta^{[0]} \sinh \alpha, \\ U_{1,0}^{\dagger}(\alpha) \beta^{[2]} U_{1,0}(\alpha) &= \beta^{[2]}, \\ U_{1,0}^{\dagger}(\alpha) \beta^{[3]} U_{1,0}(\alpha) &= \beta^{[3]}. \end{aligned} \tag{18}$$

If

$$\varphi' := U_{1,0}(\alpha) \varphi$$

and

$$j'_{A,k} := \varphi'^{\dagger} \beta^{[k]} \varphi'$$

where $(k \in \{0, 1, 2, 3\})$ then

$$\begin{aligned} j'_{A,0} &= j_{A,0} \cosh \alpha - j_{A,1} \sinh \alpha, \\ j'_{A,1} &= j_{A,1} \cosh \alpha - j_{A,0} \sinh \alpha, \\ j'_{A,2} &= j_{A,2}, \\ j'_{A,3} &= j_{A,3}. \end{aligned} \tag{19}$$

Then let

$$\begin{aligned} x'_0 &:= x_0 \cosh \alpha - x_2 \sinh \alpha, \\ x'_1 &:= x_1, \\ x'_2 &:= x_2 \cosh \alpha - x_0 \sinh \alpha, \\ x'_3 &:= x_3. \end{aligned} \tag{20}$$

Let

$$U_{2,0}(\alpha) := \cosh \frac{\alpha}{2} \cdot 1_4 - \sinh \frac{\alpha}{2} \cdot \beta^{[2]}\beta^{[0]}. \quad (21)$$

That is:

$$U_{2,0}(\alpha) = \begin{bmatrix} \cosh \frac{1}{2}\alpha & -i \sinh \frac{1}{2}\alpha & 0 & 0 \\ i \sinh \frac{1}{2}\alpha & \cosh \frac{1}{2}\alpha & 0 & 0 \\ 0 & 0 & \cosh \frac{1}{2}\alpha & i \sinh \frac{1}{2}\alpha \\ 0 & 0 & -i \sinh \frac{1}{2}\alpha & \cosh \frac{1}{2}\alpha \end{bmatrix}.$$

In this case:

$$\begin{aligned} U_{2,0}^\dagger(\alpha)\beta^{[0]}U_{2,0}(\alpha) &= \beta^{[0]}\cosh\alpha - \beta^{[2]}\sinh\alpha, \quad (22) \\ U_{2,0}^\dagger(\alpha)\beta^{[1]}U_{2,0}(\alpha) &= \beta^{[1]}, \\ U_{2,0}^\dagger(\alpha)\beta^{[2]}U_{2,0}(\alpha) &= \beta^{[2]}\cosh\alpha - \beta^{[0]}\sinh\alpha, \\ U_{2,0}^\dagger(\alpha)\beta^{[3]}U_{2,0}(\alpha) &= \beta^{[3]}. \end{aligned}$$

If

$$\varphi' := U_{2,0}(\alpha)\varphi$$

and

$$j'_{A,k} := \varphi'^\dagger \beta^{[k]} \varphi'$$

where $(k \in \{0, 1, 2, 3\})$ then

$$\begin{aligned} j'_{A,0} &= j_{A,0} \cosh \alpha - j_{A,1} \sinh \alpha, \quad (23) \\ j'_{A,1} &= j_{A,1}, \\ j'_{A,2} &= j_{A,2} \cosh \alpha - j_{A,3} \sinh \alpha, \\ j'_{A,3} &= j_{A,3}. \end{aligned}$$

Then let

$$\begin{aligned} x'_0 &:= x_0 \cosh \alpha - x_3 \sinh \alpha, \quad (24) \\ x'_1 &:= x_1, \\ x'_2 &:= x_2, \\ x'_3 &:= x_3 \cosh \alpha - x_0 \sinh \alpha. \end{aligned}$$

Let

$$U_{3,0}(\alpha) := \cosh \frac{\alpha}{2} \cdot 1_4 - \sinh \frac{\alpha}{2} \cdot \beta^{[3]}\beta^{[0]}.$$

That is:

$$U_{3,0}(\alpha) = \begin{bmatrix} e^{\frac{1}{2}\alpha} & 0 & 0 & 0 \\ 0 & e^{-\frac{1}{2}\alpha} & 0 & 0 \\ 0 & 0 & e^{-\frac{1}{2}\alpha} & 0 \\ 0 & 0 & 0 & e^{\frac{1}{2}\alpha} \end{bmatrix}. \quad (25)$$

In this case:

$$\begin{aligned} U_{3,0}^\dagger(\alpha)\beta^{[0]}U_{3,0}(\alpha) &= \beta^{[0]}\cosh\alpha - \beta^{[3]}\sinh\alpha, \quad (26) \\ U_{3,0}^\dagger(\alpha)\beta^{[1]}U_{3,0}(\alpha) &= \beta^{[1]}, \\ U_{3,0}^\dagger(\alpha)\beta^{[2]}U_{3,0}(\alpha) &= \beta^{[2]}, \\ U_{3,0}^\dagger(\alpha)\beta^{[3]}U_{3,0}(\alpha) &= \beta^{[3]}\cosh\alpha - \beta^{[0]}\sinh\alpha. \end{aligned}$$

If

$$\varphi' := U_{3,0}(\alpha)\varphi$$

and

$$j'_{A,k} := \varphi'^\dagger \beta^{[k]} \varphi'$$

where $(k \in \{0, 1, 2, 3\})$ then

$$\begin{aligned} j'_{A,0} &= j_{A,0} \cosh \alpha - j_{A,3} \sinh \alpha, \quad (27) \\ j'_{A,1} &= j_{A,1}, \\ j'_{A,2} &= j_{A,2}, \\ j'_{A,3} &= j_{A,3} \cosh \alpha - j_{A,0} \sinh \alpha. \end{aligned}$$

3 Equation of motion

Function φ submits to the following equation [2, p. 82]:

$$\begin{aligned} &\frac{1}{c}\partial_t\varphi - (i\Theta_0\beta^{[0]} + i\Upsilon_0\beta^{[0]}\gamma^{[5]})\varphi = \\ &= \left(\sum_{v=1}^3 \beta^{[v]} (\partial_v + i\Theta_v + i\Upsilon_v\gamma^{[5]}) + \right. \\ &\quad + iM_0\gamma^{[0]} + iM_4\beta^{[4]} - \\ &\quad - iM_{\zeta,0}\gamma_{\zeta}^{[0]} + iM_{\zeta,4}\zeta^{[4]} - \\ &\quad - iM_{\eta,0}\gamma_{\eta}^{[0]} - iM_{\eta,4}\eta^{[4]} + \\ &\quad \left. + iM_{\theta,0}\gamma_{\theta}^{[0]} + iM_{\theta,4}\theta^{[4]} \right)\varphi. \end{aligned}$$

That is:

$$\begin{aligned} &\left(\sum_{v=0}^3 \beta^{[v]} (\partial_v + i\Theta_v + i\Upsilon_v\gamma^{[5]}) + \right. \\ &\quad + iM_0\gamma^{[0]} + iM_4\beta^{[4]} - \\ &\quad - iM_{\zeta,0}\gamma_{\zeta}^{[0]} + iM_{\zeta,4}\zeta^{[4]} - \\ &\quad - iM_{\eta,0}\gamma_{\eta}^{[0]} - iM_{\eta,4}\eta^{[4]} + \\ &\quad \left. + iM_{\theta,0}\gamma_{\theta}^{[0]} + iM_{\theta,4}\theta^{[4]} \right)\varphi = 0. \quad (28) \end{aligned}$$

Like coordinates x_5 and x_4 [2, p. 83] here are entered new coordinates $y^\beta, z^\beta, y^\zeta, z^\zeta, y^\eta, z^\eta, y^\theta, z^\theta$ such that

$$\begin{aligned} -\frac{\pi c}{h} &\leq y^\beta \leq \frac{\pi c}{h}, -\frac{\pi c}{h} \leq z^\beta \leq \frac{\pi c}{h}, \\ -\frac{\pi c}{h} &\leq y^\zeta \leq \frac{\pi c}{h}, -\frac{\pi c}{h} \leq z^\zeta \leq \frac{\pi c}{h}, \\ -\frac{\pi c}{h} &\leq y^\eta \leq \frac{\pi c}{h}, -\frac{\pi c}{h} \leq z^\eta \leq \frac{\pi c}{h}, \\ -\frac{\pi c}{h} &\leq y^\theta \leq \frac{\pi c}{h}, -\frac{\pi c}{h} \leq z^\theta \leq \frac{\pi c}{h}. \end{aligned}$$

and like $\tilde{\varphi}$, [2, p. 83] let:

$$\begin{aligned} &[\varphi](t, \mathbf{x}, y^\beta, z^\beta, y^\zeta, z^\zeta, y^\eta, z^\eta, y^\theta, z^\theta) := \quad (29) \\ &:= \varphi(t, \mathbf{x}) \times \exp\left(i(y^\beta M_0 + z^\beta M_4 + y^\zeta M_{\zeta,0} + z^\zeta M_{\zeta,4} + \right. \\ &\quad \left. + y^\eta M_{\eta,0} + z^\eta M_{\eta,4} + y^\theta M_{\theta,0} + z^\theta M_{\theta,4})\right). \end{aligned}$$

In this case if

$$\begin{aligned}
 &([\varphi], [\chi]) := \\
 &:= \int_{-\frac{\pi c}{h}}^{\frac{\pi c}{h}} dy^\beta \int_{-\frac{\pi c}{h}}^{\frac{\pi c}{h}} dz^\beta \int_{-\frac{\pi c}{h}}^{\frac{\pi c}{h}} dy^\zeta \int_{-\frac{\pi c}{h}}^{\frac{\pi c}{h}} dz^\zeta \times \\
 &\times \int_{-\frac{\pi c}{h}}^{\frac{\pi c}{h}} dy^\eta \int_{-\frac{\pi c}{h}}^{\frac{\pi c}{h}} dz^\eta \int_{-\frac{\pi c}{h}}^{\frac{\pi c}{h}} dy^\theta \int_{-\frac{\pi c}{h}}^{\frac{\pi c}{h}} dz^\theta \times \\
 &\quad \times [\varphi]^\dagger [\chi]
 \end{aligned} \tag{30}$$

then

$$\begin{aligned}
 ([\varphi], [\varphi]) &= \rho_{\mathcal{A}}, \\
 ([\varphi], \beta^{[s]} [\varphi]) &= -\frac{j_{\mathcal{A},k}}{c},
 \end{aligned} \tag{31}$$

and in this case from (28):

$$\begin{aligned}
 &\left(\sum_{\nu=0}^3 \beta^{[\nu]} (\partial_\nu + i\Theta_\nu + i\Upsilon_\nu \gamma^{[5]}) + \right. \\
 &\quad + \gamma^{[0]} \partial_y^\beta + \beta^{[4]} \partial_z^\beta - \\
 &\quad - \gamma_\zeta^{[0]} \partial_y^\zeta + \zeta^{[4]} \partial_z^\zeta - \\
 &\quad - \gamma_\eta^{[0]} \partial_y^\eta - \eta^{[4]} \partial_z^\eta + \\
 &\quad \left. + \gamma_\theta^{[0]} \partial_y^\theta + \theta^{[4]} \partial_z^\theta \right) [\varphi] = 0.
 \end{aligned} \tag{32}$$

Because

$$\gamma_\eta^{[0]} = \begin{bmatrix} 0 & 0 & 0 & i \\ 0 & 0 & -i & 0 \\ 0 & i & 0 & 0 \\ -i & 0 & 0 & 0 \end{bmatrix}, \eta^{[4]} = i \begin{bmatrix} 0 & 0 & 0 & -i \\ 0 & 0 & i & 0 \\ 0 & i & 0 & 0 \\ -i & 0 & 0 & 0 \end{bmatrix}; \tag{33}$$

$$\gamma_\theta^{[0]} = \begin{bmatrix} 0 & 0 & -1 & 0 \\ 0 & 0 & 0 & 1 \\ -1 & 0 & 0 & 0 \\ 0 & 1 & 0 & 0 \end{bmatrix}, \theta^{[4]} = i \begin{bmatrix} 0 & 0 & 1 & 0 \\ 0 & 0 & 0 & -1 \\ -1 & 0 & 0 & 0 \\ 0 & 1 & 0 & 0 \end{bmatrix}; \tag{34}$$

$$\gamma_\zeta^{[0]} = \begin{bmatrix} 0 & 0 & 0 & -1 \\ 0 & 0 & -1 & 0 \\ 0 & -1 & 0 & 0 \\ -1 & 0 & 0 & 0 \end{bmatrix}, \zeta^{[4]} = i \begin{bmatrix} 0 & 0 & 0 & 1 \\ 0 & 0 & 1 & 0 \\ 0 & -1 & 0 & 0 \\ -1 & 0 & 0 & 0 \end{bmatrix}; \tag{35}$$

then from (32):

$$\begin{aligned}
 &\sum_{\nu=0}^3 \beta^{[\nu]} (\partial_\nu + i\Theta_\nu + i\Upsilon_\nu \gamma^{[5]}) [\varphi] + \\
 &\quad + \gamma^{[0]} \partial_y^\beta [\varphi] + \beta^{[4]} \partial_z^\beta [\varphi] + \\
 &\quad + \left(\begin{bmatrix} 0 & 0 & -\partial_y^\theta & \partial_y^\zeta - i\partial_y^\eta \\ 0 & 0 & \partial_y^\zeta + i\partial_y^\eta & \partial_y^\theta \\ -\partial_y^\theta & \partial_y^\zeta - i\partial_y^\eta & 0 & 0 \\ \partial_y^\zeta + i\partial_y^\eta & \partial_y^\theta & 0 & 0 \end{bmatrix} + \right. \\
 &\quad \left. i \begin{bmatrix} 0 & 0 & \partial_z^\theta & \partial_z^\zeta + i\partial_z^\eta \\ 0 & 0 & \partial_z^\zeta - i\partial_z^\eta & -\partial_z^\theta \\ -\partial_z^\theta & -\partial_z^\zeta - i\partial_z^\eta & 0 & 0 \\ -\partial_z^\zeta + i\partial_z^\eta & \partial_z^\theta & 0 & 0 \end{bmatrix} \right) \\
 &\quad \times [\varphi] = 0.
 \end{aligned} \tag{36}$$

Let a Fourier transformation of

$$[\varphi] (t, \mathbf{x}, y^\beta, z^\beta, y^\zeta, z^\zeta, y^\eta, z^\eta, y^\theta, z^\theta)$$

be the following:

$$\begin{aligned}
 &[\varphi] (t, \mathbf{x}, y^\beta, z^\beta, y^\zeta, z^\zeta, y^\eta, z^\eta, y^\theta, z^\theta) = \\
 &= \sum_{w, p_1, p_2, p_3, n^\beta, s^\beta, n^\zeta, s^\zeta, n^\eta, s^\eta, n^\theta, s^\theta} c(w, p_1, p_2, p_3, n^\beta, s^\beta, \\
 &\quad n^\zeta, s^\zeta, n^\eta, s^\eta, n^\theta, s^\theta) \times \\
 &\quad \times \exp \left(-i \frac{h}{c} (wx_0 + p_1 x_1 + p_2 x_2 + p_3 x_3 + \right. \\
 &\quad \left. + n^\beta y^\beta + s^\beta z^\beta + n^\zeta y^\zeta + s^\zeta z^\zeta + \right. \\
 &\quad \left. + n^\eta y^\eta + s^\eta z^\eta + n^\theta y^\theta + s^\theta z^\theta) \right).
 \end{aligned} \tag{37}$$

Let in (36) $\Theta_\nu = 0$ and $\Upsilon_\nu = 0$.

Let us design:

$$\begin{aligned}
 G_0 := &\left(\sum_{\nu=0}^3 \beta^{[\nu]} \partial_\nu + \gamma^{[0]} \partial_y^\beta + \beta^{[4]} \partial_z^\beta - \right. \\
 &\quad - \gamma_\zeta^{[0]} \partial_y^\zeta + \zeta^{[4]} \partial_z^\zeta - \\
 &\quad - \gamma_\eta^{[0]} \partial_y^\eta - \eta^{[4]} \partial_z^\eta + \\
 &\quad \left. + \gamma_\theta^{[0]} \partial_y^\theta + \theta^{[4]} \partial_z^\theta \right).
 \end{aligned} \tag{38}$$

that is:

$$\begin{aligned}
 &G_0 = \\
 &\begin{bmatrix} -\partial_0 + \partial_3 & \partial_1 - i\partial_2 & \partial_y^\beta - \partial_y^\theta & \partial_y^\zeta - i\partial_y^\eta \\ \partial_1 + i\partial_2 & -\partial_0 - \partial_3 & \partial_y^\zeta + i\partial_y^\eta & \partial_y^\beta + \partial_y^\theta \\ \partial_y^\beta - \partial_y^\theta & \partial_y^\zeta - i\partial_y^\eta & -\partial_0 - \partial_3 & -\partial_1 + i\partial_2 \\ \partial_y^\zeta + i\partial_y^\eta & \partial_y^\beta + \partial_y^\theta & -\partial_1 - i\partial_2 & -\partial_0 + \partial_3 \end{bmatrix} \\
 &+ i \begin{bmatrix} 0 & 0 & \partial_z^\beta + \partial_z^\theta & \partial_z^\zeta + i\partial_z^\eta \\ 0 & 0 & \partial_z^\zeta - i\partial_z^\eta & \partial_z^\beta - \partial_z^\theta \\ -\partial_z^\beta - \partial_z^\theta & -\partial_z^\zeta - i\partial_z^\eta & 0 & 0 \\ -\partial_z^\zeta + i\partial_z^\eta & -\partial_z^\beta + \partial_z^\theta & 0 & 0 \end{bmatrix}
 \end{aligned} \tag{39}$$

$$\begin{aligned}
 G_0 [\varphi] = &-i \frac{h}{c} \sum_{w, p_1, p_2, p_3, n^\beta, s^\beta, n^\zeta, s^\zeta, n^\eta, s^\eta, n^\theta, s^\theta} \check{g}(w, \\
 &p_1, p_2, p_3, n^\beta, s^\beta, n^\zeta, s^\zeta, n^\eta, s^\eta, n^\theta, s^\theta) \\
 &\sum_{k=0}^3 c_k(w, p_1, p_2, p_3, n^\beta, s^\beta, n^\zeta, s^\zeta, n^\eta, s^\eta, n^\theta, s^\theta) \times \\
 &\times \exp \left(-i \frac{h}{c} (wx_0 + p_1 x_1 + p_2 x_2 + p_3 x_3 + \right. \\
 &\quad \left. + n^\beta y^\beta + s^\beta z^\beta + n^\zeta y^\zeta + s^\zeta z^\zeta + \right. \\
 &\quad \left. + n^\eta y^\eta + s^\eta z^\eta + n^\theta y^\theta + s^\theta z^\theta) \right).
 \end{aligned} \tag{40}$$

Here

$$c_k(w, p_1, p_2, p_3, n^\beta, s^\beta, n^\zeta, s^\zeta, n^\eta, s^\eta, n^\theta, s^\theta)$$

is an eigenvector of

$$\check{g}(w, p_1, p_2, p_3, n^\beta, s^\beta, n^\zeta, s^\zeta, n^\eta, s^\eta, n^\theta, s^\theta)$$

and

$$\begin{aligned} \check{g}(w, p_1, p_2, p_3, n^\beta, s^\beta, n^\zeta, s^\zeta, n^\eta, s^\eta, n^\theta, s^\theta) := & (41) \\ := & \beta^{[0]}w + \beta^{[1]}p_1 + \beta^{[2]}p_2 + \beta^{[3]}p_3 + \\ & + \gamma^{[0]}n^\beta + \beta^{[4]}s^\beta - \gamma_\zeta^{[0]}n^\zeta + \zeta^{[4]}s^\zeta - \\ & - \gamma_\eta^{[0]}n^\eta - \eta^{[4]}s^\eta + \gamma_\theta^{[0]}n^\theta + \theta^{[4]}s^\theta. \end{aligned}$$

Here

$$\{c_0, c_1, c_2, c_3\}$$

is an orthonormalized basis of the complex4-vectors space.

Functions

$$\begin{aligned} c_k(w, p_1, p_2, p_3, n^\beta, s^\beta, n^\zeta, s^\zeta, n^\eta, s^\eta, n^\theta, s^\theta) \times & (42) \\ \times \exp\left(-i\frac{\hbar}{c}(wx_0 + p_1x_1 + p_2x_2 + p_3x_3 + \right. & \\ \left. + n^\beta y^\beta + s^\beta z^\beta + \right. & \\ \left. + n^\zeta y^\zeta + s^\zeta z^\zeta + n^\eta y^\eta + s^\eta z^\eta + n^\theta y^\theta + s^\theta z^\theta)\right) & \end{aligned}$$

are eigenvectors of operator G_0 .

4 Chromes under Lorentz's and Cartesian transformations

$$\varphi_y^\zeta := c(w, \mathbf{p}, f) \exp\left(-i\frac{\hbar}{c}(wx_0 + \mathbf{p}\mathbf{x} + \gamma_\zeta^{[0]}fy^\zeta)\right)$$

is a red lower chrome function,

$$\varphi_z^\zeta := c(w, \mathbf{p}, f) \exp\left(-i\frac{\hbar}{c}(wx_0 + \mathbf{p}\mathbf{x} - i\zeta^{[4]}fz^\zeta)\right)$$

is a red upper chrome function,

$$\varphi_y^\eta := c(w, \mathbf{p}, f) \exp\left(-i\frac{\hbar}{c}(wx_0 + \mathbf{p}\mathbf{x} + \gamma_\eta^{[0]}fy^\eta)\right)$$

is a green lower chrome function,

$$\varphi_z^\eta := c(w, \mathbf{p}, f) \exp\left(-i\frac{\hbar}{c}(wx_0 + \mathbf{p}\mathbf{x} - i\eta^{[4]}fz^\eta)\right)$$

is a green upper chrome function,

$$\varphi_y^\theta := c(w, \mathbf{p}, f) \exp\left(-i\frac{\hbar}{c}(wx_0 + \mathbf{p}\mathbf{x} + \gamma_\theta^{[0]}fy^\theta)\right)$$

is a blue lower chrome function,

$$\varphi_z^\theta := c(w, \mathbf{p}, s^\theta) \exp\left(-i\frac{\hbar}{c}(wx_0 + \mathbf{p}\mathbf{x} - i\theta^{[4]}fz^\theta)\right)$$

is a blue upper chrome function.

Operator $-\partial_y^\zeta \partial_y^\zeta$ is called a red lower chrome operator, $-\partial_z^\zeta \partial_z^\zeta$ is a red upper chrome operator, $-\partial_y^\eta \partial_y^\eta$ is called a green lower chrome operator, $-\partial_z^\eta \partial_z^\eta$ is a green upper chrome operator, $-\partial_y^\theta \partial_y^\theta$ is called a blue lower chrome operator, $-\partial_z^\theta \partial_z^\theta$ is a blue upper chrome operator.

For example, if φ_z^ζ is a red upper chrome function then

$$\begin{aligned} -\partial_y^\zeta \partial_y^\zeta \varphi_z^\zeta &= -\partial_y^\eta \partial_y^\eta \varphi_z^\zeta = -\partial_z^\eta \partial_z^\eta \varphi_z^\zeta = \\ &= -\partial_y^\theta \partial_y^\theta \varphi_z^\zeta = -\partial_z^\theta \partial_z^\theta \varphi_z^\zeta = 0 \end{aligned}$$

but

$$-\partial_z^\zeta \partial_z^\zeta \varphi_z^\zeta = -\left(\frac{\hbar}{c}f\right)^2 \varphi_z^\zeta.$$

Because

$$G_0[\varphi] = 0$$

then

$$UG_0U^{-1}U[\varphi] = 0.$$

If $U = U_{1,2}(\alpha)$ then $G_0 \rightarrow U_{1,2}(\alpha)G_0U_{1,2}^{-1}(\alpha)$ and $[\varphi] \rightarrow U_{1,2}(\alpha)[\varphi]$.

In this case:

$$\partial_1 \rightarrow \partial'_1 := (\cos \alpha \cdot \partial_1 - \sin \alpha \cdot \partial_2),$$

$$\partial_2 \rightarrow \partial'_2 := (\cos \alpha \cdot \partial_2 + \sin \alpha \cdot \partial_1),$$

$$\partial_0 \rightarrow \partial'_0 := \partial_0,$$

$$\partial_3 \rightarrow \partial'_3 := \partial_3,$$

$$\partial_y^\beta \rightarrow \partial_y^{\beta'} := \partial_y^\beta,$$

$$\partial_z^\beta \rightarrow \partial_z^{\beta'} := \partial_z^\beta,$$

$$\partial_y^\zeta \rightarrow \partial_y^{\zeta'} := (\cos \alpha \cdot \partial_y^\zeta - \sin \alpha \cdot \partial_y^\eta),$$

$$\partial_y^\eta \rightarrow \partial_y^{\eta'} := (\cos \alpha \cdot \partial_y^\eta + \sin \alpha \cdot \partial_y^\zeta),$$

$$\partial_z^\zeta \rightarrow \partial_z^{\zeta'} := (\cos \alpha \cdot \partial_z^\zeta + \sin \alpha \cdot \partial_z^\eta),$$

$$\partial_z^\eta \rightarrow \partial_z^{\eta'} := (\cos \alpha \cdot \partial_z^\eta - \sin \alpha \cdot \partial_z^\zeta),$$

$$\partial_y^\theta \rightarrow \partial_y^{\theta'} := \partial_y^\theta,$$

$$\partial_z^\theta \rightarrow \partial_z^{\theta'} := \partial_z^\theta.$$

Therefore,

$$-\partial_z^{\zeta'} \partial_z^{\zeta'} \varphi_z^\zeta = \left(f\frac{\hbar}{c} \cos \alpha\right)^2 \cdot \varphi_z^\zeta,$$

$$-\partial_z^{\eta'} \partial_z^{\eta'} \varphi_z^\zeta = \left(-\sin \alpha \cdot f\frac{\hbar}{c}\right)^2 \varphi_z^\zeta.$$

If $\alpha = -\frac{\pi}{2}$ then

$$-\partial_z^{\zeta'} \partial_z^{\zeta'} \varphi_z^\zeta = 0,$$

$$-\partial_z^{\eta'} \partial_z^{\eta'} \varphi_z^\zeta = \left(f\frac{\hbar}{c}\right)^2 \varphi_z^\zeta.$$

That is under such rotation the red state becomes the green state.

If $U = U_{3,2}(\alpha)$ then $G_0 \rightarrow U_{3,2}(\alpha) G_0 U_{3,2}^{-1}(\alpha)$ and $[\varphi] \rightarrow U_{3,2}(\alpha) [\varphi]$.

In this case:

$$\begin{aligned} \partial_0 &\rightarrow \partial'_0 := \partial_0, \\ \partial_1 &\rightarrow \partial'_1 := \partial_1, \\ \partial_2 &\rightarrow \partial'_2 := (\cos \alpha \cdot \partial_2 + \sin \alpha \cdot \partial_3), \\ \partial_3 &\rightarrow \partial'_3 := (\cos \alpha \cdot \partial_3 - \sin \alpha \cdot \partial_2), \\ \partial_y^\beta &\rightarrow \partial_y^{\beta'} := \partial_y^\beta, \\ \partial_y^\zeta &\rightarrow \partial_y^{\zeta'} := \partial_y^\zeta, \\ \partial_y^\eta &\rightarrow \partial_y^{\eta'} := (\cos \alpha \cdot \partial_y^\eta - \sin \alpha \cdot \partial_y^\theta), \\ \partial_y^\theta &\rightarrow \partial_y^{\theta'} := (\cos \alpha \cdot \partial_y^\theta + \sin \alpha \cdot \partial_y^\eta), \\ \partial_z^\beta &\rightarrow \partial_z^{\beta'} := \partial_z^\beta, \\ \partial_z^\zeta &\rightarrow \partial_z^{\zeta'} := \partial_z^\zeta, \\ \partial_z^\eta &\rightarrow \partial_z^{\eta'} := (\cos \alpha \cdot \partial_z^\eta - \sin \alpha \cdot \partial_z^\theta), \\ \partial_z^\theta &\rightarrow \partial_z^{\theta'} := (\cos \alpha \cdot \partial_z^\theta + \sin \alpha \cdot \partial_z^\eta). \end{aligned}$$

Therefore, if φ_y^η is a green lower chrome function then

$$\begin{aligned} -\partial_z^{\eta'} \partial_z^{\eta'} \varphi_y^\eta &= \left(\frac{\hbar}{c} \cos \alpha \cdot f\right)^2 \cdot \varphi_y^\eta, \\ -\partial_y^{\theta'} \partial_y^{\theta'} \varphi_y^\eta &= \left(\frac{\hbar}{c} \sin \alpha \cdot f\right)^2 \cdot \varphi_y^\eta. \end{aligned}$$

If $\alpha = \pi/2$ then

$$\begin{aligned} -\partial_z^{\eta'} \partial_z^{\eta'} \varphi_y^\eta &= 0, \\ -\partial_y^{\theta'} \partial_y^{\theta'} \varphi_y^\eta &= \left(\frac{\hbar}{c} f\right)^2 \cdot \varphi_y^\eta. \end{aligned}$$

That is under such rotation the green state becomes blue state.

If $U = U_{3,1}(\alpha)$ then $G_0 \rightarrow U_{3,1}(\alpha) G_0 U_{3,1}^{-1}(\alpha)$ and $[\varphi] \rightarrow U_{3,1}(\alpha) [\varphi]$.

In this case:

$$\begin{aligned} \partial_0 &\rightarrow \partial'_0 := \partial_0, \\ \partial_1 &\rightarrow \partial'_1 := (\cos \alpha \cdot \partial_1 - \sin \alpha \cdot \partial_3), \\ \partial_2 &\rightarrow \partial'_2 := \partial_2, \\ \partial_3 &\rightarrow \partial'_3 := (\cos \alpha \cdot \partial_3 + \sin \alpha \cdot \partial_1), \\ \partial_y^\beta &\rightarrow \partial_y^{\beta'} := \partial_y^\beta, \\ \partial_y^\zeta &\rightarrow \partial_y^{\zeta'} := (\cos \alpha \cdot \partial_y^\zeta + \sin \alpha \cdot \partial_y^\theta), \\ \partial_y^\eta &\rightarrow \partial_y^{\eta'} := \partial_y^\eta, \\ \partial_y^\theta &\rightarrow \partial_y^{\theta'} := (\cos \alpha \cdot \partial_y^\theta - \sin \alpha \cdot \partial_y^\zeta), \\ \partial_z^\beta &\rightarrow \partial_z^{\beta'} := \partial_z^\beta, \\ \partial_z^\zeta &\rightarrow \partial_z^{\zeta'} := (\cos \alpha \cdot \partial_z^\zeta - \sin \alpha \cdot \partial_z^\theta), \\ \partial_z^\eta &\rightarrow \partial_z^{\eta'} := \partial_z^\eta, \\ \partial_z^\theta &\rightarrow \partial_z^{\theta'} := (\cos \alpha \cdot \partial_z^\theta + \sin \alpha \cdot \partial_z^\zeta). \end{aligned}$$

Therefore,

$$-\partial_z^{\zeta'} \partial_z^{\zeta'} \varphi_z^\zeta = -\left(f \frac{\hbar}{c} \cos \alpha\right)^2 \cdot \varphi_z^\zeta,$$

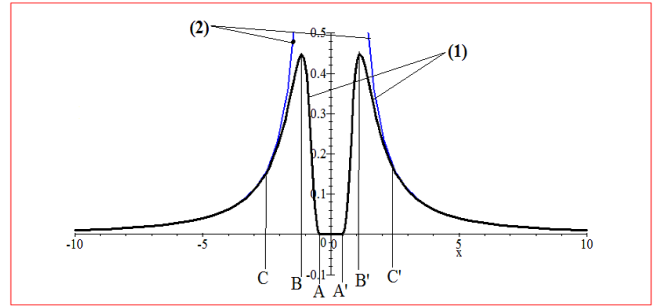


Fig. 1:

$$-\partial_z^{\theta'} \partial_z^{\theta'} \varphi_z^\zeta = -\left(\sin \alpha \cdot f \frac{\hbar}{c}\right)^2 \varphi_z^\zeta.$$

If $\alpha = \pi/2$ then

$$\begin{aligned} -\partial_z^{\theta'} \partial_z^{\theta'} \varphi_z^\zeta &= 0, \\ -\partial_z^{\theta'} \partial_z^{\theta'} \varphi_z^\zeta &= -\left(f \frac{\hbar}{c}\right)^2 \varphi_z^\zeta. \end{aligned}$$

That is under such rotation the red state becomes the blue state. Thus at the Cartesian turns chrome of a state is changed.

One of ways of elimination of this noninvariancy consists in the following. Calculations in [2, p. 156] give the grounds to assume that some oscillations of quarks states bend time-space in such a way that acceleration of the bent system in relation to initial system submits to the following law (Fig. 1):

$$g(t, \mathbf{x}) = c\lambda / (\mathbf{x}^2 \cosh^2(\lambda t / \mathbf{x}^2)).$$

Here the acceleration plot is line (1) and the line (2) is plot of λ / \mathbf{x}^2 .

Hence, to the right from point C' and to the left from point C the Newtonian gravitation law is carried out.

AA' is the Asymptotic Freedom Zone.

CB and $B'C'$ is the Confinement Zone.

Let in the potential hole AA' there are three quarks $\varphi_y^\zeta, \varphi_y^\eta, \varphi_y^\theta$. Their general state function is determinant with elements of the following type: $\varphi_y^{\zeta\eta\theta} := \varphi_y^\zeta \varphi_y^\eta \varphi_y^\theta$. In this case:

$$-\partial_y^{\zeta'} \partial_y^{\zeta'} \varphi_y^{\zeta\eta\theta} = \left(\frac{\hbar}{c} f\right)^2 \varphi_y^{\zeta\eta\theta}$$

and under rotation $U_{1,2}(\alpha)$:

$$\begin{aligned} -\partial_y^{\zeta'} \partial_y^{\zeta'} \varphi_y^{\zeta\eta\theta} &= \left(\frac{\hbar}{c} f\right)^2 (\gamma_\zeta^{[0]} \cos \alpha - \gamma_\eta^{[0]} \sin \alpha)^2 (\varphi_y^\zeta \varphi_y^\eta \varphi_y^\theta) \\ &= \left(\frac{\hbar}{c} f\right)^2 \varphi_y^{\zeta\eta\theta}. \end{aligned}$$

That is at such turns the quantity of red chrome remains.

As and for all other Cartesian turns and for all other chromes.

Baryons $\Delta^- = ddd$, $\Delta^{++} = uuu$, $\Omega^- = sss$ belong to such structures.

If $U = U_{1,0}(\alpha)$ then $G_0 \rightarrow U_{1,0}^{-1\dagger}(\alpha) G_0 U_{1,0}^{-1}(\alpha)$ and $[\varphi] \rightarrow U_{1,0}(\alpha) [\varphi]$.

In this case:

$$\partial_0 \rightarrow \partial'_0 := (\cosh \alpha \cdot \partial_0 + \sinh \alpha \cdot \partial_1),$$

$$\partial_1 \rightarrow \partial'_1 := (\cosh \alpha \cdot \partial_1 + \sinh \alpha \cdot \partial_0),$$

$$\partial_2 \rightarrow \partial'_2 := \partial_2,$$

$$\partial_3 \rightarrow \partial'_3 := \partial_3,$$

$$\partial_y^\beta \rightarrow \partial_y^{\beta'} := \partial_y^\beta,$$

$$\partial_y^\zeta \rightarrow \partial_y^{\zeta'} := \partial_y^\zeta,$$

$$\partial_y^\eta \rightarrow \partial_y^{\eta'} := (\cosh \alpha \cdot \partial_y^\eta - \sinh \alpha \cdot \partial_z^\eta),$$

$$\partial_y^\theta \rightarrow \partial_y^{\theta'} := (\cosh \alpha \cdot \partial_y^\theta + \sinh \alpha \cdot \partial_z^\theta),$$

$$\partial_z^\beta \rightarrow \partial_z^{\beta'} := \partial_z^\beta,$$

$$\partial_z^\zeta \rightarrow \partial_z^{\zeta'} := \partial_z^\zeta,$$

$$\partial_z^\eta \rightarrow \partial_z^{\eta'} := (\cosh \alpha \cdot \partial_z^\eta + \sinh \alpha \cdot \partial_y^\eta),$$

$$\partial_z^\theta \rightarrow \partial_z^{\theta'} := (\cosh \alpha \cdot \partial_z^\theta - \sinh \alpha \cdot \partial_y^\theta).$$

Therefore,

$$-\partial_y^{\eta'} \partial_y^{\eta'} \varphi_y^\eta = (1 + \sinh^2 \alpha) \cdot \left(\frac{\hbar}{c} f\right)^2 \varphi_y^\eta,$$

$$-\partial_z^{\theta'} \partial_z^{\theta'} \varphi_y^\eta = \sinh^2 \alpha \cdot \left(\frac{\hbar}{c} f\right)^2 \varphi_y^\eta.$$

Similarly chromes and grades change for other states and under other Lorentz transformation.

One of ways of elimination of this noninvariancy is the following:

Let

$$\varphi_{yz}^{\zeta\eta\theta} := \varphi_y^\zeta \varphi_y^\eta \varphi_y^\theta \varphi_z^\zeta \varphi_z^\eta \varphi_z^\theta,$$

Under transformation $U_{1,0}(\alpha)$:

$$-\partial_z^{\theta'} \partial_z^{\theta'} \varphi_{yz}^{\zeta\eta\theta} = -\left(\frac{\hbar}{c} f\right)^2 \varphi_{yz}^{\zeta\eta\theta}.$$

That is a magnitude of red chrome of this state doesn't depend on angle α .

This condition is satisfied for all chromes and under all Lorentz's transformations.

Pairs of baryons

$$\begin{aligned} \{p = uud, n = ddu\}, \\ \{\Sigma^+ = uus, \Xi^0 = uss\}, \\ \{\Delta^+ = uud, \Delta^0 = udd\} \end{aligned}$$

belong to such structures.

Conclusion

Baryons represent one of ways of elimination of the chrome noninvariancy under Cartesian and under Lorentz transformation.

Submitted on April 4, 2014 / Accepted on April 9, 2014

References

1. Amsler C. et al. (Particle Data Group). Review of particle physics — quark model. *Physics Letters B*, 2008, v. 667, 1.
2. Quznetsov G. Final Book on Fundamental Theoretical Physics. American Research Press, Rehoboth (NM), 2011.

CKM and PMNS Mixing Matrices from Discrete Subgroups of SU(2)

Franklin Potter

Sciencegems.com, 8642 Marvale Drive, Huntington Beach, CA 92646 USA E-mail: frank11hb@yahoo.com

One of the greatest challenges in particle physics is to determine the first principles origin of the quark and lepton mixing matrices CKM and PMNS that relate the flavor states to the mass states. This first principles derivation of both the PMNS and CKM matrices utilizes quaternion generators of the three discrete (i.e., finite) binary rotational subgroups of SU(2) called [3,3,2], [4,3,2], and [5,3,2] for three lepton families in \mathbb{R}^3 and four related discrete binary rotational subgroups [3,3,3], [4,3,3], [3,4,3], and [5,3,3] represented by four quark families in \mathbb{R}^4 . The traditional 3×3 CKM matrix is extracted as a submatrix of the 4×4 CKM4 matrix. The predicted fourth family of quarks has not been discovered yet. If these two additional quarks exist, there is the possibility that the Standard Model lagrangian may apply all the way down to the Planck scale.

1 Introduction

The very successful Standard Model (SM) local gauge group $SU(2)_L \times U(1)_Y \times SU(3)_C$ defines an electroweak (EW) interaction part and a color interaction part. Experiments have determined that the left-handed EW isospin flavor states are linear superpositions of mass eigenstates. One of the greatest challenges in particle physics is to determine the first principles origin of the quark and lepton mixing matrices CKM and PMNS that relate the flavor states to the mass states.

In a recent article [1] I derived the lepton PMNS mixing matrix by using the quaternion (i.e., spinor) generators of three specific discrete (i.e., finite) binary rotational subgroups of the EW gauge group $SU(2)_L \times U(1)_Y$, one group for each lepton family, while remaining within the realm of the SM lagrangian. All the derived PMNS matrix element values are within the 1σ range of the empirically determined absolute values.

The three lepton family groups, binary rotational groups called [3,3,2], [4,3,2], and [5,3,2], (or 2T, 2O, and 2I), have discrete rotational symmetries in \mathbb{R}^3 . Each group has two degenerate basis states which must be taken in linear superposition to form the two orthogonal fermion flavor states in each family, i.e., (ν_e, e) , (ν_μ, μ) , and (ν_τ, τ) .

In order to have a consistent geometrical approach toward understanding the SM, I have proposed in a series of articles [2–4] over several years that the quark flavor states represent discrete binary rotational groups also. However, one must move up one spatial dimension from \mathbb{R}^3 to \mathbb{R}^4 and use the related four discrete binary rotational subgroups [3,3,3], [4,3,3], [3,4,3], and [5,3,3], (or 5-cell, 16-cell, 24-cell, and 600-cell), for the quarks, thereby dictating four quark families. Recall that both \mathbb{R}^3 and \mathbb{R}^4 are subspaces of the unitary space \mathbb{C}^2 .

Therefore, following up the success I had deriving the neutrino PMNS matrix, the CKM mixing matrix should be derivable by using the same geometrical method, i.e., based upon the quaternion generators of the four groups of specific discrete rotational symmetries. In this quark case, however,

first one determines a 4×4 mixing matrix called CKM4 and then extracts the appropriate 3×3 submatrix as the traditional CKM matrix.

These seven closely-related groups representing specific discrete rotational symmetries dictate the three known lepton families in \mathbb{R}^3 and four related quark families in \mathbb{R}^4 , the fourth quark family still to be discovered. That is, neither leptons nor quarks are to be considered as point objects at the fundamental Planck scale of about 10^{-35} meters. If this geometrical derivation of both the PMNS and CKM mixing matrices is based upon the correct reason for the mixing of flavor states to make the mass states, then one must reconcile the empirical data with the prediction of a fourth quark family.

My proposal that leptons are 3-D entities and that quarks are 4-D entities has several advantages. There is a clear distinction between leptons and quarks determined by inherent geometrical properties such as explaining that leptons do not experience the color interaction via $SU(3)_C$ because gluons and quarks would involve 4-D rotations associated with the three color charges defined in \mathbb{R}^4 . Also, one now has a geometrical reason for there being more than one family of leptons and of quarks. In addition, the mass ratios of the fundamental fermions are determined by the group relationships to the j-invariant of the Monster Group. These physical properties and many other physical consequences are discussed in my previous papers.

2 Review of the PMNS matrix derivation

This section reviews the mathematical procedure used in my 2013 derivation [1] of the PMNS matrix from first principles. One constructs the three SU(2) generators, the $U_1 = j$, $U_2 = k$, and the $U_3 = i$, (i.e., the Pauli matrices in quaternion form), from the three quaternion generators from each of the discrete subgroups [3,3,2], [4,3,2], and [5,3,2]. As you know, the three Pauli matrices, i.e., the quaternions i , j , and k , can generate all rotations in \mathbb{R}^3 about a chosen axis or, equivalently, all rotations in the plane perpendicular to this axis. For example,

Table 1: Lepton Family Quaternion Generators U_2

| Fam. | Grp. | Generator | Factor | Angle $^\circ$ |
|------------------|------|--|---------|----------------|
| ν_e, e | 332 | $-\frac{1}{2}i - \frac{1}{2}j + \frac{1}{\sqrt{2}}k$ | -0.2645 | 105.337 |
| ν_μ, μ | 432 | $-\frac{1}{2}i - \frac{1}{\sqrt{2}}k + \frac{1}{2}j$ | 0.8012 | 36.755 |
| ν_τ, τ | 532 | $-\frac{1}{2}i - \frac{\phi}{2}j + \frac{\phi^{-1}}{2}k$ | -0.5367 | 122.459 |

the quaternion k is a binary rotation by 180° in the i - j plane.

The complete mathematical description [5] for the generators operating on the unit vector x in R^3 extending from the origin to the surface of the unit sphere S^2 is given by $R_s = i x U_s$ where $s = 1, 2, 3$ and

$$U_1 = j, \quad U_2 = -i \cos \frac{\pi}{q} - j \cos \frac{\pi}{p} + k \sin \frac{\pi}{h}, \quad U_3 = i, \quad (1)$$

with $h = 4, 6, 10$ for the three lepton flavor groups $[p, q, 2]$, respectively. Their U_2 generators are listed in Table 1.

My three lepton family binary rotational groups, $[3, 3, 2]$, $[4, 3, 2]$, and $[5, 3, 2]$, all have generators $U_1 = j$ and $U_3 = i$, but each U_2 is a different quaternion generator operating in R^3 . One obtains the correct neutrino PMNS mixing angles from the linear superposition of their U_2 's by making the total $U_2 = k$, agreeing with $SU(2)$. This particular combination of three discrete angle rotations is now equivalent to a rotation in the i - j plane by the quaternion k .

The sum of all three U_2 generators should be k , so there are three equations for the three unknown factors, which are determined to be: -5.537, 16.773, and -11.236. Let the quantity $\phi = (\sqrt{5}+1)/2$, the golden ratio. The resulting angles in Table 1 are the arccosines of these factors (normalized), i.e., their projections to the k -axis, but they are twice the rotation angles required in R^3 , a property of quaternion rotations.

Using one-half of these angles produces

$$\theta_1 = 52.67^\circ, \quad \theta_2 = 18.38^\circ, \quad \theta_3 = 61.23^\circ, \quad (2)$$

resulting in mixing angles

$$\theta_{12} = 34.29^\circ, \quad \theta_{13} = -8.56^\circ, \quad \theta_{23} = -42.85^\circ. \quad (3)$$

The absolute values of these mixing angles are all within the 1σ range of their values for the normal mass hierarchy [6–11] as determined from several experiments:

$$\theta_{12} = \pm 34.47^\circ, \quad \theta_{13} = \pm 8.73^\circ, \quad \theta_{23} = \pm (38.39^\circ - 45.81^\circ). \quad (4)$$

The experimental 1σ uncertainty in θ_{12} is about 6%, in θ_{13} about 14%, and θ_{23} has the range given. The \pm signs arise from the squares of the sines of the angles determined by the experiments.

For three lepton families, one has the neutrino flavor states ν_e, ν_μ, ν_τ , and the mass states ν_1, ν_2, ν_3 , related by the PMNS

matrix V_{ij}

$$\begin{bmatrix} \nu_e \\ \nu_\mu \\ \nu_\tau \end{bmatrix} = \begin{bmatrix} V_{e1} & V_{e2} & V_{e3} \\ V_{\mu1} & V_{\mu2} & V_{\mu3} \\ V_{\tau1} & V_{\tau2} & V_{\tau3} \end{bmatrix} \begin{bmatrix} \nu_1 \\ \nu_2 \\ \nu_3 \end{bmatrix}.$$

The PMNS entries are the products of the sines and cosines of the derived angles (3) using the standard parametrization of the matrix, producing:

$$\begin{bmatrix} 0.817 & 0.557 & -0.149e^{-i\delta} \\ -0.413 - 0.084e^{i\delta} & 0.605 - 0.057e^{i\delta} & -0.673 \\ -0.383 + 0.090e^{i\delta} & 0.562 + 0.061e^{i\delta} & 0.725 \end{bmatrix}.$$

For direct comparison, the empirically estimated PMNS matrix for the *normal hierarchy* of neutrino masses is

$$\begin{bmatrix} 0.822 & 0.547 & -0.150 + 0.038i \\ -0.356 + 0.0198i & 0.704 + 0.0131i & 0.614 \\ 0.442 + 0.0248i & -0.452 + 0.0166i & 0.774 \end{bmatrix}$$

Comparing the V_{e3} elements from each, the phase angle δ is confined to be $0^\circ \leq \delta \leq \pm 14.8^\circ$, an angle in agreement with the T2K collaboration value of $\delta \approx 0$ but quite different from other proposed $\delta \approx \pi$ values.

3 The CKM4 matrix derivation

The success of the above geometrical procedure for deriving the lepton PMNS matrix by using the quaternion generators from the 3 discrete binary rotation groups demands that the same approach should work for the quark families in R^4 using the 4 discrete binary rotation groups $[3, 3, 3]$, $[4, 3, 3]$, $[3, 4, 3]$, and $[5, 3, 3]$. If this procedure succeeds in deriving the CKM matrix elements as a 3×3 submatrix of CKM4, then a fourth sequential quark family, call its quark states b' and t' , exists in Nature.

These 4 binary rotational groups for the quark family flavors each have rotation subgroups of $SO(4) = SO(3) \times SO(3)$, and they also have the double covering $SU(2) \times SU(2)$. The $SO(4)$ is the rotation group of the unit hypersphere S^3 in R^4 , with every 4-D rotation being simultaneous rotations in two orthogonal planes.

The only finite (i.e., discrete) quaternion groups are [12]

$$2I, \quad 2O, \quad 2T, \quad 2D_{2n}, \quad 2C_n, \quad 1C_n \quad (n \text{ odd}) \quad (5)$$

with the 2 in front meaning binary (double) group, the double cover of the normal 3-D rotation group by $SU(2)$ over $SO(3)$. Mathematically, the 4 discrete binary groups for the quark families each can be identified as $(L/L_K; R/R_K)$ with the homomorphism $L/L_K = R/R_K$. Here L and R are specific discrete groups of quaternions and L_K and R_K are their kernels.

P. DuVal [13] established that one only needs the cyclic groups $2C_n$ and $1C_n$ when considering the four discrete rotational symmetry groups, i.e., the ones I am using for the

quark families. Essentially, vertices on the 4-D regular polytope can be projected to be a regular polygon on each of the two orthogonal planes in R^4 .

There will be 6 quaternion generators for each of the 4 groups, producing simultaneous rotations in two orthogonal planes. The two sets of Pauli matrices for producing continuous rotations can be identified as i, j, k, and another i, j, k, but they act on the two different S^2 spheres, i.e, in the two orthogonal planes. One can consider this 4-D rotational transformation as the result of a bi-quaternion operation [14], or equivalently, a bi-spinor or Ivanenko-Landau-Kähler spinor or Dirac-Kähler spinor operation.

For three quark families, one has the “down” flavor states d' , s' , b' , and their mass states d , s , b , related by the CKM matrix. This quark mixing matrix for the left-handed components is defined in the standard way as

$$V = U_L D_L^\dagger, \tag{6}$$

but for four quark families the mathematics is a little different, for one must consider the bi-quaternion case in which there will be Bogoliubov mixing [14], producing two subfactors for each component, i.e.,

$$U_L = W_{14,23}^u W_{12,34}^u, \quad D_L = W_{14,23}^d W_{12,34}^d \tag{7}$$

with the W^u and W^d factor on the right mixing the 1st and 2nd generations and, separately, mixing the 3rd and 4th generations. The Bogoliubov mixing in the factor on the left mixes the 1st and 4th generations and, separately, the 2nd and 3rd generations. Therefore, the CKM4 matrix derives from

$$V_{CKM4} = U_L D_L^\dagger = W_{14,23}^u W_{12,34}^u (W_{14,23}^d W_{12,34}^d)^\dagger. \tag{8}$$

The product $W_{12,34}^u W_{12,34}^{d\dagger}$ is given by

$$W_{12,34}^u W_{12,34}^{d\dagger} = \begin{bmatrix} x_1 & y_1 & 0 & 0 \\ z_1 & w_1 & 0 & 0 \\ 0 & 0 & x_2 & y_2 \\ 0 & 0 & z_2 & w_2 \end{bmatrix}.$$

The upper left block is an SU(2) matrix that mixes generations 1 and 2 while the lower right block is an SU(2) matrix that mixes generations 3 and 4. Each 2x2 block relates the rotation angles and the phases via

$$\begin{bmatrix} x & y \\ z & w \end{bmatrix} = \begin{bmatrix} \cos\theta e^{i\alpha} & -\sin\theta e^{i\beta} \\ \sin\theta e^{i\gamma} & \cos\theta e^{i\delta} \end{bmatrix}.$$

The 4x4 matrix that achieves the Bogoliubov mixing has four possible forms for the four possible isospin cases obeying $SU(2) \times SU(2)$: (0, 0), (1/2, 0), (0, 1/2), and (1/2, 1/2). The (1/2, 1/2) is the one for equal, simultaneous, isospin 1/2 rotations in the two orthogonal planes for CKM4:

$$W_{14,23}^{u,d} = \frac{1}{\sqrt{2}} \begin{bmatrix} 1 & 0 & -1 & 0 \\ 0 & 1 & 0 & -1 \\ 1 & 0 & 1 & 0 \\ 0 & 1 & 0 & 1 \end{bmatrix}.$$

Table 2: Quark Family Discrete Group Assignments for U_2

| Fam. | Grp. | Generator | Angle° | Factor | Angle° |
|-------|------|-------------------|--------|--------|--------|
| u,d | 333 | $\exp[2\pi i/5]$ | 72 | 1.132 | 81.504 |
| c,s | 433 | $\exp[2\pi i/8]$ | 45 | 1.132 | 50.940 |
| t,b | 343 | $\exp[2\pi i/12]$ | 30 | 1.132 | 33.960 |
| t',b' | 533 | $\exp[2\pi i/30]$ | 12 | 1.132 | 13.584 |

Multiplying out these three 4x4 bi-quaternion mixing matrices, one determines that

$$V_{CKM4} = \frac{1}{2} \begin{bmatrix} x_1 + x_2 & y_1 + y_2 & x_1 - x_2 & y_1 - y_2 \\ z_1 + z_2 & w_1 + w_2 & z_1 - z_2 & w_1 - w_2 \\ x_1 - x_2 & y_1 - y_2 & x_1 + x_2 & y_1 + y_2 \\ z_1 - z_2 & w_1 - w_2 & z_1 + z_2 & w_1 + w_2 \end{bmatrix}$$

in which the phases $\alpha, \beta, \gamma, \delta$ have been ignored.

One determines the angles θ_1 and θ_2 from the quaternion generators of the 4 discrete binary rotation groups for the quark families. Projections of each of the four discrete symmetry 4-D entities onto the two orthogonal planes produces a regular polygon [5, 13] with the generator $i \exp[2\pi j/h]$, as given in Table 2, where the h values are 5, 8, 12, 30, for the [3,3,3], [4,3,3], [3,4,3], and [5,3,3], respectively.

Again, we need to determine the contribution from each group generator that will make the sum add to 180° , i.e., make their collective action produce the rotation $U_2 = k$. Expanding out the exponentials in terms of sines and cosines reveals four unknowns but only two equations. Alternately, because the four rotation angles sum to only 159° , we can use the same factor for each group, i.e., the ratio $180^\circ/159^\circ = 1.132$.

In the last column of Table 2 are the normalized angles which are twice the angle required. Therefore, taking the appropriate half-angle differences produces the mixing angles

$$\theta_1 = 15.282^\circ, \quad \theta_2 = 10.188^\circ. \tag{9}$$

Substituting the cosines and sines of these two derived angles into the CKM4 matrix form above produces a mixing matrix symmetrical about the diagonal. Remember that I have ignored up to eight possible phases in the 2x2 blocks.

$$V_{CKM4} = \begin{bmatrix} 0.9744 & 0.2203 & 0.0098 & 0.0433 \\ 0.2203 & 0.9744 & 0.0433 & 0.0098 \\ 0.0098 & 0.0433 & 0.9744 & 0.2203 \\ 0.0433 & 0.0098 & 0.2203 & 0.9744 \end{bmatrix}.$$

One can compare the upper left 3x3 submatrix to the most recent *estimated absolute values* [7]

$$V_{CKM} = \begin{bmatrix} 0.9745 & 0.2246 & 0.0036 \\ 0.2244 & 0.9736 & 0.0415 \\ 0.0088 & 0.0407 & 0.9991 \end{bmatrix}.$$

Note that most of these estimated V_{CKM} values are probably good to within a few percent but some could have uncertainties as large as 10% or more.

Of concern are my low values of 0.2203 for V_{us} and V_{cd} . However, according to the Particle Data Group (2013) there are two possible values [7]: 0.2253 and 0.2204, the latter from tau decays. Also, my derived symmetric CKM4 matrix V_{ub} value is high while the V_{td} value is reasonable, i.e., V_{td} at 0.0098 compares well with the estimated value of 0.0088.

The V_{tb} element of CKM4 is 0.9744, quite a bit smaller than the suggested 0.9991 V_{tb} value for the 3×3 CKM matrix. However, if one imposes the unitarity condition on the rows and columns of the extracted CKM, the new value for this V_{tb} matrix element would be 0.999, in agreement.

My final comment is that if one calculates CKM using only the first three quark groups [3,3,3], [4,3,3], and [3,4,3], the resulting 3×3 CKM matrix will disagree significantly with the known CKM matrix. Therefore, one cannot eliminate a fourth quark family when discrete rotational subgroups of $SU(2)$ are considered.

4 Discussion

In the SM the EW symmetry group is the Lie group $SU(2)_L \times U(1)_Y$. This local gauge group operating on the lepton and quark states works extremely well, meaning that all its predictions agree with experiments so far. However, in this context there is no reason for Nature to have more than one fermion family, and certainly no reason for having 3 lepton families and at least 3 quark families. As far as I know, the normal interpretation of the SM provides no answer that dictates the actual number of families, although the upper limit of 3 lepton families with low mass neutrinos is well established via Z^0 decays and via analysis of the CMB background.

My geometrical approach with *discrete* symmetries alters the default reliance upon $SU(2)$ and its continuous symmetry transformations, for I utilize discrete binary rotational subgroups of $SU(2)$ for the fundamental fermion states, a different subgroup for each lepton family and for each quark family. In this scenario one can surmise that the enormous success of the SM occurs because $SU(2)_L \times U(1)_Y$ is acting like a mathematical “cover group” for the actual underlying discrete rotations operating on the lepton states and quark states.

Assuming that the above matrix derivations are correct, the important question is: Where is the b' quark of the predicted 4th quark family? In 1992 I predicted a top quark mass of about 160 GeV, a b' quark mass of 65–80 GeV, and a t' quark at a whopping 2600 GeV. These mass predictions were based upon the mass ratios being determined by the j-invariant function of elliptic modular functions and of fractional linear transformations, i.e., Möbius transformations. Note that all seven discrete groups I have for the fermions are related to the j-invariant and Möbius transformations, which have direct connections to numerous areas of fundamental

mathematics.

With a predicted b' mass that is much smaller than the top quark mass of 173.3 GeV and even smaller than the W mass at 80.4 GeV, one would have expected some production of the b' at LEP, Fermilab, and the LHC. Yet, no clear indication of the b' quark has appeared.

Perhaps the b' quark has escaped detection at the LHC and lies hidden in the stored data from the runs at 7 TeV and 8 TeV. With a mass value below the W and Z masses, the b' quark must decay via flavor changing neutral current (FCNC) decay channels [16] such as $b' \rightarrow b + \gamma$ and $b' \rightarrow b + \text{gluon}$. The b' could have an average lifetime too long for the colliders to have detected a reasonable number of its decays within the detector volumes and/or the energy and angle cuts. However, the b' quark and t' quark would affect certain other decays that depend upon the heaviest “top” quark in a box diagram or penguin diagram.

Another possibility is that a long lifetime might allow the formation of the quarkonium bound state b' -anti- b' , which has its own specific decay modes, to $b\bar{b}$, gg , $\gamma\gamma$, and $WW^* \rightarrow \nu\nu\ell\ell$. Depending upon the actual quarkonium bound state, the spin and parity $J^{PC} = 0^{++}$ or 0^{-+} .

And finally, there is an important theoretical problem associated with the mismatch of three lepton families to four quark families, e.g., the famous triangle anomalies do not cancel in the normal manner. Perhaps my fundamental leptons and quarks, being extended particles into 3 and 4 dimensions, respectively, can avoid this problem which occurs for point particles. Someone would need to work on this possibility.

5 The bigger picture!

We know that the SM is an excellent approximation for understanding the behavior of leptons, quarks, and the interaction bosons in the lower energy region when the spatial resolution is less than 10^{-24} meters. At smaller distance scales, perhaps one needs to consider a discrete space-time, for which the discrete binary rotation groups that I have suggested for the fundamental particles would be appropriate. Quite possibly, with this slight change in emphasis to discrete subgroups of the local gauge group, the SM lagrangian will hold true all the way down to the Planck scale.

If indeed the SM applies at the Planck scale, then one can show [2] that the Monster group dictates all of physics! The surprising consequence: The Universe *is* mathematics and is *unique*. Indeed, we humans are mathematics!

This connection to the Monster Group is present already in determining the lepton and quark mass ratios, which are proportional to the j-invariant of elliptic modular functions, the same j-invariant that is the partition function for the Monster Group in a quantum field theory [17].

The mathematics of these discrete groups does even more for us, for there is a direct connection [2] from the lepton

groups [3,3,2], [4,3,2], [5,3,2], and the quark groups [3,3,3], [4,3,3], [3,4,3], [5,3,3], in R^3 and R^4 , respectively, via special quaternions called icosians to the discrete space R^8 . One then brings in another R^8 for relativistic space-time transformations. The two spaces combine into a 10-D discrete space-time obeying the discrete symmetry transformations of “Weyl” $SO(9,1) = \text{Weyl } E_8 \times \text{Weyl } E_8$. This proposed *unique* connection to “Weyl” $SO(9,1)$ was a surprise to me because one has two 8-D spaces combining to make a 10-D space-time! Its direct and unique relationship to the SM certainly is a welcome replacement to the 10^{500} ways for M-theory.

Finally, among the advantages to having a fourth family of quarks is a possible explanation of the baryon asymmetry of the Universe (BAU). From the CKM and the PMNS matrices, one learns that the predicted CP violation (CPV) is at least 10 orders of magnitude too small to explain the BAU. That is, the important quantity called the Jarlskog value is much too small. But a 4th quark family resolves this issue [18] because substituting the fourth quark family mass values into the Jarlskog expression increases the CPV value by more than 10^{13} ! Voilà. One now has penguin diagrams distinguishing the particle and antiparticle decays with sufficient difference to have the particle Universe we experience.

6 Conclusion

The quark mixing matrix CKM4 has been derived using four quark families. Using quaternion generators from four specific related discrete binary rotational groups [3,3,3], [4,3,3], [3,4,3], and [5,3,3], I have derived the quark CKM4 and its CKM submatrix. However, neither quark of the 4th quark family has been detected at the colliders. Their appearance could mean that the Standard Model lagrangian might be a good approximation to the ultimate lagrangian all the way down to the Planck scale if space-time is discrete.

Acknowledgements

The author wishes to thank Sciencegems.com for financial support and encouragement.

Submitted on April 2, 2014 / Accepted on April 10, 2014

References

- Potter, F. Geometrical Derivation of the Lepton PMNS Matrix Values. *Progress in Physics*, 2013, v. 9 (3), 29–30.
- Potter, F. Our Mathematical Universe: I. How the Monster Group Dictates All of Physics. *Progress in Physics*, 2011, v. 7 (4), 47–54.
- Potter, F. Unification of Interactions in Discrete Spacetime. *Progress in Physics*, 2006, v. 2 (1), 3–9.
- Potter, F. Geometrical Basis for the Standard Model. *International Journal of Theoretical Physics*, 1994, v. 33, 279–305.
- Coxeter, H. S. M. Regular Complex Polytopes. Cambridge University Press, Cambridge, 1974.
- An, F.P. *et al.* (Daya Bay Collaboration). Spectral Measurement of Electron Antineutrino Oscillation Amplitude and Frequency at Daya Bay. *Physical Review Letters*, 2014, v. 112, 061801. arXiv:1310.6732.
- Beringer, J. *et al.* (Particle Data Group). The Review of Particle Physics: V_{ud} , V_{us} , the Cabbibo Angle, and CKM Unitarity. *Physical Review*, 2012 and 2013 partial update, v. D86, 010001, 6–7.
- Capozzi, F., Fogli, G. J., *et al.* Status of three-neutrino oscillation parameters, circa 2013. arXiv:1312.2878v1.
- Fogli, G. I. Global analysis of neutrino masses, mixings and phases: Entering the era of leptonic CP violation searches. *Physical Review*, 2012, v. D86, 013012. arXiv:1205.5254v3.
- Forero, D. V., Tortola, M., Valle, J. W. F. Global status of neutrino oscillation parameters after Neutrino–2012. *Physical Review*, 2012, v. D86, 073012. arXiv:1205.4018.
- T2K Collaboration, Abe, K. *et al.* Indication of Electron Neutrino Appearance from an Accelerator-produced Off-axis Muon Neutrino Beam. *Physical Review Letters*, 2011, v. 107, 041801. arXiv:1106.2822.
- Conway, J. H., Smith, D. A. On Quaternions and Octonions: Their Geometry, Arithmetic, and Symmetry. A.K. Peters, Wellesley, Massachusetts, 2003.
- Du Val, P. Homographies, Quaternions, and Rotations. Oxford University Press, Oxford, 1964.
- Jourjine, A. Scalar Spin of Elementary Fermions. *Physics Letters*, 2014, v. B728, 347–357. arXiv:1307.2694.
- Beringer, J. *et al.* (Particle Data Group). The Review of Particle Physics: Neutrino Mass, Mixing and Oscillations. *Physical Review*, 2012 and 2013 partial update, v. D86, 010001, 46–48.
- Arhrib, A., Hou, W.S. CP Violation in Fourth Generation Quark Decays. *Physical Review*, 2009, v. D80, 076005. arXiv:0908.0901v1.
- Witten, E. Three-Dimensional Gravity Reconsidered. arXiv:0706.3359.
- Hou, W. S. Source of CP Violation for the Baryon Asymmetry of the Universe. *International Journal of Modern Physics*, 2011, v. D20, 1521–1532. arXiv:1101.2161v1.

Superluminal Velocities in the Synchronized Space-Time

Sergey Yu. Medvedev

Department of Physics, Uzhgorod National University

54, Voloshyna str., Uzhgorod 88000, Ukraine. E-mail: medvefiz@gmail.com

Within the framework of the non-gravitational generalization of the special relativity, a problem of possible superluminal motion of particles and signals is considered. It has been proven that for the particles with non-zero mass the existence of anisotropic light barrier with the shape dependent on the reference frame velocity results from the Tangherlini transformations. The maximal possible excess of neutrino velocity over the absolute velocity of light related to the Earth (using the clock with instantaneous synchronization) has been estimated. The illusoriness of the acausality problem has been illustrated and conclusion is made on the lack of the upper limit of velocities of signals of informational nature.

1 Introduction

In the special relativity (SR) the velocity of establishing connection between two events “1” and “2” (particle motion, information transfer, quantum teleportation and so on) could not exceed the velocity of light c in vacuum. The attempts to overcome such a prohibition encounter the problem of causality principle violation, namely, if in the initial inertial reference frame (IRF) K a signal moves with the superluminal velocity $u > c$, then exists such IRF K' that moves with the velocity $v < c$, but $\mathbf{v} \cdot \mathbf{u} > c^2$, in which the event-effect “2” anticipates the event-cause “1”, $t'_2 < t'_1$ (while in the K IRF $-t_2 > t_1$). In some papers (see, e.g. [1]) the extreme paradoxicalness of this problem, namely, the appearance of the acausal loops, when the cyclic process terminates at the point of its beginning, but before its beginning, is discussed. The absurdity of acausality leads one to the conclusion about the existence of the isotropic light barrier, i.e. in the space of the possible velocities of particles and signals that realize the cause-and-effect relationship the velocity vectors lie inside the sphere of the radius c . In other words, the 4-interval between the cause-and-effect events could be the time-like one only. The event-effect must be inside the light cone of the future event-cause. All the mentioned above follows from the Lorentz transformations (LT).

Below, however, we will show that the causality principle violation is illusory, and the assumption about the possibility of the appearance of the acausal loop is wrong. This problem is discussed in detail in Sect. 6, while here we will indicate only the important fact noted by Leonid I. Mandelstam in his SR-related lectures [2]: the time involved in LT is measured by the clock synchronized by the light signals with *a priori* assumption about the light velocity invariance. The consequence of such synchronization (in fact, the consequence of the light velocity invariance postulate) is the relativity of simultaneity: the spatially split events, simultaneous in one IRF, are not simultaneous in the other one, i.e. $t'_2 \neq t'_1$ at $t_2 = t_1$. Mandelstam in the same lectures explained also that in case of using the clock with instantaneous synchronization at

the spatially split points the simultaneity of events will be absolute. Hence the irrefutable logical conclusion follows about the non-invariance of the velocity of light measured using the clock with instantaneous synchronization (because from the light velocity invariance the simultaneity relativity follows). The principal possibility of such synchronization was proven in the works by Vitaliy L. Ginzburg and his followers (see, e.g. [3]). Namely, the clock at the points “1” and “2” could be synchronized by means of a photo relays switched on by the light spot that moves from “1” to “2” with the velocity $V = \omega R$ at the light source rotation with the angular velocity ω (the light source being located at the distance R). Since the product ωR could be, in principle, unrestrictedly large, $\omega R \gg c$, then $V \gg c$ as well, i.e. such synchronization can be considered almost instantaneous. For instance, the above light spot produced by the emission of the *NP.0532* pulsar in the Crab nebula moves the Earth surface with the velocity $V = 1.2 \times 10^{22}$ m/s ($\omega = 200$ rad/s, $R = 6 \times 10^{19}$ m). Another way of almost instantaneous synchronization was realized in Marinov's experiments [4, 5] on measuring the velocity of the Earth with respect to the ether (see below Sect. 3).

Note that in the classical physics the clock at the spatially split points is considered synchronized just by the instantaneous signals. As shown below, to explain the lack of interference in the Michelson-Morley (MM) experiment [6] there was no necessity to change the above synchronization and, thus, discard such a fundamental property of time as the absolute simultaneity of the spatially split events. The theoretical model of relativistic processes for the case of instantaneously synchronized clock was developed, mainly, in the Frank R. Tangherlini's Ph.D thesis [7, 8] (see also [9]). In this model, the existence of a dedicated absolute inertial reference system (AIRF), in which the velocity of light is isotropic, is postulated. It seems most naturally to represent this reference system as resting with respect to the ether. Note that the lack of the ether does not follow from the MM experiment, this experiment failed only to find its presence for the reason explained in Sect. 2. The second postulate of this theory is the

invariance of the average velocity of light at the motion along the closed contour, just this property of the light velocity follows with the necessity from the MM experiment and all the following interference experiments, in which the light either passed twice the same distance or moved around a closed loop (see, e.g. [10, 11]). The following space-time transformations (i.e. the Tangherlini transformations, TT) [7, 8] are obtained from the above postulates:

$$x' = \gamma(x - vt), \quad y' = y, \quad z' = z; \quad (1)$$

$$t' = \frac{t}{\gamma}, \quad \gamma = \left(1 - \frac{v^2}{c^2}\right)^{-1/2}. \quad (2)$$

Here (x, y, z, t) are the coordinates and time of the point event in AIRF K , whereas (x', y', z', t') are those in the IRF K' that moves with the velocity v along the X -axis in AIRF K .

A detailed discussion of the above transformations as well as the new ways of their deriving could be found in [12–19]. Relation (2) demonstrates the absolute simultaneity: from the condition $\Delta t = 0$ follows that $\Delta t' = 0$ as well. Therefore, one may, similarly to [18, 19], call TT the “synchronized transformations”.

One may call the TT-based theory the “non-gravitational SR generalization” (see Sect. 7 below).

As shown in the pioneer work [7, 8], the main experimentally verified LT and TT consequences coincide (since they do not depend on the way of synchronizing the clock). In particular, both TT and LT equally successfully explain the MM experiment [6] and all the following interference experiments. The same results are obtained by calculating the momentum-energy characteristics as well (see below equations (29) and (30)).

Only the values of velocities (and other physical values determined by the time derivative) differ. In Sect. 2, the transformation properties of the velocity characteristics in the Tangherlini theory (TTh) are described and the “coefficient of recalculation” of these characteristics from TTh to SR and *vice versa* is obtained. These results are used in Sect. 3 to obtain the theoretical estimates of the possibility of the excess of the neutrino velocity u' (with respect to the Earth) over the absolute velocity of light c , i.e. the velocity of light with respect to AIRF. It is proved in Sect. 4 that the particle having a non-zero rest mass cannot go before the light when moving in the same direction in any IRF. Its velocity u' may only exceed the absolute velocity of light c , i.e. the situation may occur when $c < u'(\theta') < c'(\theta')$, where c' is the velocity of light with respect to IRF K' . Thus, in TTh the light barrier (isotropic in SR) appears to be anisotropically deformed, and the degree of such deformation depends on the velocity v of IRF K' . The light cone undergoes the similar deformation (see Sect. 4). It is explained in Sect. 5 why the mass of the particle moving with the velocity exceeding the absolute velocity of light c remains real (unlike the tachyon mass in SR). Section 6 is dedicated to the discussion of the properties of time in

TTh and SR. The illusoriness of the problem of violation of the causality principle in SR and, hence, that of prohibition of motion with superluminal velocity have been found. The final remarks and conclusions are presented in Sect. 7.

2 Transformational properties of the velocity characteristics in the Tangherlini theory

Let $\mathbf{u} = (u_x; u_y; u_z)$ be the vector of the velocity of the particle with respect to AIRF K . Let us determine the value and direction of the velocity \mathbf{u}' in IRF K' that moves with the velocity v along the X -axis in AIRF K . From TT (1), (2) we obtain [7, 8]:

$$u'_x = \gamma^2(u_x - v), \quad u'_y = \gamma u_y, \quad u'_z = \gamma u_z. \quad (3)$$

Hence, the below expressions for the velocity $u' \equiv |\mathbf{u}'|$ and angle $\theta' = (\mathbf{u}', \mathbf{v})$ follow from here:

$$u'(\mathbf{u}, \mathbf{v}) = \frac{\sqrt{(\mathbf{u} - \mathbf{v})^2 - \left(\frac{\mathbf{u} \times \mathbf{v}}{c}\right)^2}}{1 - \frac{v^2}{c^2}}, \quad (4)$$

$$\cos \theta' = \frac{\cos \theta - \frac{v}{u}}{\sqrt{\left(\cos \theta - \frac{v}{u}\right)^2 + \left(1 - \frac{v^2}{c^2}\right) \sin^2 \theta}}. \quad (5)$$

If we use LT to calculate the velocity projections in IRF K' , we obtain:

$$\tilde{u}'_x = \frac{u - v}{1 - \frac{uv \cos \theta}{c^2}}, \quad \tilde{u}'_y = \frac{u_y}{\gamma \left(1 - \frac{uv \cos \theta}{c^2}\right)}, \quad \tilde{u}'_z = \frac{u_z}{\gamma \left(1 - \frac{uv \cos \theta}{c^2}\right)}. \quad (6)$$

Here and below “ \sim ” denotes characteristics calculated from LT.

As seen, each of projections of the vector \mathbf{u}' is obtained by multiplying the relevant projection of the vector $\tilde{\mathbf{u}}'$ onto the same “coefficient of recalculation”

$$\chi = \frac{1 - \frac{v \cdot \mathbf{u}}{c^2}}{1 - \frac{v^2}{c^2}}; \quad (7)$$

$$u'_x = \tilde{u}'_x \chi, \quad u'_y = \tilde{u}'_y \chi, \quad u'_z = \tilde{u}'_z \chi. \quad (8)$$

Hence, two conclusions result here:

1. The directions of the vectors \mathbf{u}' and $\tilde{\mathbf{u}}'$ coincide.
2. The value of the velocity in TTh is obtained by multiplying this value in SR u' by χ : $u' = \chi \tilde{u}'$, where

$$\tilde{u}'(\mathbf{u}, \mathbf{v}) = \frac{\sqrt{(\mathbf{u} - \mathbf{v})^2 - \left(\frac{\mathbf{u} \times \mathbf{v}}{c}\right)^2}}{1 - \frac{v \cdot \mathbf{u}}{c^2}}. \quad (9)$$

The nature of the coefficient χ is easy to understand: it arises due to the difference in the ways of synchronizing the clock in SR and TTh. As the consequence of this difference, we obtain the following relation between the time intervals in

TTh and SR for the particle that moves with the velocity \mathbf{u} in AIRF K (see Sect. 6):

$$dt' = \frac{d\tilde{t}'}{\chi}. \quad (10)$$

Thus, the time interval between two events (in the same IRF) differs dependent of the way of the clock synchronization. What time is more adequate to the physical reality — t' or \tilde{t}' ? The answer to this question is discussed below in Sect. 6.

Using the reverse TT, one may express the coefficient χ through \mathbf{u}' and \mathbf{v} (and through $\tilde{\mathbf{u}}'$, \mathbf{v}):

$$\chi = 1 - \frac{\mathbf{u}' \cdot \mathbf{v}}{c^2} = \frac{1}{1 + \frac{\tilde{\mathbf{u}}' \cdot \mathbf{v}}{c^2}}. \quad (11)$$

Consider an important particular case: i.e. the transformational properties of the velocity of light. If in AIRF K the light propagates with the velocity c at the angle θ with respect to the X -axis, then we obtain from (4) and (5):

$$c'(v, \theta) = c \frac{1 - \frac{v}{c} \cos \theta}{1 - \frac{v^2}{c^2}}, \quad (12)$$

$$\cos \theta' = \frac{\cos \theta - \frac{v}{c}}{1 - \frac{v}{c} \cos \theta}. \quad (13)$$

From (13) we obtain:

$$\cos \theta = \frac{\cos \theta' + \frac{v}{c}}{1 + \frac{v}{c} \cos \theta'}. \quad (14)$$

Relations (13) and (14) coincide with the relevant SR formulae. Inserting (14) into (12) we obtain [7, 8]:

$$c'(v, \theta') = \frac{c}{1 + \frac{v}{c} \cos \theta'}. \quad (15)$$

In the 1st degree of expansion in v/c , expression (15) coincides with that resulted from the Galilean velocity addition:

$$c'(v, \theta') = c - v \cos \theta' + o\left(\frac{v^2}{c^2}\right). \quad (16)$$

Formula (15) describes the anisotropy of the velocity of light in IRF K' . Such anisotropy was observed in [20, 21]. Note that formula (15) does not contradict the postulate of the light velocity invariance in SR, what is meant here are the two different velocities differing in the way of synchronizing the clock they are determined by. It is easy to state that formula (15) explains the lack of interference in the MM experiment [6] since the time of the “back and forth” motion is

$$t_{\uparrow\downarrow} = t_{\uparrow} + t_{\downarrow} = \frac{L}{c'(\theta')} + \frac{L}{c'(\theta' + \pi)} = \frac{2L}{c} = \text{invar.} \quad (17)$$

Formula (15) enables one to understand how the ether “hided” from Michelson (more exactly, it did not allow him to

find it), i.e. at adding the reverse velocities in (17) the “ether terms” are mutually abolished. The reader has to recognize the methodological value of formula (15), since it indicates that the lack of interference in the MM experiment could be explained not postulating the assumption about the independence of the velocity of light on the observer’s motion velocity. All the difficulties in the time behavior in SR seat in this assumption.

3 Estimation of the possible excess of the absolute velocity of light in IRF related to the Earth

Let us use equation (4) to obtain the estimate of the possible excess of the neutrino velocity over the absolute velocity of light. Let v and u be the velocity of the Earth and that of neutrino with respect to AIRF K (conditionally speaking, with respect to the ether), respectively, u' be the neutrino velocity value with respect to the Earth. According to Marinov’s measurements [4, 5]

$$v = (360 \pm 40) \text{ km/s.} \quad (18)$$

The same estimate follows from the analysis of the experimental data on the light velocity anisotropy [20, 21].

Let us assume that the velocity u is very close to the velocity of light c : $u = c - \delta$, $\delta \ll c$. Taking also into account that $v \ll c$, we obtain from (4) to the accuracy of the first-order values over v/c and δ/c :

$$\frac{u' - c}{c} = -\frac{v}{c} \cos \theta - \frac{\delta}{c}, \quad \theta = (\widehat{\mathbf{u}, \mathbf{v}}). \quad (19)$$

At the neutrino energies of the order of GeV, taking into account the smallness of the neutrino rest mass (several eV), $\delta \ll v$. Then

$$\frac{u' - c}{c} = -\frac{v}{c} \cos \theta. \quad (20)$$

The maximal value of the above excess is reached at $\theta = \pi$:

$$\left(\frac{u' - c}{c}\right)_{MAX} = (121 \pm 13.3) \times 10^{-5}, \quad (21)$$

This is approximately 50 times larger than the infamous CERN result [22] obtained with a technical mistake that, obviously, could not be considered the contestation of theoretical estimates (20) and (21). It is important to achieve the correct confirmation of estimates (20) and (21) for the sake of the further progress of physics. To do this it is necessary to ensure the clock synchronization close to instantaneous. One may also use the “light synchronization” (GPS) that is more convenient technically, but in this case one has to take into account in (15) the difference of velocities of electromagnetic signals propagating in the opposite directions.

Note that in case of the use of the clock synchronized “according to Einstein” we may obtain from (9) for the situation under discussion:

$$\frac{\tilde{u}' - c}{c} = -\left(\frac{v}{c} \cos \theta\right)^2 \Rightarrow \tilde{u}' < c, \quad (22)$$

i.e. the “superluminal” motion would not be observed as is true according to SR.

Note a specific circumstance: the estimate (20) could be obtained from the Galilean velocity addition $\mathbf{u}' = \mathbf{u} - \mathbf{v}$, despite the fact that the velocities \mathbf{u}' and \mathbf{u} are relativistic. This is due to the fact that the Tangherlini transformations are the less correction of the Galilean transformations (GT) than the Lorentz ones. To make the velocity addition law (3)–(5) (that follows from TT) coincide in the first order with the Galilean one, the fulfillment of the condition $v \ll c$ is sufficient, whereas formulae (6) and (9) coincide with the Galilean ones only when $u \ll c$ and $v \ll c$, and this is demonstrated by formula (22).

4 Anisotropic deformation of the light barrier and light cone in the Tangherlini theory

It follows from (4) and (15) that the velocities of the particle u' and light c' in IRF K' that moves with respect to the ether may exceed the absolute velocity of light c . However, the following holds true:

Statement 1 *The velocity u' of the particle with a non-zero rest mass is always less than the velocity c' of light that moves in the same direction:*

$$u'(\theta') < c'(\theta') \quad (23)$$

Proof. Using formulae (4), (9), (11) and (15), we obtain:

$$\frac{u'(\theta')}{c'(\theta')} = \frac{\tilde{u}' \left(1 + \frac{v}{c} \cos \theta'\right)}{c \left(1 + \frac{\tilde{u}' v}{c^2} \cos \theta'\right)} = \frac{1 + \frac{v}{c} \cos \theta'}{\frac{c}{\tilde{u}'} + \frac{v}{c} \cos \theta'}. \quad (24)$$

Since always $c > \tilde{u}'$, it follows from (24) that $\frac{u'(\theta')}{c'(\theta')} < 1$, i.e. *quod erat demonstrandum*.

Thus, it follows from TT that in IRF K' that moves with respect to the ether with the velocity v an anisotropically deformed light barrier appears:

$$u' < \frac{c}{1 + \frac{v}{c} \cos \theta'}.$$

Only in AIRF K ($v = 0$) this barrier takes a form of an absolute SR barrier. In other IRTs, the value of deformation depends on the velocity v of IRF with respect to the ether. Therefore, even in case when the velocity of particle exceeds, according to (20), the absolute velocity of light, it will not overcome the light barrier, this barrier is simply such deformed that the motion with the velocity exceeding the absolute velocity of light ($c < u' < c'$) becomes possible. Therefore, one has not to expect the “vacuum” Cherenkov effect. If the neutrino outruns its self-radiation, then, according to Kohen-Glashow calculations [23], it would lose almost its total energy for the production of a pair of particles, which has not been observed experimentally.

Thus, for the particle with the non-zero mass, even at $u' > c$, the term “superluminal motion” is conditional.

To obtain the equation that describes the light “quasi-cone” in TTh, we will use the non-invariant metric tensor [7, 8]:

$$g'_{\mu\nu}(v) = \begin{pmatrix} 1 & -\frac{v}{c} & 0 & 0 \\ -\frac{v}{c} & \frac{v^2}{c^2} - 1 & 0 & 0 \\ 0 & 0 & -1 & 0 \\ 0 & 0 & 0 & -1 \end{pmatrix}. \quad (25)$$

The invariant 4-interval is:

$$dS'^2 = g'_{\mu\nu} dx'^{\mu} dx'^{\nu} = g_{\mu\nu} dx^{\mu} dx^{\nu} = c^2 dt^2 - (dx^2 + dy^2 + dz^2). \quad (26)$$

For the light “quasi-cone” we obtain the following equation:

$$ct' - \frac{v}{c} x' = \pm \sqrt{x'^2 + y'^2 + z'^2}. \quad (27)$$

At $v \ll c$, this “quasi-cone” transforms into the SR light cone. Taking into account relation (15), equation (27) should be written in a form:

$$c'(\theta')t' = \pm \sqrt{x'^2 + y'^2 + z'^2}, \quad (28)$$

and this vindicates the use of the term “light quasi-cone”.

5 Energy and momentum of the “superluminal” particle

Let us ascertain that at the “superluminal” motion, i.e. at $u' > c$, the mass of the particle remains real. According to TT (1), (2), one may obtain the following expressions for the momentum \mathbf{P}' and energy E' :

$$\mathbf{P}' = \frac{m\mathbf{u}'}{\sqrt{\chi^2 - \left(\frac{u'}{c}\right)^2}} = \tilde{\mathbf{P}}', \quad (29)$$

$$E' = \frac{\chi mc^2}{\sqrt{\chi^2 - \left(\frac{u'}{c}\right)^2}} = \tilde{E}'. \quad (30)$$

These expressions were obtained in [7, 8] from the extreme action principle with the certain-type Lagrangian. In [17], the same expressions were obtained by means of the two simpler methods: a) by using the notion “proper time” and b) by applying TT to the 4-vector of energy-momentum. It is easy to show that the Statement 1 provides the positiveness of the radicand expression in (29) and (30), including that at $u' > c$. Hence, there is no necessity to postulate the imaginary character of the rest mass m (in contrary to the tachyon hypothesis in SR).

6 Notion of time in TTh and SR. Acausality illusoriness

Let us discuss now the difference of the properties of time in TTh and SR resulting from the difference of the ways of the clock synchronizing. The TT set (1), (2) does not form a group, but, substituting:

$$t' \rightarrow \tilde{t}' = t' - \frac{v}{c^2} x', \quad (31)$$

we obtain the time part of LT:

$$\tilde{t} = \gamma \left(t - \frac{v}{c^2} x \right) \quad (32)$$

(the co-ordinate parts in TT and LT are the same).

The Lorentz transformations form a group and, therefore, seem to be more preferred than TT. However, is it correct to call the time the value \tilde{t} that is a linear combination of the time t' and co-ordinate x' ? One may call the quantity \tilde{t} the “quasi-time”, and the derivative with respect to \tilde{t} the radius-vector \mathbf{r}' – the “quasi-velocity”. Then the second SR postulate sounds as follows: “the quasi-velocity of light is invariant”. This coincides with the second TTh postulate, since the quasi-velocity of light equals to the average velocity of light when moving along the closed contour.

Let us express the relation between the intervals dt' and $d\tilde{t}$ through the velocities v and $u'_x = dx'/dt'$. From (31) we obtain:

$$d\tilde{t} = \left(1 - \frac{vu'_x}{c^2} \right) dt' = \left(1 - \frac{\mathbf{v} \cdot \mathbf{u}'}{c^2} \right) dt' = \chi dt' \quad (33)$$

and this explains the relation between the velocities in TTh and SR (see Section 2).

In IRF related to the Earth ($v \approx 360$ km/s), deviation of the coefficient χ from unit is insufficient (i.e. it is about 10^{-3}). However, for the precise measuring the velocities with announced error less than 10^{-3} (as in the CERN experiment [22] on finding the superluminal neutrino motion) this difference should be taken into account. Of particular consideration is the situation of the “superluminal” motion, i.e. when $u' > c$. It is seen from (2) that at $dt > 0$ the condition $dt' > 0$ always holds true as well, i.e. the time in TTh, as it has been always in physics, varies in any IRF towards one side, i.e. from the past to the future. No “backward time motion” does exist. As regards the interval $d\tilde{t}$, it follows from (33) that given the fulfillment of the condition $\mathbf{v} \cdot \mathbf{u}' > c^2$ this interval becomes negative, i.e. $d\tilde{t} < 0$ (at $dt' > 0$). This allows one to understand the illusoriness of the so-called problem of violation of the causality principle in SR: the illusion of the acausality arises due to neglecting the difference in the velocities of light in case of the opposite directions. Let us dwell upon this problem in more detail. Let the superluminal signal propagate in IRF K' along the X -axis from the point “1” to the point “2”. According to the instantaneously synchronized clock, the motion time interval is $\Delta t' = t'_2 - t'_1$. If one uses the light synchronization (GPS) with fixing at the point “3” the light signals emitted at the points “1” and “2” (let us consider for simplicity that $x_3 = (x_1 + x_2)/2$), then the motion time interval is:

$$\Delta \tilde{t} = \tilde{t}_2 - \tilde{t}_1 = \Delta t' - \frac{Lv}{c^2}, \quad L = x_2 - x_1. \quad (34)$$

Thus, at $Lv/c^2 > \Delta t'$ (that is equal to the condition $u'v > c^2$) the “acausality” takes place, i.e. $\tilde{t}_2 < \tilde{t}_1$. Everything is extremely

simple here, i.e. the light signal from the event-effect “2” is detected earlier than the light signal from the event-cause “1” due to the fact that the signal from the event-cause “1” moves (along the IRF motion direction) for a time longer than the total time of the superluminal motion and the reverse (i.e. in the opposite to the IRF motion) light beam motion from the point “2” to the point “3”. The acausality illusion vanishes, if one, formulating the causality principle, clearly states the things implied as well, i.e. the event-effect always occurs later than the event-cause according to the clock with the instantaneous synchronization.

Perception of the illusoriness lifts the ban on the superluminal motion: the velocity of the signals of the informational origin (in particular, the quantum teleportation) could be arbitrarily large.

It is easy to understand that the assumption about the possibility of appearance of the acausal loop is wrong. Indeed, the intervals $\Delta t'$ and $\Delta \tilde{t}$ between the events taking place at the same point coincide. Therefore, it follows from $\Delta t' > 0$ for the cyclic process that $\Delta \tilde{t} > 0$ as well.

Note that in TTh, as seen from (2), the experimentally proven delay of time also exists. However, unlike SR, this delay depends not on the relative velocity of the two reference frames, but on the velocity of motion of a given IRF with respect to the ether. For the two reference systems K'_1 and K'_2 moving with the same velocities in the opposite directions \mathbf{v}' and $\mathbf{v}'' = -\mathbf{v}'$ the time varies similarly, i.e. $t'' = t'$, though their relative velocity $2v'/(1 - (v'/c)^2)$ could be as much as desired large.

Obviously, the clock paradox doesn't take place in TTh.

7 Final comments and conclusions

The above discussion allows one to conclude that TTh is a wider theory than SR, however, all the TTh results almost coincide with those of SR in the cases when one may neglect the non-invariance of the velocity of light (this is a kind of application of the Bohr's correspondence principle). In IRF related to the Earth, this condition holds true very frequently. Just due to this, such a brilliant agreement of the SR calculations with a huge number of experimental data does exist. However, the motion with the superluminal velocities is out of the SR competence. As it had been shown above, the apparent violation of the causality principle at the superluminal velocities in SR is due to neglecting the light velocity difference in case of motion in opposite directions. Therefore, no restrictions on the velocity of particles and signals are imposed by the causality principle. However, as proven in Statement 1, when comparing the velocity of particle with the non-zero mass u' with that of the light c' in the arbitrary reference frame, condition $u' < c'$ is always valid (though in this case u' could be arbitrarily large, including the case $u' > c$).

In the case of the non-local correlation interaction between the “entangled states” of the quantum objects, the ve-

locity of its propagation is not restricted at all. The experimental excess of this velocity over the velocity of light has been observed for the first time in the paper by Alan Aspect et al. [24] devoted to the correlation of the photon pairs polarized states. The theoretical justification of the possibility of information transfer with the superluminal velocity could be easily found, say, in [25]. The possibility of the technical realization of the superluminal signals in the communication networks is discussed in [26] in the section with the characteristic name “Superluminal communications”.

Submitted on April 06, 2014 / Accepted on April 07, 2014

Received after revision on April 21, 2014

References

1. Barashenkov V.S. Tachyons: particles moving with velocities greater than the speed of light. *Review Soviet Physics Uspekhi*, 1975, v. 17 (5), 774–782.
2. Mandelshtam L.I. Lectures on the Physical Principles of Relativity Theory (1933–1934). In: Rytov S.M. (ed.). Academician L.I. Mandelshtam. Lectures on Optics, Relativity Theory and Quantum Mechanics. Nauka, Moscow, 1972. Pages 83–285. (In Russian).
3. Bolotovskii B. M., Ginzburg V. L. The Vavilov-Cerenkov effect and the Doppler effect in the motion of sources with superluminal velocity in vacuum. *Soviet Physics Uspekhi*, 1972, v. 15 (2), 184–192.
4. Marinov S. Measurement of the laboratory’s absolute velocity. *General Relativity and Gravitation*, 1980, v. 12 (1), 57–66.
5. Marinov S. New measurement of the Earth’s absolute velocity with the help of the “Coupled Shutters” experiment. *Progress in Physics*, 2007, v. 3 (1), 31–37.
6. Michelson A. A., Morley E. W. On the relative motion of the Earth and the luminiferous ether. *American Journal of Science*, 1887, v. 34 (203), 333–345.
7. Tangherlini F.R. The velocity of light in uniformly moving frames. A dissertation. Stanford University, 1958. *The Abraham Zelmanov Journal*, 2009, v. 2, 44–110.
8. Malykin G. B., Malykin E. G. Tangherlini’s dissertation and its significance for physics of the 21th century. *The Abraham Zelmanov Journal*, 2009, v. 2, 121–147.
9. Tangherlini F.R. Light travel times around a closed Universe. *Nuovo Cimento B*, 1994, v. 109 (9), 929–951.
10. Kennedy R. J., Thorndike E. M. Experimental establishment of the relativity of time. *Physical Review*, 1932, v. 43 (3), 400–418.
11. Ragul’skii V. V. An experimental study of the optical isotropy of space. *Soviet Physics Uspekhi*, 1997, v. 40 (9), 972–974.
12. Malykin G. B. Para-Lorentz transformations. *Soviet Physics Uspekhi*, 2009, v. 52 (3), 263–266.
13. Chavarga M. M. Relative motion of solitons in the light-carrying ether. *Uzhhorod National University Scientific Herald. Series Physics*, 2000, v. 7, 174–194. (In Ukrainian).
14. Obukhov Yu. A., Zakharchenko N. N. The light-carrying ether and the violation of the principle of relativity. *Physical Thought of Russia*, 2001, v. 3, 71–83. (In Russian).
15. Kupryaev N. V. Extended representation of the Lorentz transformations. *Russian Physical Journal*, 1999, v. 42 (7), 592–597.
16. Chepick A. M. Absolute. Main principles (to discussion). *Modern Problems of Statistical Physics*, 2007, v. 6, 111–134. (In Russian).
17. Medvedev S. Yu., Halamba I. F. About some consequences from the Tangherlini transformations. *Uzhhorod National University Scientific Herald. Series Physics*, 2012, v. 31, 174–184. (In Ukrainian)
18. Homem G. On Abreu’s theory of space and time and new measurements of absolute velocities. arXiv: physics/0212050 [physics.gen-ph].
19. Homem G. Physics in a synchronized space-time. In: Projecto de Final de Curso da LEFT 2002/2003 orientado por prof. de Abreu Rodrigo, 2003. 38 Pages.
20. Smoot G. F., Gorenstein M. V., Muller R. A. Detection of anisotropy in the Cosmic Blackbody Radiation. *Physical Review Letters*, 1977, v. 39 (14), 898–901.
21. Gurzadayan V. G. et.al. Probing the light speed anisotropy with respect to the Cosmic Microwave Background Radiation dipole. *Modern Physics Letters A*, 2005, v. 20 (1), 19.
22. Adam T. et.al. Measurement of the neutrino velocity with the OPERA detector in the CNGS beam. arXiv: 1109.4897 [hep-ex].
23. Cohen A. G., Glashow S. L. Pair creation constrains superluminal neutrino propagation. *Physical Review Letters*, 2011, v. 107 (18), 181803.
24. Aspect A., Dalibard J., Roger G. Experimental test of Bell’s inequalities using time-varying analyzers. *Physical Review Letters*, 1982, v. 49 (25), 804–1807.
25. Gadosky O. N., Altunin K. K. Quantum teleportation and resonance information transfer from one atom to another at arbitrary interatomic distances. *Russian Physical Journal*, 2000, v. 43 (11), 893–898.
26. Kadomtsev B. B. Dynamics and information. *Soviet Physics Uspekhi*, 1994, v. 37 (5), 425–499.

On the Equation which Governs Cavity Radiation II

Pierre-Marie Robitaille

Department of Radiology, The Ohio State University, 395 W. 12th Ave, Columbus, Ohio 43210, USA.
robitaille.1@osu.edu

In this work, the equation which properly governs cavity radiation is addressed once again, while presenting a generalized form. A contrast is made between the approach recently taken (P.M. Robitaille. On the equation which governs cavity radiation. *Progr. Phys.*, 2014, v. 10, no. 2, 126–127) and a course of action adopted earlier by Max Planck. The two approaches give dramatically differing conclusions, highlighting that the derivation of a relationship can have far reaching consequences. In Planck's case, all cavities contain black radiation. In Robitaille's case, only cavities permitted to temporarily fall out of thermal equilibrium, or which have been subjected to the action of a perfect absorber, contain black radiation. Arbitrary cavities do not emit as blackbodies. A proper evaluation of this equation reveals that cavity radiation is absolutely dependent on the nature of the enclosure and its contents. Recent results demonstrating super-Planckian thermal emission from hyperbolic metamaterials in the near field and emission enhancements in the far field are briefly examined. Such findings highlight that cavity radiation is absolutely dependent on the nature of the cavity and its walls. As previously stated, the constants of Planck and Boltzmann can no longer be viewed as universal.

Science enhances the moral value of life, because it furthers a love of truth and reverence. . .

Max Planck, Where is Science Going? 1932 [1]

1 Introduction

Recently [2], the equation which governs radiation in an arbitrary cavity, Eq. 1, has been derived by combining Kirchhoff's law of thermal emission [3, 4] with Stewart law [5, 6]:

$$\epsilon_\nu = f(T, \nu) - \rho_\nu, \quad (1)$$

where ϵ_ν corresponds to the frequency dependent emissivity, ρ_ν to the frequency dependent reflectivity, and $f(T, \nu)$ to the function defined by Max Planck [7, 8].* This expression is valid under assumptions made by the German scientist in neglecting the effects of diffraction and scattering [8, §2]. At the same time, it implies that all materials used to assemble blackbodies will act as Lambertian emitters/reflectors. The total emission will vary with the cosine of the polar angle in accordance with Lambert's Law (see e.g. [9, p. 19] and [11, p. 22–23]). Planck assumes that white reflectors, which are Lambertian in nature, can be utilized in the construction of blackbodies (e.g. [8, §61, §68, §73, §78]). But very few materials, if any, are truly Lambertian emitters/reflectors.

*The emissivity of an object is equal to its emissive power, E , divided by the emissive power of a blackbody of the same shape and dimension. Similarly, the reflectivity can be taken as the reflected portion of the incoming radiation, divided by the total incoming radiation, as often provided by a blackbody [9, 10]. Like emissivity, the reflectivity of an object is an intrinsic property of the material itself. Once measured, its value does not depend on the presence of incident radiation. As a result, Eq. 1 can never be undefined, since ρ_ν can only assume values between 0 and 1. For a perfect blackbody, $\rho_\nu = 0$ and $\epsilon_\nu = 1$. In that case, the Planck function is normalized.

Consequently, a fully generalized form of Eq. 1 must take into account that all of these conditions might not necessarily be met:

$$\epsilon_{\nu, \theta, \phi} = f(T, \nu, \theta, \phi, s, d, N) - \rho_{\nu, \theta, \phi}, \quad (2)$$

where θ and ϕ account for the angular dependence of the emission and reflection in real materials, s and d account for the presence of scattering and diffraction, respectively, and N denotes the nature of the materials involved.

Since laboratory blackbodies must be Lambertian emitters [11, p. 22–23], they are never made from materials whose emissivity is strongly directional. This explains why strong specular reflectors, such as silver, are not used to construct blackbodies. It is not solely that this material is a poor emitter. Rather, it is because all reflection within blackbodies must be diffuse or Lambertian, a property which cannot be achieved with polished silver.

It should also be noted that when Eq. 1 was presented in this form [2], the reflectivity term was viewed as reducing the emissive power from arbitrary cavities. There was nothing within this approach which acted to drive the reflection. Within the cavity, the absorptivity must equal the emissivity. Hence, any photon which left a surface element to arrive at another must have been absorbed, not reflected. The overall probability of emission within the cavity must equal the probability of absorption under thermal equilibrium. This precludes the buildup of reflective power and, thereby, prevents a violation of the 1st law of thermodynamics.

However, are there any circumstances when the reflection term can be driven? In order to answer this question, it is valuable to return to the work of Max Planck [8].

2 Max Planck's treatment of reflection

In his derivation of Eq. 1,* Max Planck had also sought to remove the undefined nature of Kirchhoff's law, when expressed in term of emission and absorption [8, §45–49]. However, in order to address the problem, he actively placed the surface of interest in contact with a perfect emitter [8, §45–49]. In so doing, Planck permitted a perfectly emitting body to drive the reflection and, thereby, build the radiation within his cavities, noting in §49 that “*the amount lacking in the intensity of the rays actually emitted by the walls as compared with the emission of a black body is supplied by rays which fall on the wall and are reflected there*”. In §45, he had informed the reader that the second medium was a blackbody. It is for this reason that Planck insists that all cavities must contain black radiation.

Thus, despite the advantage of expressing Eq. 1 in terms of reflection, Planck abandoned the relationship he had presented in §49 [8], as reflection became inconsequential if it could be driven by a carbon particle. He subsequently summarized “*If we now make a hole in one of the walls of a size $d\sigma$, so small that the intensity of the radiation directed towards the hole is not changed thereby, then radiation passes through the hole to the exterior where we shall suppose there is the same diathermanous medium as within. This radiation has exactly the same properties as if $d\sigma$ were the surface of a black body, and this radiation may be measured for every color together with the temperature T* ” [8, §49].

The problem of radiation emitted by an arbitrary cavity had not been solved, because Planck ensured, throughout his *Theory of Heat Radiation* [8], that he could place a minute particle of carbon within his perfectly reflecting cavities in order to release the “stable radiation” which he sought [12]. He advanced that the carbon particle simply had a catalytic role [8, 12]. In fact, since he was placing a perfect emitter within his cavities at every opportunity [8, 12], he had never left the confines of the perfectly absorbing cavity, as represented by materials such as graphite or soot. His cavities all contained black radiation as a direct result. Perhaps this explains why he did not even number Eq. 1 in his derivation. Since he was driving reflection, all cavities contained the same radiation and Eq. 1 had no far reaching consequences.

Planck's approach stands in contrast to the derivation of Eq. 1 presented recently [2]. In that case, particles of carbon are never inserted within the arbitrary cavities. Instead, the emissivity of an object is first linked by Stewart's law [5, 6] to its reflectivity, before a cavity is ever constructed

$$\epsilon_v + \rho_v = \kappa_v + \rho_v = 1. \quad (3)$$

*Planck obtains $I = E + (1 - A)I = E + RI$, where E corresponds to emitted power, $R(= \epsilon)$ is the fraction of light reflected and $I(= f(T, \nu))$ is the blackbody power which, in Planck's case, also drives the reflection [8, §49]. This is because he places a carbon particle inside the cavity to produce the black radiation.

This is how the emissivity of a real material is often measured in the laboratory. The experimentalist will irradiate the substance of interest with a blackbody source and note its reflectivity. From Stewart's law (Eq. 3), the emissivity can then be easily determined.

It is only following the determination of the emissivity and reflectivity of a material that the author constructs his arbitrary cavity. As such, the recent derivation of Eq. 1 [2], does not require that materials inside the cavity can drive the reflectivity term to eventually “build up” a blackbody spectrum. This is a fundamental distinction with the derivation provided by Max Planck [8, §49].

The emissivity of a material is defined relative to the emissivity of a blackbody at the same temperature. To allow, therefore, that reflectivity would “build up” black radiation, within an arbitrary cavity in the absence of a perfect emitter, constitutes a violation of the first law of thermodynamics (see [2] and references therein). Planck himself must have recognized the point, as he noted in §51 of his text that “*Hence in a vacuum bounded by perfectly reflecting walls any state of radiation may persist*” [8].

Consequently, one can see a distinction in the manner in which Eq. 1 has been applied. This leads to important differences in the interpretation of this relationship. For Planck, all cavities contain black radiation, because he has insisted on placing a small carbon particle within all cavities. The particle then actively drives the reflection term to produce black radiation.

In contrast, in the author's approach, arbitrary cavity radiation will never be black, because a carbon particle was not placed within the cavity. Emissivity and reflectivity are first determined in the laboratory and then the cavity is constructed. That cavity will, therefore, emit a radiation which will be distinguished from that of a blackbody by the presence of reflectivity. This term, unlike the case advocated by Max Planck, acts to decrease the net emission relative to that expected from a blackbody.

In this regard, how must one view arbitrary cavities and which approach should guide physics? Answers to such questions can only be found by considering the manner in which blackbodies are constructed and utilized in the laboratory.

3 Laboratory blackbodies

Laboratory blackbodies are complex objects whose interior surfaces are always manufactured, at least in part, from nearly ideal absorbers of radiation over the frequency of interest (see [13], [14, p. 747–759], and references therein). This fact alone highlights that Kirchhoff's law cannot be correct. Arbitrary cavities are not filled with blackbody radiation. If this was the case, the use of specialized surfaces and components would be inconsequential. Blackbodies could be made from any opaque material. In practice, they are never constructed from surfaces whose emissive properties are poor and whose

emissivity/reflectivity are far from Lambertian.

Sixty years ago, De Vos summarized black body science as follows: “Resuming, it must be concluded that the formulae given in the literature for the quality of a blackbody can be applied only when the inner walls are reflecting diffusely to a high degree and are heated quite uniformly” [15]. De Vos was explicitly stating that mathematical rules only apply when a cavity is properly constructed. Even if the temperature was uniform, the walls must have been diffusely reflecting. Everything was absolutely dependent on the nature of the walls. Lambertian emitters/reflectors had to be utilized. Specialized materials were adopted in the laboratory, in sharp contrast to Kirchhoff’s claims (see [2] and references therein).

At the same time, there is another feature of laboratory blackbodies which appears to have been overlooked by those who accept universality and Planck’s use of reflection to produce black radiation.

Laboratory blackbodies (see [13], [14, p.747–759], and references therein) are heated devices: “In photometry and pyrometry often use is made of blackbodies i.e. opaque hollow bodies which are provided with one or more small holes and whose walls are heated uniformly” [15]. They tend to be cylindrical or spherical objects heated in a furnace, by immersion in a bath of liquid (water, oil, molten metal), through electrical means like conduction (where resistive elements are placed in the walls of the cavity) and induction (where electromagnetic fields are varied), and even by electron bombardment [13–15].

The question becomes, when does the heating in a laboratory blackbody stop? For most experiments, the answer is never. Once the desired temperature is achieved, additional heat continues to be transferred to the blackbody with the intent of maintaining its temperature at the desired value. The consequences of this continual infusion of energy into the system are ignored. Since temperature equilibrium has been achieved, scientists believe that they have now also reached the conditions for thermal equilibrium. The two, however, are completely unrelated conditions.

4 Theoretical considerations

As an example, an object can maintain its temperature, if it is heated by conduction, or convection, and then radiates an equivalent amount of heat away by emission. In that case, it will be in temperature equilibrium, but completely out of thermal equilibrium. For this reason, it is clear that heated cavities cannot be in thermal equilibrium during the measurements, as this condition demands the complete absence of *net* conduction, convection, or radiation (neglecting the amount of radiation leaving from the small hole for discussion purposes).

Planck touched briefly on the subject of thermal equilibrium in stating, “Now the condition of thermodynamic equilibrium required that the temperature shall be everywhere the

same and shall not vary with time. Therefore in any given arbitrary time just as much radiant heat must be absorbed as is emitted in each volume-element of the medium. For the heat of the body depends only on the heat radiation, since, on account of the uniformity in temperature, no conduction of heat takes place” [8, §25]. Clearly, if the experimentalists were adding energy into the system in order to maintain its temperature, they could not be in thermal equilibrium, and they could not judge what the effect of this continual influx of energy might be having on the radiation in the cavity.

4.1 Consequences of preserving thermal equilibrium

Consider an idealized isothermal cavity in thermal equilibrium whose reflection has not been driven by adding a carbon particle. Under those conditions, the emissivity and absorptivity of all of its surface elements will be equal. Then, one can increase the temperature of this cavity, by adding an infinitesimal amount of heat. If it can be assumed that the walls of the cavity all reach the new temperature simultaneously, then the emissivity of every element, ϵ_v , must equal the absorptivity of every element, κ_v , at that instant. The process can be continued until a much higher temperature is eventually achieved, but with large numbers of infinitesimal steps. Under these conditions, reflection can play no part, as no energy has been converted to photons which could drive the process. All of the energy simply cycles between emission and absorption. The cavity will now possess an emissive power, E , which might differ substantially from that set forth by Kirchhoff for all cavities. In fact, at the moment when the desired temperature has just been reached, it will simply correspond to

$$E = \epsilon_v \cdot f(T, \nu), \quad (4)$$

because the emissivity of a material remains a fundamental property at a given temperature. This relationship will deviate from the Planckian solution by the extent to which ϵ_v deviates from 1.

4.2 Consequences of violating thermal equilibrium

At this stage, an alternative visualization can be examined. It is possible to assume that the influx of energy which enters the system is not infinitesimal, but rather, causes the emissivity of the cavity to temporarily become larger than its absorptivity. The cavity is permitted to move out of thermal equilibrium, if only for an instant. Under these conditions, the temperature does not necessarily increase. The additional energy can simply be converted, through emission, to create a reflective component. Thermal equilibrium is violated. Emissivity becomes greater than absorptivity and the difference between these two values enters a reflected pool of photons. A condition analogous to

$$\epsilon_v = \kappa_v + \delta\rho_v \quad (5)$$

has been reached, where $\delta\rho_v$ is that fraction of the reflectivity which has actually been driven.

The emissive power might still not be equal to the Kirchhoff function in this case, depending on the amount of photons that are available from reflection. If one assumes that the radiation inside the cavity must be governed in the limiting case by the Planck function, then the emissive power under these circumstances will be equal to the following:

$$E = (\epsilon_v + \delta\rho_v) \cdot f(T, \nu). \quad (6)$$

The cavity is still not filled with blackbody radiation, as the reflective term has not yet been fully driven. Nonetheless, the process can be continued until $\delta\rho_v = \rho_v$ and the reflective component has been fully accessed. At the end of the process, Eq. 3 becomes valid in accordance to Stewart's Law [5, 6]. The temperature has not yet increased, but the energy which was thought to heat the cavity has been transformed to drive the reflective component.

Finally, thermal equilibrium can be re-established by limiting any excess heat entering the system. The reflected photons will bounce back and forth within the cavity. Balfour Stewart referred to these photons as "banded" [5] and, for historical reasons, the term could be adopted. Thus, given enough transfer of energy into the system, and assuming that the material is able to continue to place excess emitted photons into the reflected pool, then eventually, the cavity might become filled with black radiation, provided that emission and reflection are Lambertian. In that case, the Planckian result is finally obtained:

$$E = (\epsilon_v + \rho_v) \cdot f(T, \nu). \quad (7)$$

In practice, when a blackbody is being heated, some reflected photons will always be produced at every temperature, as the entire process is typically slow and never in thermal equilibrium. However, for most materials, the introduction of photons into the reflected pool will be inefficient, and the temperature of the system will simply increase. That is the primary reason that arbitrary cavities can never contain black radiation. Only certain materials, such as soot, graphite, carbon black, gold black, platinum black, etc. will be efficient in populating the reflected pool over the range of temperatures of interest. That is why they are easily demonstrated to behave as blackbodies. Blackbodies are not made from polished silver, not only because it is a specular instead of a diffuse reflector, but because that material is inefficient in pumping photons into the reflected pool. With silver, it is not possible to adequately drive the reflection through *excessive* heating. The desired black radiation cannot be produced.

In order to adequately account for all these effects, it is best to divide the reflectivity between that which eventually becomes banded, $\delta\rho_{v,b}$, and that which must be viewed as unbanded, $\delta\rho_{v,ub}$:

$$\rho_v = \delta\rho_{v,b} + \delta\rho_{v,ub}. \quad (8)$$

The unbanded reflection is that component which was never driven. As such, it must always be viewed as subtracting from the maximum emission theoretically available, given applicability of the Planck function. With this in mind, Eq. 1 can be expressed in terms of emissive power in the following form:

$$E = (1 - \delta\rho_{v,ub}) \cdot f(T, \nu), \quad (9)$$

where one assumes that the Planckian conditions can still apply in part, even if not all the reflectivity could be banded. In a more general sense, then the expression which governs the radiation in arbitrary cavities can be expressed as:

$$E = (1 - \delta\rho_{v,\theta,\phi,ub}) \cdot f(T, \nu, \theta, \phi, s, d, N). \quad (10)$$

In this case, note that $f(T, \nu, \theta, \phi, s, d, N)$ can enable thermal emission to exceed that defined by Max Planck. The specialized nature of the materials utilized and the manner in which the cavity is physically assembled, becomes important. In this regard, Eqs. 1, 9, and 10, do not simply remove the undefined nature of Kirchhoff's formulation when considering a perfect reflector, but they also properly highlight the central role played by reflectivity in characterizing the radiation contained within an arbitrary cavity.

5 Discussion

Claims that cavity radiation must always be black or normal [7,8] have very far reaching consequences in physics. Should such statements be true, then the constants of Planck and Boltzmann carry a universal significance which provide transcendent knowledge with respect to matter. Planck length, mass, time, and temperature take on real physical meaning throughout nature [8, §164]. The advantages of universality appear so tremendous that it would be intuitive to protect such findings. Yet, universality brings with it drawbacks in a real sense, namely the inability to properly discern the true properties of real materials.

Moreover, because of Kirchhoff's law and the associated insistence that the radiation within a cavity must be independent of the nature of the walls, a tremendous void is created in the understanding of thermal emission. In this respect, Planckian radiation remains the only process in physics which has not been linked to a direct physical cause. Why is it that a thermal photon is actually emitted from a material like graphite or soot?

This question has not yet been answered, due to the belief that Kirchhoff's law was valid. Thus, Kirchhoff's law has enabled some to hope for the production of black radiation in *any* setting and in a manner completely unrelated to real processes taking place within graphite or soot. It is for this reason that astronomers can hold that a gaseous Sun can produce a thermal spectrum. Such unwarranted extensions of physical reality are a direct result of accepting the validity of Kirchhoff's formulation. Real materials must invoke the same mechanism to produce thermal photons. Whatever happens

within graphite and soot to generate a blackbody spectrum must also happen on the surface of the Sun.

The belief that arbitrary materials can sustain black radiation always results from an improper treatment of reflection and energy influx. In Max Planck's case, this involved the mandatory insertion of a carbon particle within his cavities. This acted to drive reflection. In the construction of laboratory blackbodies, it involves departure from thermal equilibrium as the inflow of energy enables the emissivity to drive the reflection. In the belief that optically thick gases can emit blackbody radiation [16], it centers upon the complete dismissal of reflection and a misunderstanding with respect to energy inflow in gases [17].

Relative to the validity of Kirchhoff's Law, it is also possible to gain insight from modern laboratory findings. Recent experiments with metamaterials indicate that super-Planckian emission can be produced in the near field [18–20]. Such emissions can exceed the Stefan-Boltzmann law by orders of magnitude [18–20].

Guo et al. summarize the results as follows: “*The usual upper limit to the black-body emission is not fundamental and arises since energy is carried to the far-field only by propagating waves emanating from the heated source. If one allows for energy transport in the near-field using evanescent waves, this limit can be overcome*” [18]. Beihls et al. states that, “*Accordingly, thermal emission is in that case also called super-Planckian emission emphasizing the possibility to go beyond the classical black-body theory*” [19].

Similar results have been obtained, even in the far-field, using a thermal extraction device [21, 22]. In that case, the spatial extent of the blackbody is enhanced by adding a transparent material above the site of thermal emission. A four-fold enhancement of the far-field emission could thus be produced. In their *Nature Communications* article, the authors argue that this does not constitute a violation of the Stefan-Boltzmann law, because the effective “emitting surface” is now governed by the transmitter, which is essentially transparent [21]. However, this was not the position advanced when the results were first announced and the authors wrote: “*The aim of our paper here is to show that a macroscopic blackbody in fact can emit more thermal radiation to far field vacuum than $P = \sigma T^4 S$ ” [22].*

In the end, the conclusion that these devices do not violate the Stefan-Boltzmann relationship [21] should be carefully reviewed. It is the opaque surface of an object which must be viewed as the area which controls emission. Kirchhoff's law, after all, refers to opaque bodies [3, 4]. It is an extension of Kirchhoff's law beyond that previously advanced to now claim that transparent surface areas must now be considered to prevent a violation of the laws of emission.

In this regard, Nefedov and Milnikov have also claimed that super-Planckian emission can be produced in the far-field [23]. In that case, they emphasize that Kirchhoff's law is not violated, as energy must constantly flow into these sys-

tems. There is much truth in these statements. Obviously, modern experiments [18–23] fall short of the requirements for thermal equilibrium, as the cavities involved are heated to the temperature of operation. But given that all laboratory blackbodies suffer the same shortcomings, the production of super-Planckian emission in the near and far fields [18–23] cannot be easily dismissed. After all, in order for Planck to obtain a blackbody spectrum in every arbitrary cavity, he had to drive the reflection term, either by injecting a carbon particle or by permitting additional heat to enter the system, beyond that required at the onset of thermal equilibrium.

An interesting crossroads has been reached. If one assumes that modern experiments cannot be invoked, as they require an influx of conductive energy once temperature equilibrium has been reached, then the same restriction must be applied to all laboratory blackbodies. Yet, in the absence of banded reflection, very few cavities indeed would adhere to Kirchhoff's law. In fact, many cavities can never be filled with black radiation, even if one attempts to drive the reflection term. That is because certain materials are not conducive to emission and prefer to increase their temperature rather than drive reflection. Arbitrary cavities do not contain black radiation, and that is the measure of the downfall of Kirchhoff's law.

Taken in unison, all of these observations, even dating back to the days of Kirchhoff himself, highlight that the universality of blackbody radiation has simply been overstated. The emissive characteristics of a cavity are absolutely dependent on the nature of the cavity walls (see [13], [14, p. 747–759], and references therein). This has broad implications throughout physics and astronomy.

Dedication

This work is dedicated to our mothers on whose knees we learn the most important lesson: love.

Submitted on: April 28, 2014 / Accepted on: April 29, 2014
First published online on: May 1, 2014

References

1. Planck M. The new science – 3 complete works: Where is science going? The universe in the light of modern physics; The philosophy of physics. [Translated from the German by James Murphy and W.H. Johnston], Meridian Books, New York, 1959.
2. Robitaille P.-M. On the equation which governs cavity radiation. *Progr. Phys.*, v. 2, no. 2, 126–127.
3. Kirchhoff G. Über das Verhältnis zwischen dem Emissionsvermögen und dem Absorptionsvermögen. der Körper für Wärme und Licht. *Poggendorfs Annalen der Physik und Chemie*, 1860, v. 109, 275–301. (English translation by F. Guthrie: Kirchhoff G. On the relation between the radiating and the absorbing powers of different bodies for light and heat. *Phil. Mag.*, 1860, ser. 4, v. 20, 1–21).
4. Kirchhoff G. Über den Zusammenhang zwischen Emission und Absorption von Licht und Wärme. *Monatsberichte der Akademie der Wissenschaften zu Berlin*, sessions of Dec. 1859, 1860, 783–787.
5. Stewart B. An account of some experiments on radiant heat, involving an extension of Prévost's theory of exchanges. *Trans. Royal Soc.*

- Edinburgh*, 1858, v. 22, no. 1, 1–20 (also found in Harper's Scientific Memoirs, edited by J. S. Ames: The Laws of Radiation and Absorption: Memoirs of Prévost, Stewart, Kirchhoff, and Kirchhoff and Bunsen, translated and edited by D. B. Brace, American Book Company, New York, 1901, 21–50).
6. Robitaille P.-M. A critical analysis of universality and Kirchhoff's law: A return to Stewart's law of thermal emission. *Progr. Phys.*, 2008, v. 3, 30–35.
 7. Planck M. Über das Gesetz der Energieverteilung im Normalspektrum. *Annalen der Physik*, 1901, v. 4, 553–563.
 8. Planck M. The theory of heat radiation. P. Blakiston's Son & Co., Philadelphia, PA, 1914.
 9. Modest M.F. Radiative Heat Transfer. McGraw-Hill, New York, 1993, pp. 26–ff.
 10. Palmer J.M. The Measurement of Transmission, Absorption, Emission, and Reflection, in: Handbook of Optics (2nd Ed.), Part II, M. Bass, Ed., McGraw-Hill, NY, 1994.
 11. Burns D.A. and Ciurczak E.W. Handbook of Near-Infrared Analysis (3rd Edition), CRC Press, Boca Raton, FL, 2008.
 12. Robitaille P.-M. Blackbody radiation and the carbon particle. *Progr. Phys.*, 2008, v. 3, 36–55.
 13. Robitaille P.-M. Kirchhoff's law of thermal emission: 150 Years. *Progr. Phys.*, 2009, v. 4, 3–13.
 14. DeWitt D. P. and Nutter G. D. Theory and Practice of Radiation Thermometry. John Wiley and Sons Inc., New York, NY, 1988.
 15. de Vos J.C. Evaluation of the quality of a blackbody. *Physica*, 1954, v. 20, 669–689.
 16. Finkelburg W. Conditions for blackbody radiation in gases. *J. Opt. Soc. Am.*, 1949, v. 39, no. 2, 185–186.
 17. Robitaille P.M. Blackbody radiation in optically thick gases? *Progr. Phys.*, 2014, v. 10, no. 3, submitted for publication.
 18. Guo Y., Cortez C.L., Molesky S., and Jacob Z. Broadband super-Planckian thermal emission from hyperbolic metamaterials. *Appl. Phys. Lett.*, 2012, v. 101, 131106.
 19. Biehs S.A., Tschikin M., Messina R. and Ben-Abdallah P. Super-Planckian near-field thermal emission with phonon-polaritonic hyperbolic metamaterials. *Appl. Phys. Lett.*, 2013, v. 102, 131106.
 20. Petersen S.J., Basu S. and Francoeur M. Near-field thermal emission from metamaterials. *Photonics and Nanostructures — Fund. Appl.*, 2013, v. 11, 167–181.
 21. Yu Z., Sergeant N.P., Skauli T., Zhang G., Wang H., and Fan S. Enhancing far-field thermal emission with thermal extraction. *Nature Comm.*, 2013, DOI: 10.1038/ncomms2765.
 22. Yu Z., Sergeant N., Skauli T., Zhang G., Wang H. and Fan S. Thermal extraction: Enhancing thermal emission of finite size macroscopic blackbody to far-field vacuum. 4 Nov 2012, arXiv:1211.0653v1 [physics.optics].
 23. Nefedov I.S. and Melnikov L.A. Super-Planckian far-zone thermal emission from asymmetric hyperbolic metamaterials. 14 Feb 2014, arXiv:1402.3507v1 [physics.optics].
-

Digital Gamma-Neutron Discrimination with Organic Plastic Scintillator EJ 299-33

Sheth Nyibule¹, Eric Henry², Jan Töke², Wojtek Skulski¹, Wolf-Udo Schröder^{2,1}

¹Department of Physics and Astronomy, University of Rochester, P.O. Box 270171, 14627, Rochester, New York. E-mail: sochieng@pas.rochester.edu

²Department of Chemistry, University of Rochester, P.O. Box 270216, 14627, Rochester, New York. E-mail: schroeder@chem.rochester.edu

The neutron/gamma pulse shape discrimination (PSD) is measured for the newly discovered plastic scintillator EJ 299-33 using a fast digitizer DDC10. This plastic scintillator (EJ 299-33) discovered by Lawrence Livermore National Laboratory (LLNL) is now commercially available by Eljen Technology. Some of its properties include light output emission efficiency of 56/100 (of Anthracene), wavelength of maximum emission of 420 nm, C:H ratio of 1:1.06 and density of 1.08 g/cm³. The PSD between neutrons and gamma rays in this plastic scintillator is studied using a 5.08-cm diameter by 5.08-cm thick sample irradiated by a neutron-gamma source AmBe-241 and employing charge integration method. The results show that EJ 299-33 has a very good PSD, having a figure of merit of approximately 0.80, 2.5 and 3.09 at 100 KeV, 450 KeV and 750 KeV light outputs respectively. The performance of this new material is compared to that of a liquid scintillator with a well proven excellent PSD performance NE213, having a figure of merit of 0.93, 2.95 and 3.30 at 100 KeV, 450 KeV and 750 KeV respectively. The PSD performance of EJ 299-33 is found to be comparable to that of NE 213.

1 Introduction

For several years efforts to develop plastic scintillators with efficient neutron/gamma discrimination yielded little success [1, 2]. Plastic scintillators are preferred over liquid scintillators for a number of attractive features including low cost, self-containment, and ease of machining. This is why the invention of the plastic scintillator EJ 299-33 [3], with a very good PSD capability has generated a great interest in the community [4–8].

Applications of this type of scintillator in complex nuclear physics experiments or in homeland security and nonproliferation and safeguards are now possible. The goal of this paper is to report our recent off-line evaluation of PSD capability of EJ 299-33.

2 Experimental method

The experiment was performed at Nuclear Science Research Laboratory in Rochester. This experiment was done prior to our in-beam experiment at Laboratori Nazionali del Sud (LNS) in Catania [8]. It was meant to test the response of the organic plastic scintillator EJ 299-33, the same scintillator used in the in-beam experiment. Our results from the in-beam experiments have since been published elsewhere [8].

The experiment was done using a fast digital signal processing module, DDC10 made by SkuTek instruments [9]. The DDC10 is fashioned with 10 analog inputs, each of which is capable of a 14bit analog to digital conversions operating at 100 Ms/s. The neutron/gamma study was performed using neutron-gamma source AmBe-241, shielded with a 5.0-cm lead block which reduced the γ rates to a magnitude comparable to that of neutrons, to irradiate the 5.08-cm diameter

\times 5.08-cm thick EJ 299-33 sample. The plastic scintillator EJ 299-33 was coupled to the photomultiplier (PMT) Hamamatsu R7724 and PMT base of ELJEN model VD23N-7724 operated at 1750 Volts. The liquid scintillator NE-213 was however coupled to PMT XP-2041 operated at 1750 Volts.

In order to separate neutrons from γ -rays, integration is performed in two parts of the pulse from the digital waveforms. The first integration is done from the beginning of the pulse rise time and the other integration is done over the tail part. These two integrals are designated Q_{total} and Q_{tail} respectively. The ratio between them is used to separate neutrons from γ -rays. Thus PSD is defined as

$$PSD = \frac{Q_{tail}}{Q_{total}} \quad (1)$$

The point where the tail begins can be optimized for better neutron/gamma separation. For this case, the tail begins 40-ns after the rise time.

The quantitative evaluation of PSD was made using figures of merit (FOM) defined below.

$$FOM = \frac{\Delta X}{(\delta_{\gamma} + \delta_{neutron})} \quad (2)$$

where ΔX is the separation between the gamma and neutron peaks, and δ_{γ} and $\delta_{neutron}$ are the full width at half maximum of the corresponding peaks (see Figs. 2A-F). The separation, ΔX was calculated as the difference between the mean delayed light fraction $\frac{Q_{tail}}{Q_{total}}$, for neutrons and gamma-rays taken as a normal distribution in PSD over a specified energy range [3]

A reference parameter to define a good PSD in the tested sample is arrived at by noting that a reasonable definition

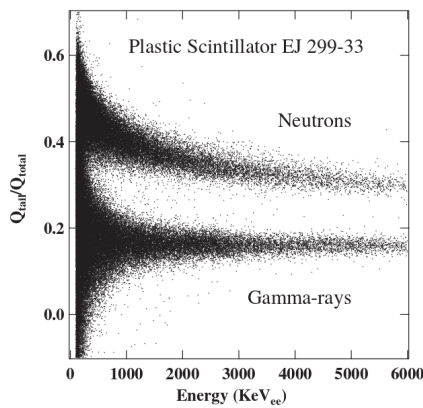


Fig. 1A: Pulse shape discrimination patterns for γ -rays and neutrons obtained using charge integration method for the plastic scintillator EJ 299-33.

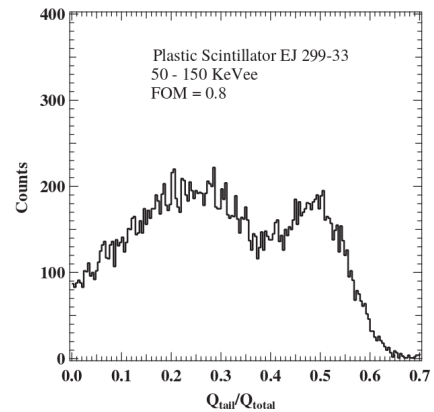


Fig. 2A: PID pattern obtained with organic plastic scintillator EJ 299-33 showing n/ γ separation for the light output cut 50-150 KeVee.

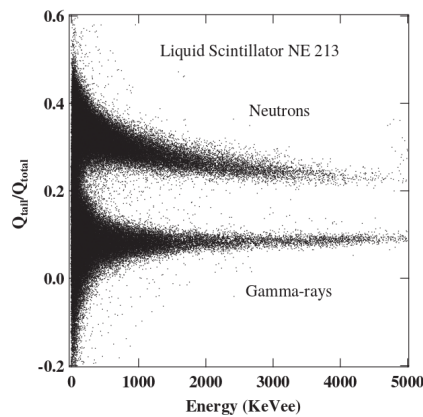


Fig. 1B: Pulse shape discrimination patterns for γ -rays and neutrons obtained using charge integration method for the liquid scintillator NE213.

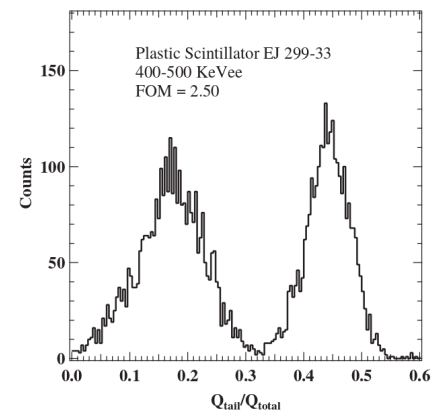


Fig. 2B: PID pattern obtained with organic plastic scintillator EJ 299-33 showing n/ γ separation for the light output cut 400-500 KeVee.

for well separated Gaussian distributions of similar populations sizes is $\Delta X > 3(\sigma_{\text{gamma}} + \sigma_{\text{neutron}})$, where σ is the standard deviation for each corresponding peak. Considering that full width at half maximum for each peak is related to the standard deviation by the expression, $\text{FWHM} \approx 2.36\sigma$, $\text{FOM} \geq 3(\sigma_{\text{gamma}} + \sigma_{\text{neutron}}) / 2.36(\sigma_{\text{gamma}} + \sigma_{\text{neutron}}) \approx 1.27$ is considered a good PSD [3].

3 Experimental results

The main experimental results are represented in Figs. 1A-1B and Figs. 2A-2F. The quality of PSD achieved with the plastic scintillator EJ 299-33 is illustrated in Fig. 1A, where one observes a very good separation of intensity ridges due to γ -rays (effectively recoil electrons) and neutrons (effectively recoil protons). Fig. 1B illustrates similar result but for the standard liquid scintillator NE 213 with proven excellent PSD capability for purposes of comparison. As one observes in 1A-B, the

degree of separation of neutrons from γ -rays for the EJ 299-33 and NE 213 is comparable. This excellent PSD capability is what makes this new scintillator unique among the plastic scintillators and is a welcome feature from the point of neutron detection and identification in the presence of gamma-ray background.

The quality of particle identification (PID) i.e. separation of neutrons and γ -rays is further evidenced by the figure of merit (FOM) as illustrated in Figs. 2A-2C for EJ 299-33 for the energy cuts 100 KeVee, 450 KeVee and 750 KeVee respectively, as indicated by the labels. Figs. 2D-2F show similar results but this case for the liquid scintillator NE 213 included for the purpose of comparison. In order to calculate the FOM, we make energy cut and project only the points within the energy cut along the y -axis. The resulting plot has a PSD along the x -axis and counts on the y -axis as shown in Figs. 2A-2F. The obtained figures of merit suggest the per-

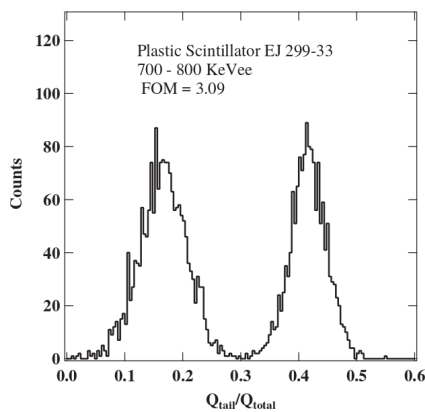


Fig. 2C: PID pattern obtained with organic plastic scintillator EJ 299-33 showing n/γ separation for the light output cut 700-800 KeVee.

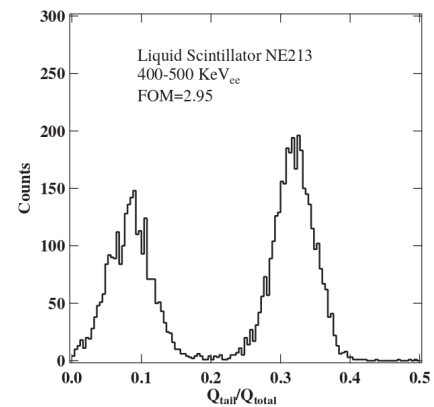


Fig. 2E: PID pattern obtained with organic liquid scintillator NE213 showing n/γ separation for the light output cut 400-500 KeVee.

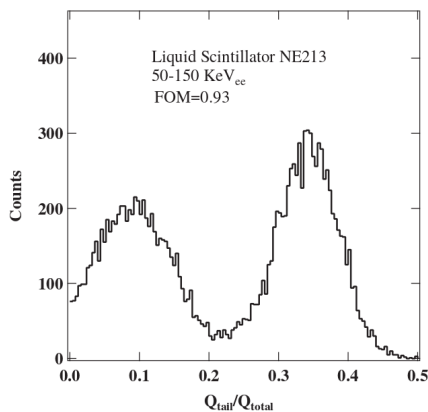


Fig. 2D: PID pattern obtained with organic liquid scintillator NE213 showing n/γ separation for the light output cut 50-150 KeVee.

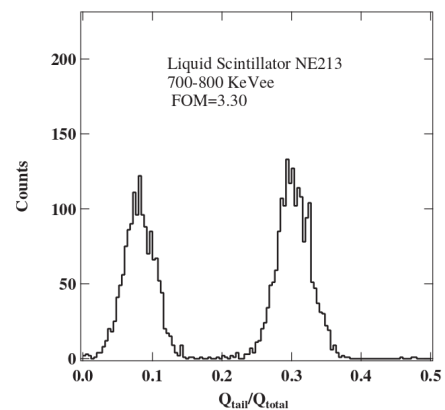


Fig. 2F: PID pattern obtained with organic liquid scintillator NE213 showing n/γ separation for the light output cut 700-800 KeVee.

formance of the standard liquid scintillator NE 213 and the new plastic scintillator are comparable. This results suggest that the replacement of liquid scintillators by plastic scintillators for applications challenged by the well known problems of liquids such as toxicity, flammability, high freezing points, among others is now possible [3, 4].

4 Summary

The results show excellent PSD capability of the new plastic scintillator EJ 299-33 to a level useful for practical applications in complex nuclear physics experiments, nuclear forensics etc. Along with its good charged particle identification [8], EJ 299-33 is expected to provide a viable alternative to the widely used CsI(Tl) detector.

Acknowledgements

The work was supported by the U.S. Department of Energy Grant no. DE-FG02-88ER40414.

Submitted on April 17, 2014 / Accepted on April 26, 2014

References

1. Birks J. B. The theory and Practice of Scintillation Counting. Pergamon Press, London, 1963.
2. Knoll G.F. Radiation Detection and Measurements. John Wiley and Sons, Inc. 2007.
3. Zaitzeva N., Benjamin L. P., Iwona P., Andrew G., Paul H. M., Leslie C., Michele F., Nerine C., Stephen P. *Nuclear Instruments and Methods in Physics Research*, 2012, v. A668, 88–93.
4. Pozzi S. A., Bourne M. M., Clarke S. *Nuclear Instruments and Methods in Physics Research*, 2013, v. A723, 19–23.
5. Cester D., Nebbia G., Pino F., Viesti G. *Nuclear Instruments and Methods in Physics Research*, 2014, v. A748, 33–38.
6. Preston R. M., Eberhard J. E., Tickner J. R. *Journal of Instrumentation*, 2013, issue 8, P12005.
7. Favalli A. *IEEE Nuclear Science*, 2013, v. 60, 1053.
8. Nyibule S., Henry E., Töke J., Schöder U. W. *Nuclear Instruments and Methods in Physics Research*, 2013, v. A728, 36–39.
9. <http://www.skutek.com>

LETTERS TO PROGRESS IN PHYSICS**Blackbody Radiation in Optically Thick Gases?**

Pierre-Marie Robitaille

Department of Radiology, The Ohio State University, 395 W. 12th Ave, Columbus, Ohio 43210, USA.
robitaille.1@osu.edu

In this work, the claim that optically thick gases can emit as blackbodies is refuted. The belief that such behavior exists results from an improper consideration of heat transfer and reflection. When heat is injected into a gas, the energy is primarily redistributed into translational degrees of freedom and is not used to drive emission. The average kinetic energy of the particles in the system simply increases and the temperature rises. In this respect, it is well-known that the emissivity of a gas can drop with increasing temperature. Once reflection and translation are properly considered, it is simple to understand why gases can never emit as blackbodies.

Supposing all the above conditions to have been verified, then the physicist's picture of the external universe has only one further requirement to fulfill. Throughout its whole composition it must be free from everything in the nature of a logical incoherence. Otherwise the researcher has an entirely free hand. [Intellectual freedom]... is not a mere arbitrary flight into the realms of fancy.

Max Planck, Where is Science Going? 1932 [1]

1 Introduction

In the laboratory, blackbodies are specialized, heated, and opaque enclosures, whose internal radiation is determined by the Planckian function [2, 3]. Not all cavities contain this type of radiation, even if Kirchhoff's law of thermal emission had dictated such an outcome [4, 5]. There are demonstrable shortfalls in Kirchhoff's ideas [6–15] and arbitrary cavities are not black. Everything is very much dependent on the nature of the walls [6–15].

Nonetheless, it can be shown that the interior of a cavity is lined with a nearly ideal absorber, or subjected to the action of a carbon particle [8–10], then it can support black body radiation [15]. It is also possible, under special circumstances, to drive the reflectivity of a cavity through a temporary violation of thermal equilibrium [15]. Under those conditions, a cavity, if it has walls which can support Lambertian radiation, might also come to be filled with black radiation. These are unique settings which do not ratify Kirchhoff's claims [15].

In its proper formulation, the law which governs radiation in arbitrary cavities [14, 15] under the limits set by Max Planck [2, 3], combines the laws of Kirchhoff [4, 5] and Stewart [16] (see Eq. 1 and 9 in [15]). These solutions include the effect of reflectivity, which can act to produce substantial deviations from the behavior expected for cavity radiation, as advanced in 1860 [4, 5]. That real materials possess reflectivity implies that they cannot generate a blackbody spectrum without driving this reflective component [15].

2 Optically thick gases

Finkelburg [17] advocated that optically thick gases can also produce blackbody radiation [3–6], since he did not properly consider reflection and energy transfer within a gas. Real gases can never meet the requirements for generating a blackbody spectrum, as they possess both convection and reflection.

Relative to the claim that optically thick gases [17] can sustain blackbody radiation [2, 3], the arguments advanced [17] fail to properly address the question. It is easy to demonstrate that, if reflection is not considered, cavity radiation will always be black, independent of the nature of the walls [8–10, 15]. However, real materials, including gases, possess reflection. As a direct consequence, this property must be included.

In his classic paper [17], Finkelburg makes the suggestion that even if gases are transparent at certain frequencies, they can come to absorb slightly over all frequencies because “*a thermally excited gas by necessity is ionized to a certain, though occasionally small degree*”. He continues, “*As a consequence of this ionization, a continuous spectrum resulting from the stopping of the free discharge electrons in the fields of the positive ions covers the whole spectral region. The same applies (with largely varying intensity) for a number of continuous spectra beyond the series limits where the emission results from recombination of free electrons with ions into different excited states of atoms. Even if any broadening of the discrete lines or bands emitted by the gas is disregarded the absorption coefficient of every luminous gas thus is different from zero for 'all' wave-lengths*” [17]. In this respect, Finkelburg has overlooked that internal reflection within the gas is also likely to be different from zero at all wavelengths.

Finkelburg failed to properly address the reflection. That is why he advocated that optically thick gases could emit as blackbodies. He made the assumption that surface reflectivity was negligible in a gas [17]. Yet, since gases have no surfaces,

there can be little relevance in such statements.

The reality remains that all gases possess internal reflection over certain wavelengths and that this characteristic cannot be distinguished from emissivity.* Unlike the transmissivity, the reflective properties of a gas remain independent of path length and is an ever present property which cannot be ignored. Photons can be reflected within a gaseous system, even if no surface exists. This is not the same as if the photons were emitted because reflection is a driven phenomenon which involves an external source to drive the departure from thermal equilibrium [15].

It has recently been argued that, in order to obtain black radiation in an arbitrary cavity, the reflectivity of a material must be driven [15]. While gases cannot be characterized by reflectivity, since they do not have a surface, they do possess internal reflection. In order for a gas to gain a blackbody appearance, it is this reflection which must be driven.

Yet, there are only two ways in which reflection can be driven. The first method, adopted by Max Planck, involves placing a small carbon particle within the cavity of interest [15]. Obviously, this cannot be achieved when considering optically dense gases in space. The second method involves driving the reflection, by the addition of energy [15], without an associated change in temperature.†

For a gas to emit like a blackbody, it must be possible to channel energy into this system and produce an excess of emission over absorption. This must occur in a manner which can serve to drive reflection [16], rather than promote convection and increase temperature. However, within a gas, this is extremely unlikely to occur. Gases are known to increase their temperature in response to the inflow of energy. They do not easily increase their emissivity [18]. In fact, the emissivities of some gases are known to drop with increasing temperature, directly confirming this conclusion [18, p.214–217]. Gases primarily respond to energy by channeling it into translational (not simply in their vibrational, rotational, or electronic) degrees of freedom. Gases increase their average kinetic energy, hence their temperature. When confronted with heat, the atoms of a gas do not simply conserve their kinetic energy in order to promote emission. Therefore, gases can never act as blackbodies, since they can easily access convection. This situation is completely unlike a solid, like graphite, which cannot invoke convection to deal with the influx of energy. Planck insisted that blackbodies have rigid walls [3].

*When monitoring a gas, it is impossible to ascertain whether a photon which reaches the detector from the “interior of the gas” has been directly produced by emission, or whether the photon has undergone one or more reflections before arriving at the detector.

†This second method relies on a temporary departure from thermal equilibrium. In the case of real cavities, a situation such as $\epsilon_v = \kappa_v + \delta\rho_v$ must be considered, where ϵ_v corresponds to emissivity, κ_v to absorptivity, and $\delta\rho_v$ to that fraction of the reflectivity which has been driven [15]. In a gas, we can reformulate this relationship in terms of emissive and absorptive powers, E and A , and obtain $E = A + \delta R \cdot I$, where δR is the fraction of the internal reflection which has been driven by some function, I [15].

There can be no convection.

As a side note, all experiments on pure gases on Earth involve some form of container. This places the gas within the confines of an enclosure, which though not necessarily opaque to photons, will act to permit gaseous atoms to experience collisional broadening. Such an effect can dramatically alter the conclusions reached, when studying gases in the laboratory versus how gases behave in the unbounded conditions of space. It is not possible for Finkelburg to assert that “*Even if any broadening of the discrete lines or bands emitted by the gas is disregarded the absorption coefficient of every luminous gas thus is different from zero for ‘all’ wavelengths*” [4], as the experimentalist who is studying a gas remains restricted to his container and the effects which it imposes on his conclusions. Obviously, if no broadening of the lines can be observed, then the gas under study is even further from approaching the blackbody spectrum. If broadening does not occur, then the lines, by definition, remain sharp and this implies no absorption between the bands.

3 Discussion

When the interaction between a photon and a gas is considered, one must include the effect of reflection or scattering. Such processes are ignored in all derivations which lead to the conclusion that gases can act as blackbodies, when they are sufficiently optically thick [17]. A gaseous atom can interact briefly with a photon and this can result in diffuse reflection or scattering. This term prevents any mathematical proof that all gases, given sufficient optical thickness, can act as blackbodies. The proper equations for radiation in thermal equilibrium with an enclosure, even in the illogical scenario that a gas can be in thermal equilibrium with a self-provided enclosure, involves reflection [15]. The momentary loss of thermal equilibrium, associated with the injection of an infinitesimal amount of heat into a gas, is seldom associated with increased emissivity and the ability to drive reflection [15]. Rather, the additional energy is channeled towards the translational degrees of freedom.

Gases can easily support convection. That is why no gas can ever behave as a blackbody, even when “optically thick”.

Long ago, Sir William Huggins and his wife, Margaret Lindsay Huggins [19], demonstrated that planetary nebula can manifest extremely sharp lines in spite of their great spatial extent [20, p. 87]. These findings provide strong evidence that astronomical gases do not emit as blackbodies.

As previously emphasized [6–15], condensed matter is absolutely required for the production of a thermal spectrum.

Dedication

This work is dedicated to Larry and Winifred, in thanksgiving for their friendship and encouragement.

Submitted on: May 1, 2014 / Accepted on: May 4, 2014
First published online on: May 7, 2014

References

1. Planck M. The new science — 3 complete works: Where is science going? The universe in the light of modern physics; The philosophy of physics. [Translated from the German by James Murphy and W.H. Johnston], Meridian Books, New York, 1959, p. 45.
2. Planck M. Über das Gesetz der Energieverteilung im Normalspektrum. *Annalen der Physik*, 1901, v. 4, 553–563.
3. Planck M. The Theory of Heat Radiation. P. Blakiston's Son & Co., Philadelphia, PA, 1914.
4. Kirchhoff G. Über das Verhältnis zwischen dem Emissionsvermögen und dem Absorptionsvermögen der Körper für Wärme und Licht. *Poggendorfs Annalen der Physik und Chemie*, 1860, v. 109, 275–301. (English translation by F. Guthrie: Kirchhoff G. On the relation between the radiating and the absorbing powers of different bodies for light and heat. *Phil. Mag.*, 1860, ser. 4, v. 20, 1–21).
5. Kirchhoff G. Über den Zusammenhang zwischen Emission und Absorption von Licht und Wärme. *Monatsberichte der Akademie der Wissenschaften zu Berlin*, sessions of Dec. 1859, 1860, 783–787.
6. Robitaille P.-M. On the validity of Kirchhoff's law of thermal emission. *IEEE Trans. Plasma Sci.*, 2003, v. 31, no. 6, 1263–1267.
7. Robitaille P.M. Robitaille P. M. L. An analysis of universality in blackbody radiation. *Progr. Phys.*, 2006, v. 2, 22–23; arXiv:physics 0507007.
8. Robitaille P.-M. A critical analysis of universality and Kirchhoff's law: A return to Stewart's law of thermal emission. *Progr. Phys.*, 2008, v. 3, 30–35.
9. Robitaille P.-M. Blackbody radiation and the carbon particle. *Progr. Phys.*, 2008, v. 3, 36–55.
10. Robitaille P.-M. Kirchhoff's law of thermal emission: 150 years. *Progr. Phys.*, 2009, v. 4, 3–13.
11. Robitaille P.-M. Blackbody radiation and the loss of universality: Implications for Planck's formulation and Boltzmann's constant. *Progr. Phys.*, 2009, v. 4, 14–16.
12. Robitaille P.-M. Further insight relative to cavity radiation: A thought experiment refuting Kirchhoff's law. *Progr. Phys.*, 2014, v. 10(1), 38–40.
13. Robitaille P.-M. Further insight relative to cavity radiation II: Gedanken experiments and Kirchhoff's law. *Progr. Phys.*, 2014, v. 10(2), 116–120.
14. Robitaille P.M. On the equation which governs cavity radiation. *Progr. Phys.*, 2014, v. 10, no. 2, 126–127.
15. Robitaille P.M. On the equation which governs cavity radiation II. *Progr. Phys.*, 2014, v. 10, no. 3, 157–162.
16. Stewart B. An account of some experiments on radiant heat, involving an extension of Prévost's theory of exchanges. *Trans. Royal Soc. Edinburgh*, 1858, v. 22, no. 1, 1–20.
17. Finkelburg W. Conditions for blackbody radiation of gases. *J. Opt. Soc. Am.*, 1949, v. 39, no. 2, 185–186.
18. DeWitt D. P. and Nutter G. D. Theory and Practice of Radiation Thermometry. John Wiley and Sons Inc., New York, NY, 1988.
19. Becker B.J. Dispelling the myth of the able assistant: Margaret and William Huggins at work in the Tulse Hill Observatory, in *Creative Couples in the Sciences*, (H.M. Pycior, N.G. Slack, and P.G. Abir-Am, eds.), 1996, Rutgers University Press, 88–111.
20. Watts W.M. and Huggins W. An Introduction to the Study of Spectrum Analysis. Longmans, Green, and Co., London, 1904.

Black Hole Structure in Schwarzschild Coordinates

David Proffitt

Sheerness, UK. E-mail: proffittcenter@gmail.com

In the analysis of the interior region of both stationary and rotating black holes, it is customary to switch to a set of in-falling coordinates to avoid problems posed by the coordinate singularity at the event horizon. I take the view here that to understand the physics of black holes, we need to restrict ourselves to bookkeeper or Schwarzschild coordinates of a distant observer if we are to derive measurable properties. I show that one can derive interesting properties of black holes that might explain some of the observational evidence available without the necessity of introducing further ad hoc conjectures.

1 The Schwarzschild black hole

Birkhoff's theorem [1] assures us that for any non-rotating spherically symmetric distribution of matter, the gravitational effect on any test mass is solely due to whatever mass lies closer to the center of symmetry. This allows us to infer what happens inside the event horizon, by comparing a hypothetical distribution of matter that is identical but with all mass outside the point of interest removed, with that of (say) a collapsing star. Making no further assumptions, let the density at any point inside the event horizon be $\rho_{initial}(r)$ where r is the reduced distance from the center of symmetry. Now consider a test mass m at a distance r_p from the center of a black hole, but inside an event horizon of radius r_{eh} . Now compare this in a thought experiment with a similar test mass m with an identical distribution of mass but with all mass at a distance greater than r_p set to zero. Clearly, our test mass in both cases will head towards the origin, but so too will every other particle that makes up the mass distribution $\rho_{initial}$ but is not yet at the origin. In our thought experiment, the spherical mass distribution will become increasingly compressed with our test particle riding on the collapsing surface. A point in time will be reached in our thought experiment where the mass enclosed by the collapsing surface becomes a black hole in its own right. To a distant observer, the test mass can then never in a finite time cross the event horizon formed by this newly created black hole. This will be true in our thought experiment, and thus must be equally true in the original black hole. At this point in time, to have formed a black hole, we must have

$$r' = \frac{2Gm'}{c^2},$$

where m' is the total mass enveloped by a surface with a radius of r' . As the test mass was at an arbitrary distance from the origin, this will become equally true for every point within the event horizon of the original black hole. As a consequence, the eventual distribution of mass must be such that for all r less than r_{eh}

$$r = \frac{2G}{c^2} \int_0^r 4\pi r'^2 \rho(r') dr'$$

with $\rho(r)$ being the eventual mass distribution function. This relation is satisfied by

$$\rho(r) = \frac{c^2}{8\pi G r^2}.$$

The black hole has a density inside its outer event horizon that is inversely proportional to the square of the (reduced) distance from the origin.

2 The Kerr black hole

In Boyer-Lindquist coordinates [2], there is a spherical inner event horizon for a Kerr black hole [3]; also in the limit of zero rotation, these coordinates, not surprisingly, reduce to Schwarzschild coordinates. The curvature tensors at the surfaces of the (inner) event horizons seem very different but are in fact identical. To understand this, see section 3, below. Therefore, in Boyer-Lindquist coordinates, both the Kerr black hole and the Schwarzschild black hole, have identical gravitational fields at their respective event horizons and therefore identical internal structure as a consequence of the holographic principle [4]. Let us clarify this: they are identical in Boyer-Lindquist coordinates but not from a viewing platform here on earth. From here, the spinning black hole will have an event horizon that appears as an oblate spheroid.

3 Comparing infinities

Consider two men with infinite piles of money, but with one having additional small piles of money. Which is the richer? Clearly they are equal. This was an example using scalar quantities, but let us extend this to vectors. Two vectors each have an infinite component but one of them has additional non-zero components at right angles. Which is the larger? Convert to polar coordinates to see that again they are equal. The same is true for tensors. Consider first two tensors each with one large and equal (but not infinite) component, but one tensor having small non-zero additional components (the other having all other components at zero). Now scale all components to the size of the largest by dividing through by the largest component. Then let the largest component increase without limit. The largest component remains at unity

whilst all other components approach zero. Thus we are left with two identical tensors.

4 Consequences

With this solution, every point inside a black hole is sitting on a local event horizon, where, to a distant observer, time stands still, and so no two points inside a black hole will ever move closer together. Consequently, the black hole must be truly rigid in a way that no other physical object can be; it then follows directly from consideration of the Ehrenfest paradox [5] that the angular velocity of a black hole can never increase — it is fixed at birth. When a black hole increases in mass, it must also increase in angular momentum in order to keep the angular velocity constant up to the maximum speed of rotation set by the periphery being unable to exceed the speed of light, which thus limits the ultimate size a black hole can grow to. We thus formulate a new fifth law of black hole dynamics: **it is never possible to change the angular velocity of a black hole**. Rigidity means that black holes cannot be deformed by any outside processes, so it is difficult to comprehend a process that will allow black holes to coalesce. Ignoring this problem, it can be seen that the limitations of the laws of black hole dynamics severely restrict the possible outcomes whenever two black holes meet.

5 Observational justification

No definitive experimental evidence to confirm these results is produced at this time, but observe that with stellar black holes we would expect that at creation they would have to have a typical mass range of 3–30 solar masses. One would also expect them to be created with high spin due to the conservation of the angular momentum of the collapsing (spinning) star. This limits the maximum mass that a stellar mass black hole could ever grow to. This may apparently be justified by current observations but leaves the unanswered question of how supermassive black holes are ever formed. I suggest that although black holes may never merge, neutron stars can, and with counter-rotating neutron stars, this can give rise to a stellar mass black hole with exceptionally low spin. These black holes are not so limited in growth as normal stellar mass black holes and could grow to become supermassive. All measurements to date suggest that the spin rates for supermassive black holes are extremely high; that is they are approaching the end of their growth phase.

6 Counterarguments

In general relativity, any convenient system of coordinates can be used and is valid [6]. I suggest that as far as observational data goes, Schwarzschild coordinates are the most appropriate as these alone can correlate with observations. Two different coordinate systems — Schwarzschild and in-falling coordinates — give very different results in the vicinity of a black hole horizon and yet we know that they must

describe the same reality for different observers. Understanding the relation between these two results is therefore crucial to accepting the validity of this result. Consider twins, one of whom descends towards the event horizon of a black hole. We accept that one, the traveler, will appear to be slowing down due to the gravitational effect on the passage of time. However, the traveler sees the opposite: time for the stay at home twin seems to speed up. There is nothing fictitious or illusory about this — if the traveler returns home, he will certainly be younger than his twin. Depending upon how close to the event horizon he travels, he could be many days or years younger. In principal, he could be 100,000 years younger and still not have crossed the event horizon. (Apart from the technical difficulties, we are assuming eternal life.) So when does the traveler cross the event horizon. By his own watch, it may be just a few hours but for the stay at home twin it will be eternity. So the traveler does arrive at the real singularity at the center, but for the stay at home twin, this is after the Universe has ceased to exist. Both are real but only one produces a measurable outcome.

Acknowledgements

I thank Anna Proffitt for many challenging discussions leading to this work.

Submitted on May, 19, 2014 / Accepted on May 21, 2014

References

1. Johansen N. V., Ravndal F. On the discovery of Birkhoff's theorem. arXiv:physics/0508163, 2005
2. Bondi H. Boyer–Lindquist coordinates. *Review of Modern Physics*, 1957, v. 29 (3), 423–428.
3. Kerr R. P. The Kerr and Kerr-Schwarzschild metrics. In: *The Kerr Spacetime*. Cambridge Univ. Press, Cambridge, 2009, pp. 38–72.
4. Susskind L., Lindesay J., and Scarpetta G. An Introduction to Black Holes, Information and the String Revolution. *Hologr. Universe*, 2014, pp. 1–200.
5. Ehrenfest P. Gleichförmige Rotation starrer Körper und Relativitätstheorie. *Physikalische Zeitschrift*, 1909, Bd. 10, 918.
6. Einstein A. How I Constructed the Theory of Relativity. Translated by M. Morikawa. *Association of Asia Pacific Physical Societies (AAPPS) Bulletin*, 2005, v. 15, no. 2, 17–19.

Drude-Schwarzschild Metric and the Electrical Conductivity of Metals

Paulo Roberto Silva

Departamento de Física (Retired Associate Professor), ICEx, Universidade Federal de Minas Gerais, Belo Horizonte, MG, Brazil.
E-mail: prsilvafis@gmail.com

Starting from a string with a length equal to the electron mean free path and having a unit cell equal to the Compton length of the electron, we construct a Schwarzschild-like metric. We found that this metric has a surface horizon with radius equal to the electron mean free path and its Bekenstein-like entropy is proportional to the number of squared unit cells contained in this spherical surface. The Hawking temperature is inversely proportional to the perimeter of the maximum circle of this sphere. Also, interesting analogies on some features of the particle physics are examined.

1 Introduction

Drude model of the electrical conductivity of metals [1, 2], considers that in this medium the free electrons (the electrons in conductors) undergo Brownian motion with an average characteristic time τ between collisions. Due to the Pauli's exclusion principle, only the electrons with energies which are close to the Fermi energy participate in the conduction phenomena. These electrons travel freely on average by a distance called electron mean free path equal to $\ell = v_F \tau$, where v_F is the Fermi velocity.

Meanwhile, let us note the following feature of black hole physics [3]: an observer at a distance greater than R_S (the Schwarzschild or the surface horizon radius) of the black hole's origin, does not observe any process occurring inside the region bounded by this surface.

Going back to the phenomena of electrical conductivity in metals. let us consider (for instance in a copper crystal) an electron in the conduction band which just suffered a collision. In the absence of an external electric field, all the directions in space have equal probability to be chosen in a starting new free flight. Therefore if we take a sphere centered at the point where the electron have been scattered, with radius equal to the electron mean free path, the surface of this sphere may be considered as an event horizon for this process. Any electron starting from this center will be, on average, scattered when striking the event horizon, losing the memory of its previous free flight. Besides this, all lattice sites of the metallic crystal are treated on equal footing, due to the translational symmetry of the system.

This analogy between two branches of physics, general relativity (GR) and the electrical conduction in metals (ECM), will be considered in the present work. As we will see, we are going to use the GR tools to evaluate some basic quantities related to ECM. We are also going to use some concepts related to the study of particle lifetimes in particle physics (PP).

2 The electron mean free path as a Schwarzschild radius

Let us consider a string of length ℓ (coinciding with the electron mean free path), composed by N unit cells of size equal

to the Compton wavelength of the electron (λ_C). Associating a relativistic energy pc to each of these cells, we have an overall kinetic energy K given by

$$K = Npc = \frac{\ell}{\lambda_C} pc = \left(\frac{\ell mc^2}{h} \right) p. \quad (1)$$

In a paper entitled: "Is the universe a vacuum fluctuation?", E.P. Tryon [4] considers a universe created from nothing, where half of the mass-energy of a created particle just cancels its gravitational interaction with the rest of matter in the universe. Inspired by the Tryon proposal we can write

$$K + U = 0 \quad (2)$$

implying that

$$U = -K = - \left(\frac{\ell mc^2}{h} \right) p. \quad (3)$$

However, we seek for a potential energy which depends on the radial coordinate r , and by using the uncertainty relation $p = \frac{h}{r}$, we get

$$U = - \left(\frac{\ell mc^2}{r} \right). \quad (4)$$

Next we deduce a metric, in the curved space, which is governed by the potential energy defined in (4). We follow the procedure established in reference [5]. A form of equivalence principle was proposed by Derek Paul [6], and when it is applied to the potential energy (4) yields

$$\hbar d\omega = dU = \frac{\ell mc^2}{r^2} dr. \quad (5)$$

Now we consider de Broglie relation

$$\hbar\omega = 2mc^2. \quad (6)$$

Dividing (5) by (6) yields

$$\frac{d\omega}{\omega} = \frac{\ell}{2r^2} dr. \quad (7)$$

Performing the integration of (7) between the limits ω_0 and ω , and between R and r , we get

$$\omega = \omega_0 \exp\left(-\frac{\ell}{2}\left(\frac{1}{r} - \frac{1}{R}\right)\right) \quad (8)$$

and

$$\omega^2 = \omega_0^2 \exp\left(-\ell\left(\frac{1}{r} - \frac{1}{R}\right)\right). \quad (9)$$

Making the choice $R = \ell$, leads to

$$\omega^2 = \omega_0^2 \exp\left(1 - \frac{\ell}{r}\right) \quad (10)$$

Then we construct the auxiliary metric

$$d\sigma^2 = \omega^2 dt^2 - k^2 dr^2 - r^2 (d\theta^2 + \sin^2 \theta d\phi^2). \quad (11)$$

In (11) we take k^2 , such that

$$\frac{k^2}{k_0^2} = \frac{\omega_0^2}{\omega^2}. \quad (12)$$

Relation (12) is a reminiscence of the time dilation and space contraction of special relativity. Now we seek for a metric which becomes flat in the limit $r \rightarrow \infty$. This can be accomplished by defining [7]

$$\omega^2 = \ln\left(\frac{\omega^2}{\omega_0^2}\right), \quad \text{and} \quad k^2 = \frac{1}{\omega^2}. \quad (13)$$

Making the above choices we can write

$$ds^2 = \left(1 - \frac{\ell}{r}\right) dt^2 - \left(1 - \frac{\ell}{r}\right)^{-1} dr^2 - r^2 (d\theta^2 + \sin^2 \theta d\phi^2). \quad (14)$$

We observe that (14) is the Schwarzschild metric, where ℓ is just the Schwarzschild radius of the system.

3 A Schwarzschild-like metric

In the last section we deduced a metric where the so called Schwarzschild radius is just the conduction's electron mean free path. But that construction seems not to be totally satisfactory, once the viscous character of the fluid embedding the charge carriers has not yet been considered. By taking separately in account the effect of the viscous force, we can write

$$m \frac{dv}{dt} = -\frac{p}{\tau^*}. \quad (15)$$

In (15), τ^* is a second characteristic time, which differs from the first one τ that was defined in the previous section. Pursuing further we write

$$v dt = dr, \quad \text{and} \quad p = \frac{h}{r}. \quad (16)$$

Upon inserting (16) into (15), and multiplying (15) by v and integrating, we get the decreasing change in the kinetic energy of the conduction's electron as

$$\Delta K_{qt} = -\frac{h}{\tau^*} \ln\left(\frac{r}{R}\right), \quad (17)$$

where R is some radius of reference.

Next, by defining $\Delta U_{qt} = -\Delta K_{qt}$, we have the total potential energy U_t , namely

$$U_t = U + \Delta U_{qt} = -\frac{mc^2 \ell}{r} + \frac{h}{\tau^*} \ln\left(\frac{r}{R}\right). \quad (18)$$

In the next step, we consider the equivalence principle [6] and de Broglie frequency to a particle pair, writing

$$\frac{dU}{2mc^2} = \frac{d\omega}{\omega} = \frac{\ell}{2} \left(\frac{dr}{r^2}\right) + \frac{1}{2} \left(\frac{dr}{r}\right). \quad (19)$$

Upon integrating we get

$$\omega = \omega_0 \exp\left(-\frac{\ell}{2r} + \frac{1}{2} \ln\left(\frac{er}{\ell}\right)\right). \quad (20)$$

In obtaining (20), we have also made the choices

$$mc^2 \tau^* = h, \quad \text{and} \quad \frac{r}{R} = \frac{er}{\ell}. \quad (21)$$

Squaring (20), yields

$$\omega^2 = \omega_0^2 \exp\left(-\frac{\ell}{r} + \ln\left(\frac{er}{\ell}\right)\right). \quad (22)$$

Defining

$$\omega^2 = \ln\left(\frac{\omega^2}{\omega_0^2}\right), \quad \text{and} \quad k^2 = \frac{1}{\omega^2}, \quad (23)$$

we finally get

$$ds^2 = \left(\ln\left(\frac{er}{\ell}\right) - \frac{\ell}{r}\right) dt^2 - \left(\ln\left(\frac{er}{\ell}\right) - \frac{\ell}{r}\right)^{-1} dr^2 - r^2 d\Omega^2. \quad (24)$$

Relation (24) is a Schwarzschild-like metric [5], that displays the same qualitative behavior like that describing the Schwarzschild geometry. We also have used in (24) a compact form of writing the solid angle differential, namely $d\Omega$ (please compare with the last term of eq. (11)).

4 Average collision time as a particle lifetime

There are two characteristics linear momenta that we can associate to the free electrons responsible for the electrical conductivity of metals. They are the Fermi momentum mv_F and the Compton momentum mc . By taking into account the fermionic character of the electron, we will write a non-linear

Dirac-like equation describing the “motion” of this particle. We have [8]

$$\frac{\partial\psi}{\partial x} - \frac{1}{c} \frac{\partial\psi}{\partial t} = \frac{mv_F}{\hbar} \psi - \frac{mc}{\hbar} |\psi^* \psi|. \quad (25)$$

We see that eq. (25) contains only first order derivatives of the field ψ . Besides this, the field ψ exhibits not a spinorial character. Taking the zero of (25) and solving for $|\psi^* \psi|$, we get

$$|\psi^* \psi| = \frac{v_F}{c}. \quad (26)$$

On the other hand in the collision process, the conduction's electron loss its memory. We may think that this feature looks similar to the annihilation of a particle-anti particle pair, each of mass-energy equal to E_F . Putting this in a form of the uncertainty principle yields

$$2E_F \Delta t = \frac{h}{2} \quad \text{or} \quad \frac{h\nu}{2} = 2E_F. \quad (27)$$

Solving equation (27) for ν , we get

$$\nu = \frac{1}{\Delta t} = 4 \frac{E_F}{h}. \quad (28)$$

By combining the results of (28) and (26) we obtain the line width Γ tied to the “particle” decay

$$\Gamma = \nu |\psi^* \psi| = \frac{4E_F v_F}{hc}. \quad (29)$$

The averaged time between collisions τ is then given by

$$\tau = \frac{1}{\Gamma} = \frac{hc}{4E_F v_F}. \quad (30)$$

Now, let us compare the two characteristic times appearing in this work. By considering (21) and (30), we get

$$\frac{\tau}{\tau^*} = \frac{1}{2} \left(\frac{c}{v_F} \right)^3 \quad (31)$$

and the electron mean free path

$$\ell = v_F \tau = \frac{1}{2} \left(\frac{c}{v_F} \right)^2 \frac{h}{mc}. \quad (32)$$

Evaluating the number of unit cells in the string of size ℓ , we have

$$N = \frac{\ell}{\lambda_C} = \frac{mc^2}{4E_F}. \quad (33)$$

It is also possible to define an effective gravitational constant G_W as

$$\ell = 2 \frac{G_W N m}{c^2} = \frac{G_W m^2}{2E_F}. \quad (34)$$

Taking $M = Nm$, we can write

$$2 \frac{G_W M}{c^2} = \ell = \frac{G_W m}{v_F^2}, \quad (35)$$

which leads to

$$M = \frac{1}{2} m \left(\frac{c}{v_F} \right)^2. \quad (36)$$

In order to better numerically evaluate the quantities we have described in this work, let us take

$$E_F = \frac{1}{4} \alpha^2 m c^2. \quad (37)$$

This value for E_F [eq. (37)], is representative of the Fermi energy of metals, namely it is close to the Fermi energy of the copper crystal. Using (37) as a typical value of E_F , we get

$$\left(\frac{c}{v_F} \right)^2 = \frac{2}{\alpha^2}. \quad (38)$$

Inserting (38) into the respective quantities we want to evaluate, we have

$$\ell = \frac{h}{\alpha^2 m c}, \quad \tau = \frac{\sqrt{2} h}{\alpha^3 m c^2}, \quad M = \frac{m}{\alpha^2}. \quad (39)$$

Putting numbers in (39) yields

$$\ell = 453 \text{ \AA}, \quad \tau = 2.93 \cdot 10^{-14} \text{ s}, \quad M = 9590 \frac{\text{MeV}}{c^2}. \quad (40)$$

It would be worth to evaluate the strength of G_W . We have

$$G_W M^2 \sim 10^{-8} \hbar c. \quad (41)$$

We notice that M is approximately equal to ten times the proton mass.

5 The event horizon temperature and entropy

To obtain the Hawking [9, 11, 12] temperature of this model, we proceed following the same steps outlined in reference [5]. First, by setting $t \rightarrow i\tau$, we perform Wick rotation on the metric given by (24). We write

$$ds^2 = -(y d\tau^2 + y^{-1} dr^2 + r^2 d\Omega^2), \quad (42)$$

where y is given by

$$y = \ln \left(\frac{er}{\ell} \right) - \frac{\ell}{r}. \quad (43)$$

Now, let us make the approximation

$$y^{\frac{1}{2}} \sim \ell^{-\frac{1}{2}} \left(r \ln \left(\frac{er}{\ell} \right) - \ell \right)^{\frac{1}{2}} = \ell^{-\frac{1}{2}} u^{\frac{1}{2}}. \quad (44)$$

In the next step we make the change of coordinates

$$R d\alpha = \ell^{-\frac{1}{2}} u^{\frac{1}{2}} d\tau, \quad \text{and} \quad dR = \ell^{\frac{1}{2}} u^{-\frac{1}{2}} dr. \quad (45)$$

Upon integrating, taking the limits between 0 and 2π for α , from 0 to β for τ , and from ℓ to r for r , we get

$$R = \ell^{\frac{1}{2}} u^{\frac{1}{2}}, \quad \text{and} \quad R 2\pi = \ell^{-\frac{1}{2}} u^{\frac{1}{2}} \beta. \quad (46)$$

Finally from (46), we find the temperature T of the horizon of events, namely

$$T \equiv \frac{1}{\beta} = \frac{1}{2\pi\ell}. \quad (47)$$

Once we are talking about event's horizon, it would be worth to evaluate the Bekenstein [10–12] entropy of the model. Let us write

$$\Delta F = \Delta U - T\Delta S. \quad (48)$$

In (48), we have the variations of the free energy F , the internal energy U , and the entropy S . In an isothermal process, setting $\Delta F = 0$, and taking $\Delta U = Nmc^2$, and inserting T given by (47), we have

$$\Delta F = \left(\frac{\ell}{\lambda_C}\right)mc^2 - \frac{hc}{2\pi\ell}\Delta S = 0 \quad (49)$$

which leads to

$$\Delta S = 2\pi\left(\frac{\ell}{\lambda_C}\right)^2. \quad (50)$$

The entropy of the event's horizon is then (putting $S_0 = 0$)

$$S = S_0 + \Delta S = 2\pi\left(\frac{\ell}{\lambda_C}\right)^2. \quad (51)$$

6 Conclusion

Therefore the analogy developed in this work between black hole physics and the electrical conductivity of metals is very encouraging. This feature was discussed in a previous paper [8] where the connection with the cosmological constant problem [13] has also been considered

Submitted on May 19, 2014 / Accepted on May 23, 2014

References

1. Kittel C. Introduction to Solid State Physics. 5th Edition, Wiley, 1976, Chapter 6.
2. Silva P.R. et al, Quantum conductance and electric resistivity, Phys. Lett. A, 2006, v. 358, 358–362.
3. Damour T. arXiv: hep-th/0401160.
4. Tryon E.P. Nature, 1973, v. 246, 396.
5. Silva P.R. arXiv: 1302.1491.
6. Paul D. Amer. J. Phys., 1980, v. 48, 283.
7. Jacobson T. arXiv: gr-qc/0707.3222.
8. Silva P.R. Progress in Physics, 2014, v. 10, issue 2, 121–125.
9. Hawking S.W. Commun. Math. Phys., 1975, v. 43, 199.
10. Bekenstein J.D. Phys. Rev. D, 1973, v. 7, 2333.
11. Zee A. Quantum Field Theory in a Nutshell. Princeton University Press, 2003.
12. Silva P.R. arXiv: gr-qc/0605051.
13. Hsu S. and Zee A. arXiv: hep-th/0406142.

Why the Proton is Smaller and Heavier than the Electron

William C. Daywitt

National Institute for Standards and Technology (retired), Boulder, Colorado. E-mail: wcdawitt@me.com

This paper argues that the proton is smaller and heavier (more massive) than the electron because, as opposed to the electron, the proton is negatively coupled to the Planck vacuum state. This negative coupling appears in the coupling forces and their potentials, in the creation of the proton and electron masses from their massless bare charges, and in the Dirac equation. The mass calculations reveal: that the source of the zero-point electric field is the primordial zero-point agitation of the Planck particles making up the Planck vacuum; and that the Dirac-particle masses are proportional to the root-mean-square random velocity of their respective charges.

1 Introduction

The Planck vacuum (PV) is an omnipresent degenerate continuum of negatively charged Planck particles, each of which is represented by $(-e_*, m_*)$, where e_* is the massless bare charge and m_* is the Planck mass [1]. Associated with each of these particles is a Compton radius $r_* = e_*^2/m_*c^2$. This vacuum state is a negative energy state separate from the free space in which the proton and electron exist. That is, the proton and electron do not propagate through the Planck particles within the PV, but their charge- and mass-fields do penetrate that continuum.

The proton and electron cores denoted by (e_*, m_p) and $(-e_*, m_e)$ are “massive” bare charges. The two cores are “shrouded” by the local response of the PV that surrounds them and gives the proton and electron their so-called structure [2]. These two particles are referred to here as Dirac particles because they are stable, possess a Compton radius, $r_p (= e_*^2/m_p c^2)$ and $r_e (= e_*^2/m_e c^2)$ respectively, and obey the Dirac equation. They are connected to the PV state via the three Compton relations

$$r_e m_e c^2 = r_p m_p c^2 = r_* m_* c^2 = e_*^2 \quad (= c\hbar) \quad (1)$$

which are derived from the vanishing of the coupling equations in (2).

In their rest frames the Dirac particles exert a two-term coupling force on the PV that takes the form [3]

$$F(r) = \mp \left(\frac{e_*^2}{r^2} - \frac{mc^2}{r} \right) = \mp \frac{e_*^2}{r^2} \left(1 - \frac{r}{r_c} \right) \quad (2)$$

where the \mp sign refers to the proton and electron respectively. The force vanishes at the Compton radius $r_c (= e_*^2/mc^2)$ of the particles, where m is the corresponding mass. The PV response to the forces in (2) is the pair of Dirac equations

$$\mp e_*^2 \left(i \frac{\partial}{\partial ct} + \boldsymbol{\alpha} \cdot i\nabla \right) \psi = \mp mc^2 \beta \psi \quad (3)$$

(with the Compton radius $\frac{\mp e_*^2}{\mp mc^2} = r_c$) which describe the dynamical motion of the free Dirac particles.

The potential defined in the range $r \leq r_c$

$$V(r) = \int_r^{r_c} F(r) dr \quad \left(F(r) = -\frac{dV(r)}{dr} \right) \quad (4)$$

leads to (with the help of (1))

$$\frac{V(r)}{mc^2} = \mp \left(\frac{r_c}{r} - 1 - \ln \frac{r_c}{r} \right) \quad (5)$$

with

$$V_p(r \leq r_p) \leq 0 \quad \text{and} \quad V_e(r \leq r_e) \geq 0. \quad (6)$$

For $r \ll r_c$, the potentials become

$$V_p(r) = -\frac{e_*^2}{r} = \frac{(e_*)(-e_*)}{r} \ll 0 \quad (7)$$

and

$$V_e(r) = +\frac{e_*^2}{r} = \frac{(-e_*)(-e_*)}{r} \gg 0 \quad (8)$$

where the final $(-e_*)$ in (7) and (8) refers to the Planck particles at a radius r from the stationary Dirac particle at $r = 0$. The leading (e_*) and $(-e_*)$ in (7) and (8) give the free proton and electron cores their negative and positive coupling potentials.

Equations (6)–(8) show that the proton potential is negative relative to the electron potential — so the proton is more tightly bound than the electron. Thus the Compton relations in (1) imply that the proton is smaller and heavier than the electron. These results follow directly from the fact that the proton has a positive charge, while the electron and the Planck particles in the PV have negative charges.

The masses of the proton and electron [4] [5] are the result of the proton charge $(+e_*)$ and the electron charge $(-e_*)$ being driven by the random zero-point electric field \mathbf{E}_{zp} , which is proportional to the Planck particle charge $(-e_*)$ of the first paragraph. A nonrelativistic calculation (Appendix A) describes the random motion of the proton and electron charges as

$$\frac{2 \ddot{\mathbf{r}}_{\pm}}{3} = \mp \left(\frac{\pi}{2} \right)^{1/2} \frac{c^2}{r_c} \mathbf{I}_{zp} \quad (9)$$

where the upper and lower signs refer to the proton and electron respectively, r_c to their respective Compton radii, and where \mathbf{I}_{zp} is a random variable of zero mean and unity mean square. The radius vector \mathbf{r} [NOT to be confused with the radius r of equations (2) thru (8)] represents the random excursions of the bare charge about its average position at $\langle \mathbf{r} \rangle = 0$. The $2/3$ factor on the left comes from the planar motions (Appendix A) of the charges $\pm e_*$ that create the Dirac masses m_{\pm} . The \mp sign on the right side of (9) is the result of the \mp sign on the right side of the potentials in (5).

After the charge accelerations in (9) are “time integrated” and their root-mean-square (rms) calculated [5], the following Dirac masses emerge (with the help of (1))

$$\frac{m_{\pm}}{m_*} = \frac{2}{3} \frac{\langle \dot{\mathbf{r}}_{\pm}^2 \rangle^{1/2}}{c} \quad (10)$$

where m_{\pm} are the derived masses whose sources are the driven charges — consequently the average center of charge and the average center of mass are the same. Equations (10) and (1) lead to the following ratios

$$\frac{\langle \dot{\mathbf{r}}_+^2 \rangle^{1/2}}{\langle \dot{\mathbf{r}}_-^2 \rangle^{1/2}} = \frac{m_p}{m_e} = \frac{r_e}{r_m} \approx 1800 \quad (11)$$

where the rms random velocity of the proton charge is 1800 times that of the electron charge because of the proton’s negative coupling potential.

2 Summary and comments

The negative and positive potentials in (6)–(8) imply that the proton is smaller and heavier than the electron. Furthermore, these two facts are manifest in the \mp signs of the random motion of the bare charges that create, with the help of the zero-point field \mathbf{E}_{zp} , the Dirac masses m_{\pm} .

In the PV theory, the radian-frequency spectrum of the zero-point electric field is approximately $(0, c/r_*)$, where the upper limit is the Planck frequency c/r_* ($\sim 10^{43}$ rad/s). On the other hand, the rms accelerations and velocities associated with the random variables $\ddot{\mathbf{r}}$ and $\dot{\mathbf{r}}$ in (9)–(11) are predominately associated with the two decades

$$\frac{c}{100r_*}, \quad \frac{c}{10r_*}, \quad \frac{c}{r_*} \quad (12)$$

at the top of that spectrum [6]. Thus the continuous creation of the Dirac masses m_{\pm} takes place in a “cycle time” approximately equal to $200\pi r_*/c \sim 10^{-41}$ sec, rapid enough for the masses in (2) and (3) to be considered constants of the motion described by (3).

The theory of the PV model suggests that the proton and electron are stable particles because the PV response to the coupling forces in (2), i.e. the Dirac equation in (3) with $r_c = e_*^2/mc^2$, maintains the separate identities of the two coupling constants e_*^2 and mc^2 . In other words, the charge and

mass of the free Dirac particle are separate characteristics of the motion in (3), even though the m_{\pm} are derived from the random motion of the bare charges $\pm e_*$.

Appendix A: Dirac masses

The nonrelativistic planewave expansion (perpendicular to the propagation vector $\widehat{\mathbf{k}}$) of the zero-point electric field that permeates the free space of the Dirac particles is [1] [5]

$$\mathbf{E}_{zp}(\mathbf{r}, t) = -e_* \text{Re} \sum_{\sigma=1}^2 \int d\Omega_k \int_0^{k_{c*}} dk k^2 \widehat{\mathbf{e}}_{\sigma} \left(\frac{k}{2\pi^2} \right)^{1/2} \times \exp [i(\mathbf{k} \cdot \mathbf{r} - \omega t + \Theta)] \quad (A1)$$

where $(-e_*)$ refers to the negative charge on the separate Planck particles making up the PV, $k_{c*} = \sqrt{\pi}/r_*$ is the cutoff wavenumber (due to the fine granular nature of the PV [7]), $\widehat{\mathbf{e}}_{\sigma}$ is the unit polarization vector perpendicular to $\widehat{\mathbf{k}}$, and Θ is the random phase that gives the field its stochastic nature.

Equation (A1) can be expressed in the more revealing form

$$\mathbf{E}_{zp}(\mathbf{r}, t) = \left(\frac{\pi}{2} \right)^{1/2} \left(\frac{-e_*}{r_*^2} \right) \mathbf{I}_{zp}(\mathbf{r}, t) \quad (A2)$$

where \mathbf{I}_{zp} is a random variable of zero mean and unity mean square; so the factor multiplying \mathbf{I}_{zp} (without the negative sign) is the rms zero-point field. This equation provides direct theoretical evidence that the zero-point field has its origin in the primordial zero-point agitation of the Planck particles (thus the ratio $-e_*/r_*^2$) within the PV. The random phase Θ in (A1) is a manifestation of this agitation.

The random motion of the massless charges that lead to the Dirac masses m_p and m_e are described by [4] [5]

$$\pm e_* \frac{2}{3} \ddot{\mathbf{r}}_{\pm} = \frac{c^2}{r_c} r_*^2 \mathbf{E}_{zp} = \left(\frac{\pi}{2} \right)^{1/2} \frac{c^2}{r_c} (-e_* \mathbf{I}_{zp}) \quad (A3)$$

which yield the accelerations in (9). The upper and lower signs in (A3) and (9) refer to the proton and electron respectively. The $2/3$ factor is related to the two-dimensional charge motion in the $\widehat{\mathbf{e}}_{\sigma}$ plane. The physical connection leading to these equations is the particle-PV coupling $\mp e_*^2$ in (2).

Finally, there is a detailed (uniform and isotropic at each frequency) spectral balance between the radiation absorbed and re-radiated by the driven dipole $\pm e_* \mathbf{r}$ in (A3); so there is no net change in the spectral energy density of the zero-point field as it continuously creates the proton and electron masses [5] [8].

Submitted on June 7, 2014 / Accepted on June 12, 2014

References

1. Daywitt W.C. The Planck Vacuum. *Progress in Physics*, 2009, v. 1, 20.
2. Daywitt W.C. The Dirac Proton and its Structure. This paper is to be published in the International Journal of Advanced Research in Physical Science (IJARPS). See also www.planckvacuum.com.

3. Daywitt W.C. The Electron and Proton Planck-Vacuum Forces and the Dirac Equation. *Progress in Physics*, 2014, v. 2, 114.
 4. Daywitt W.C. The Source of the Quantum Vacuum. *Progress in Physics*, 2009, v. 1, 27. In the first line of the last paragraph in Appendix A of this paper " $p = \hbar/r_L$ " should read " $myc = \hbar/r_L$ ".
 5. Puthoff H.E. Gravity as a Zero-Point-Fluctuation Force. *Phys. Rev. A*, 1989, v. 39, no. 5, 2333–2342.
 6. Daywitt W.C. Neutron Decay and its Relation to Nuclear Stability. To be published in *Galilean Electrodynamics*. See also www.planckvacuum.com.
 7. Daywitt W.C. The Apparent Lack of Lorentz Invariance in Zero-Point Fields with Truncated Spectra. *Progress in Physics*, 2009, v. 1, 51.
 8. Boyer T.H. Random Electrodynamics: the Theory of Classical Electrodynamics with Classical Electrodynamical Zero-Point Radiation. *Phys. Rev. D*, 1975, v. 11, no. 4, 790–808.
-

The Dichotomous Cosmology with a Static Material World and Expanding Luminous World

Yuri Heymann

3 rue Chandieu, 1202 Geneva, Switzerland. E-mail: y.heyman@yahoo.com

The dichotomous cosmology is an alternative to the expanding Universe theory, and consists of a static matter Universe, where cosmological redshifts are explained by a tired-light model with an expanding luminous world. In this model the Hubble constant is also the photon energy decay rate, and the luminous world is expanding at a constant rate as in de Sitter cosmology for an empty Universe. The present model explains both the luminosity distance versus redshift relationship of supernovae Ia, and ageing of spectra observed with the stretching of supernovae light curves. Furthermore, it is consistent with a radiation energy density factor $(1+z)^4$ inferred from the Cosmic Microwave Background Radiation.

1 Introduction

Our model is inspired by the tired-light theory that was first proposed by [1] to explain cosmological redshifts, which has been subject to other investigations [2–4]. Generally, tired-light models describe a static Universe; however, in the present model only the matter component of the Universe is static, and the luminous component is expanding. The idea of a static Universe was proposed in Einstein’s cosmological model [5], which is the first of the relativist cosmologies. Einstein had to introduce a cosmological constant to make his Universe static; otherwise it would have collapsed due to the gravitational field. Einstein came to the conclusion that his cosmology describes a spatially finite spherical Universe, as he encountered a degeneracy of coefficient $g_{\mu\nu}$ at infinity. Also, Poisson’s equation, $\nabla^2\Phi = 4\pi G\rho$, where Φ is the scalar potential and ρ the matter density, played an important role in Einstein’s cosmology. As Einstein’s wrote in [5]: “It is well known that Newton’s limiting condition of the constant limit for Φ at spatial infinity leads to the view that the density of matter becomes zero at infinity.”

Let us do a simple thought experiment for inertial bodies in an infinite Universe that is isotropic and has no edge in Newton’s absolute Euclidean space. Imagine you are a galaxy, there is a galaxy on your left and on your right, and both exert a gravitational force of same magnitude on you; the two forces would offset and you would not move from your position. From this view, based on the principle of inertia in an absolute Euclidean space, each galaxy in an isotropic Universe would be in this position of equilibrium, and the Universe would be static overall. However, for galaxy clusters where the cluster has an edge, we would expect that the galaxies will end up merging.

De Sitter introduced the concept of “relativity of inertia” based on his analysis of the degeneracy of the $g_{\mu\nu}$ at infinity in Einstein cosmology [6]. To overcome this problem, de Sitter found a solution by extending Einstein’s cosmology in three-

dimensional space to the four dimensional Minkowski space-time — a world of hyperboloid shape — and with no matter. De Sitter’s cosmological model is a solution to Einstein’s field equation applied to a vacuum, with a positive vacuum energy density, and describes an expanding Universe. Contemporary cosmological models based on general relativity such as the Λ CDM assume a uniform distribution of matter in space, but the effect of the deformation of space-time due to massive bodies may be preponderant only locally, hence this hypothesis may not be valid. In special relativity, light moves along the geodesics of the Minkowski space-time, whereas matter is confined in the three-dimensional Euclidean space. From the equivalence principle in curved space-time, an inertial particle and a pulse of light both follow the same geodesic. Contrary to Newtonian physics which describes interactions between bodies, general relativity is often employed to describe the dynamics of light, such as the deflection of light, or the event horizon of black holes. In contrast, the theory of general relativity does not establish such a dichotomy between matter and light; based on the weak field approximation of general relativity [7], Newton’s laws are a good approximation of the properties of physical space only when the gravitational field is weak. As a matter of fact, in the present cosmological model, the luminous portion of the Universe is expanding at a constant rate as in the de Sitter cosmology in a flat Universe; this is also the condition required in order for the model to match the luminosity distance versus redshift relationship of supernovae Ia. The dichotomous cosmology differs in the sense that it is the light wavelength that gets stretched due to a tired-light process and not space itself that expands.

The present model describes the dynamics of light using two transformations. First, we allow a time-varying light wavefront in order to accommodate the stretching of light’s wavelength when photons lose energy. Second, a time dilation is incorporated into the model in order for the light wavefront to stay at the celerity of light. A consequence of this

model is the “time-dilation effect” (a.k.a. the ageing of spectra) observed for supernovae light curves [8] with a stretching of the light curves by a factor $(1 + z)$. In addition, the expanding luminous world is consistent with the radiation energy density factor $(1 + z)^4$ inferred from the CMBR (Cosmic Microwave Background Radiation).

2 Light ageing model

In the tired-light cosmology where redshifts are explained by a decay of the photon energy, the following equation replaces the cosmological redshift equation of the expanding Universe theory:

$$1 + z = \frac{\lambda_{obs}}{\lambda_{emit}} = \frac{E(z)}{E_0}, \tag{1}$$

where λ_{obs} and λ_{emit} are the observed and emitted light wavelength respectively, E_0 the photon energy at reception, and $E(z)$ the photon energy when emitted at redshift z .

A simple law of decay of the photon energy is considered:

$$\frac{\dot{E}}{E} = -H, \tag{2}$$

where E is the photon energy, and H the decay of photon energy. From now on we assume that the decay rate of photon energy is constant over time and is always equal to H_0 .

By integrating (2) we get:

$$E(t) = E_0 \exp(-H_0 t), \tag{3}$$

where t is the time which is equal to zero time of observation, and E_0 the photon energy at reception.

Let us apply the following change of coordinates $T = t_0 - t$, where T is the light travel time when looking back in the past and t_0 the present time. Hence, (3) can be rewritten as follows:

$$E(T) = E_0 \exp(H_0 T), \tag{4}$$

where T is the light travel time when looking back in the past from the earth.

It is shown below that a constant decay rate for the photon energy conforms to the supernovae luminosity distance versus redshift relationship.

3 Light travel time with respect to the point of emission and luminosity distance

Here, we consider a set of two transformations to describe the photon energy decay. During this process the number of light wave cycles is constant, but due to the stretching of light wavelengths when photons lose energy we allow a superluminal light wavefront, resulting in an expansion. Then a time dilation is applied in order to maintain the speed of light at the celerity with respect to the emission point. The velocity of the light wavefront before time dilation is expressed as follows:

$$v(t) = c \frac{E_{emit}}{E(t)}, \tag{5}$$

where E_{emit} is the photon energy at emission, $E(t)$ the photon energy at time t , and c the celerity of light. We note that in (5) the light wavefront is at the speed of light at the point of emission.

In order to maintain the light wavefront at the speed of light with respect to the emission point, the following time dilation is applied:

$$\frac{\delta t'}{\delta t} = \frac{E_{emit}}{E(t)}, \tag{6}$$

where $\frac{\delta t'}{\delta t}$ is a time scale factor between time t' and time t . The light travel time with respect to the point of emission is:

$$T' = \int_{-T}^0 \frac{\delta t'}{\delta t} dt = \int_{-T}^0 \frac{E_{emit}}{E(t)} dt, \tag{7}$$

where T' is the light travel time with respect to the point of emission, and T the light travel time with time-varying speed of light.

Introducing (3) into (7) we get:

$$T' = \frac{E_{emit}}{E_0} \int_{-T}^0 \exp(H_0 t) dt. \tag{8}$$

Integrating (8) we obtain:

$$T' = \frac{E_{emit}}{E_0} \frac{1}{H_0} (1 - \exp(-H_0 T)). \tag{9}$$

By substitution of (4) into (9), we get:

$$T' = \frac{E_{emit}}{E_0} \frac{1}{H_0} \left(1 - \frac{E_0}{E_{emit}} \right). \tag{10}$$

Introducing (1) into (10) we get:

$$T' = \frac{z}{H_0}. \tag{11}$$

After the time dilation (6), the light wavefront is at the speed of light, hence the luminosity distance is expressed as follows:

$$\frac{dr_L}{dT'} = c. \tag{12}$$

By integrating (12) between 0 and T' we get the following equation:

$$r_L(T') = cT'. \tag{13}$$

By combining (11) and (13) we get the following relationship between luminosity distance and redshifts:

$$r_L = \frac{c}{H_0} z. \tag{14}$$

Ultimately, we find the linear relationship between luminosity distance and redshifts which is observed in supernovae Ia data. A rectilinear plot of the luminosity distance versus redshift of slope of 14.65 where the luminosity distance is

expressed in *Gly* (billion light years) was obtained in [9] using the redshift adjusted distance modulus [10] which is based on photon flux. The corresponding decay rate of photon energy which is the inverse of the slope from (11) is equal to $H_0 = 2.16 \times 10^{-18} \text{ sec}^{-1}$ or $67.3 \text{ km s}^{-1} \text{ Mpc}^{-1}$.

To compute the luminosity distance, the light travel time with respect to the emission point must be used. In the luminosity distance the light wavefront is maintained at the speed of light with respect to the emission point where the time dilation is equal to unity. For an indication of distances of an object with respect to the observer, the light travel time with respect to the point of observation is used for which the time dilation is equal to unity.

4 Light travel time with respect to the observer

The light travel time measured with respect to the observer is the light travel time obtained with a time dilation equal to unity at the point of observation. In this scenario, the velocity of the light wavefront before time dilation is as follows:

$$v(t) = c \frac{E_0}{E(t)}, \tag{15}$$

Thus, the time-dilation effect is:

$$\frac{\delta t_0}{\delta t} = \frac{E_0}{E(t)}, \tag{16}$$

where $\frac{\delta t_0}{\delta t}$ is a time scale factor between present time t_0 and time t .

Therefore, the light travel time with respect to the observer is:

$$T_0 = \int_{-T}^0 \frac{\delta t_0}{\delta t} dt = \int_{-T}^0 \frac{E_0}{E(t)} dt, \tag{17}$$

where T_0 is the light travel time with respect to the point of observation, and T the light travel time with time-varying speed of light.

Introducing (3) into (17) and integrating we get:

$$T_0 = \frac{1}{H_0} (1 - \exp(-H_0 T)), \tag{18}$$

Introducing (4) into (18) we get:

$$T_0 = \frac{1}{H_0} \left(1 - \frac{E_0}{E_{emit}} \right). \tag{19}$$

Finally, introducing (1) into (19):

$$T_0 = \frac{1}{H_0} \frac{z}{(1+z)}. \tag{20}$$

We note that in (20) when redshift tends to infinity, the light travel time with respect to the observer converges towards $1/H_0$. This is the farthest distance from which light can reach an observer in the Universe. There is a squeezing

effect by the factor $(1+z)$ for the light travel time when measured with respect to the point of observation instead of the point of emission. This squeezing of light travel time is due to the fact that time dilation is relative to the reference point in time from which the light wavefront is measured.

5 Equivalence in the de Sitter cosmology for an expanding Universe

The de Sitter cosmology is dominated by a repulsive cosmological constant Λ which in a flat Universe yields an expansion rate of the Universe H that does not vary over time.

In this cosmology, the luminosity distance is calculated as follows:

$$\frac{dr_L}{dT} = c + H r_L \tag{21}$$

with boundary condition $r_L = 0$ at $T = 0$, where r_L is the luminosity distance, T the light travel time between emission and observation of the light source, and H the Hubble constant at time T .

By integrating (21) we get:

$$r_L = \frac{c}{H_0} (\exp(H T) - 1). \tag{22}$$

Because $dt = \frac{da}{H a}$, where a is the scale factor, the light travel time versus redshift is as follows:

$$T = \int_{1/(1+z)}^1 \frac{da}{H a} = \frac{1}{H} \ln(1+z). \tag{23}$$

Eqs. (22) and (23) yield:

$$r_L = \frac{c}{H} z, \tag{24}$$

which is the same equation as (14).

A measure of distance is obtained by calculating the corresponding the distance if there were no expansion of the Universe, which we call the Euclidean distance. Consider a photon at a Euclidean distance y from the observer, moving towards the observer. Hence:

$$\frac{dy}{dt} = -c + H y. \tag{25}$$

By setting time zero at a reference T_b in the past, we get $t = T_b - T$; therefore, $dt = -dT$. Hence, (25) becomes:

$$\frac{dy}{dT} = c - H y, \tag{26}$$

with boundary condition $y(T = 0) = 0$.

Solving (26) we get:

$$y = \frac{c}{H} (1 - \exp(-HT)). \tag{27}$$

By substitution of (23) into (27) we get:

$$y = \frac{c}{H} \frac{z}{(1+z)}, \tag{28}$$

which is the same equation as (20) where $T_0 = \frac{y}{c}$.

We have shown that de Sitter cosmology is the equivalent to our light ageing model in an expanding Universe. In the de Sitter cosmology, the cosmological constant Λ corresponding to a positive vacuum energy density sets the expansion rate $H = \sqrt{\frac{1}{3}\Lambda}$ for a flat Universe, which is the photon energy decay rate of light traveling in vacuum.

6 Radiation density and the CMBR

The CMBR was a prediction of the work of George Gamow, Ralph Alpher, Hans Bethe and Robert Herman on the Big Bang nucleosynthesis [11, 12], and was discovered later in 1964 by Penzias and Wilson. It is believed that the CMBR is the remnant radiation of a primordial Universe made of plasma, and that galaxies are formed by gravitational collapse of this plasma phase. Here, we investigate a requirement for the CMBR to originate from a hot plasma.

From Wien's displacement law for thermal radiation from a black body, there is an inverse relationship between the wavelength of the peak of the emission spectrum and its temperature is expressed as follows:

$$\lambda_p T = b, \quad (29)$$

where λ_p is the peak wavelength and T the absolute temperature.

From this law we get:

$$\lambda_{obs} T_0 = \lambda_{emit} T_{emit}, \quad (30)$$

where T_0 is the temperature of the black body spectrum today, which is 2.7 K for the CMBR, and T_{emit} the temperature of the emitting plasma.

Hence:

$$T_{emit} = T_0 \frac{\lambda_{obs}}{\lambda_{emit}} = T_0(1+z). \quad (31)$$

From the Stefan-Boltzmann's law, the energy flux radiating from a black body is as follows:

$$\text{Flux} = \sigma T^4, \quad (32)$$

where σ is the Stefan-Boltzmann constant, and T the temperature of the black body.

Combining (31) and (32), we find that the energy flux of the source of a black body that is redshifted is of order $(1+z)^4$. Hence, the energy flux of the emitting black body must be diluted by a factor $(1+z)^4$. For an expanding luminous phase, the photon flux is diluted by a factor $(1+z)^3$. Because photons lose energy as the light wavelength is stretched, another factor $(1+z)$ must be accounted for, and the resulting energy flux is diluted by a factor $(1+z)^4$. This is the required condition for the redshifted spectrum of a black body to be a black body spectrum itself. It appears that our cosmology with an expanding luminous world is consistent with the radiation energy density inferred from the CMBR.

7 Conclusion

The dichotomous cosmology is inspired by the tired-light model and consists of a static material world and an expanding luminous world. In this model the luminous world is expanding at a constant rate as in de Sitter cosmology. The model consists of two transformations, respectively: (1) to compensate for the stretching of the light's wavelength when the photon loses energy, we allow a time-varying light wavefront; (2) a time-dilation effect is incorporated into the model in order for the light wavefront to stay at the speed of light. This model explains both the luminosity distance versus redshift relationship of supernovae Ia, and "time-dilation effect" observed with the stretching of supernovae light curves. Furthermore, it is consistent with a radiation energy density factor $(1+z)^4$ inferred from the CMBR. This alternative cosmology only differs from the expanding Universe theory from the viewpoint that it is the light wavelength that is stretched due to a tired light process and not space itself that expands.

Submitted on June 8, 2014 / Accepted on June 10, 2014

References

1. Zwicky F. Red shift of spectral lines. *Proc. Nat. Acad. Sci.*, 1929, v. 15 773–779.
2. Pecker, J.-C. and Vigier, J.-P. A possible tired-light mechanism. *Observational Cosmology*, edited by A. Hewitt, G. Burbidge, and L.Z. Fang, 1987. p. 507.
3. Sorrell W.H. Misconceptions about the Hubble recession law. *Astrophysics and Space Science*, 2009, v. 323 205–211.
4. Shao M.H. The energy loss of photons and cosmological redshift. *Physics Essays*, 2013, v. 26 183–190.
5. Einstein A. Kosmologische Betrachtungen zur allgemeinen Relativitätstheorie. *Königlich Preussische Akademie der Wissenschaften (Berlin). Sitzungsberichte (1917)*. Engl. tr.: *Cosmological considerations in the General Theory of Relativity*. The Collected Papers of Albert Einstein, Volume 6, Princeton University Press, 1997. p. 421.
6. De Sitter W. On the relativity of inertia. Remarks concerning Einstein's latest hypothesis. *Koninklijke Nederlandsche Akademie van Wetenschappen Proceedings*, 1917, v. 19 1217–1225.
7. Carroll S.M. *An Introduction to General Relativity Spacetime and Geometry*. Addison Wesley, 2004. p. 153.
8. Blondin S., Davis T.M., Krisciunas K., Schmidt B.P., Sollerman J., Wood-Vasey W.M., Becker A.C., Challis P., Clocchiatti A., Damke G., Filippenko A.V., Foley R.J., Garnavich P.M., Jha S.W., Kirshner R.P., Leibundgut B., Li W., Matherson T., Miknaitis G., Narayan G., Pignata G., Rest A., Riess A.G., Silverman J.M., Smith R.C., Spyromilios J., Stritzinger M., Stubbs C.W., Suntzeff N.B., Tonry J.L., Tucker B.E., and Zenteno A. Time dilation in Type Ia Supernovae spectra at high redshift. *The Astrophysical Journal*, 2008, v. 682 724–736.
9. Heymann Y. On the Luminosity Distance and the Hubble Constant. *Progress in Physics*, 2013, v. 3 5–6.
10. Heymann Y. Redshift Adjustment to the Distance Modulus. *Progress in Physics*, 2012, v. 1 6–7.
11. Alpher R.A., Bethe H. and Gamow G. The origin of chemical elements. *Physical Review*, 1948, v. 73 803–804.
12. Alpher R.A. and Herman R.C. On the relative abundance of the elements. *Physical Review*, 1948, v. 74 1737–1742.

LETTERS TO PROGRESS IN PHYSICS

Tractatus Logico-Realismus: Surjective Monism and the Meta-Differential Logic of the Whole, the Word, and the World

Indranu Suhendro

The Zelmanov Cosmological Group; Secretary of the Abraham Zelmanov Journal for General Relativity, Gravitation, and Cosmology

“Surjective Monism” is a creation of a whole new stage after: 1) “Primitive Monism” of Leibniz, Pascal, and to some extent also the dualist Descartes. 2) “Reflexive-Geometric-Substantial Monism” of Spinoza’s geometric “Tractatus” and “Ethics”, which Einstein embraced, loved and lived, and its variants which he deemed more profound than Kantianism and which one can see very profoundly present in the scientific creation and philosophy of Zelmanov. 3a) “Machian Empirico-Monism” (as formulated in its final form by Bogdanov) along with “Pavlovian Material Monism” (a form defined as supposedly strict “materialistic ontology” in close connection with the school of Sechenov and Pavlov). 3b) “Russellian Neutral-Primitive Monism” (used in process philosophy). Thus “Surjective Monism” finally goes beyond Husserlian Phenomenology, Substantialism, Psychologism, Existentialism, Picture/Logo Theory and the Analytical Philosophy of Mind and Language (of Wittgenstein’s “Tractatus” and its “Language Game Theory” sublimation). It also complements Smarandachean Neutrosophic Logic and Multi-Space Theory. In the above, 3a) and 3b) simply ran developmentally parallel and somewhat competing in history.

Dedicated to the vastly profound intellection, memory, and solitude of A. L. Zelmanov (1913–1987), fountainhead of the celebrated Zelmanov Cosmological School; and to the closely following centennial anniversary of Einstein’s General Theory of Relativity (1915–2015)

1 OMNUS: “Omnetic Reality” and the Summary-Quiddity of Surjective Monism (the Surjective Monad Theory of Reality)

In condensed form, we can present our Reality Theory — Surjective Monism — as the following singular meta-differential picture, i.e., “Qualon-Logos” (“OMNUS” or “Metanon”):

$$M : N(U(g, dg)) \sim S .$$

- 1.1 Reality is absolutely ONE, one-in-itself, beyond concrete and abstract count, beyond even the oft-defined “phenomena” and “noumena” (the way most philosophical abstractions define or attempt them self-limitedly); such that
- 1.2 Between Reality (M), i.e., Reality-in-itself, and Phenomenality (O) there $BE(S)$ — in the four-fold, asymmetric, anholonomic, meta-categorical (meta-differential) Unity of Sight and Sense (i.e., “Universum” (U) of Subject-Reality (g) and Surjectivity-Quality (dg)) of Surjective Monism — (capitalized with emphasis) a Surjective-Reflexive, Omnetic-

Ontometric, Verizontal-Horizontal, Meta-Differential, Diffeo-Unitic Meta-Picture of Reality and Phenomenality, of Being and Existence, of Surject and Reflex, of the Verizon and the Horizon, of Onticity and Epistemicity, of Unity, Unicity, and Multiplicity, of the Infinite, the Infinitesimal, and the (Trans-) Finite, of the Whole, the Word, and the World, of Eidos, Nous, Noema, and Plaeroma, i.e., of the most fundamental “Qualon” (N) (Reality as its own Quality — “Qualicity”); such that

- 1.3 That which is meta-categorically between Phenomenality and Reality is EXISTENCE (X), i.e., Existence-in-itself: the reflexive Mirror and Boundary and the meta-differential Horizon, while that which is between Reality and Phenomenality is BEING (M), i.e., Being-in-itself: the surjective Reality, Unity, and Difference (the Qualon) and the meta-differential Verizon; such that
- 1.4 The meta-categorical Distance between Reality and Phenomenality is Different from that between Phenomenality and Reality: $OM \neq MO$ — unless by way of Surjection (Reality’s singular Exception, just Reality is, in itself, the “surjective-diffeonic” Exception of itself); such that
- 1.5 Reality contains all things phenomenal but these contain Reality not; such that
- 1.6 Reality is meta-categorically Different from all differences and similarities — and Different still; such that

1.7 If Reality were not SUCH, Reality and Non-Reality (Unreality), Being and Non-Being, Existence and Non-Existence would be absolutely NOT, once and for-ever, which is meta-categorically absurd.

As such Reality, as outlined in Surjective Monism, has 7 (seven) meta-differential ontic-epistemic levels. In addition, Reality possesses 4 (four) asymmetric, anholonomic, meta-categorical logical modalities/foliages encompassing:

- M1. Meta-Onticity of (A, non-A, non-non-A, and none of these);
- M2. Meta-Ergodicity of (without, within, within-the-within, without-the-without);
- M3. Meta-Universality of (the material Universe, the abstract Universe, the Universe-in-itself, Reality);
- M4. Meta-Epistemicity of (thought, anti-thought, Unthought, Reality).

In the above surdetermination and most direct presentation of Reality, the Whole Object ([O]bject, Surject, Qualon) that intrinsically (in the utmost eidetic-noetic sense) transcends and overcomes all logical predication (transitive and intransitive) between object and subject — as well as between occasionalism and substantivalism, i.e., between existentialism and essentialism — is uniquely determined by the meta-differential “Qualon-Logos” (“Metanon”) of [O]bject = (Surject, Prefect, Abject, Subject, Object), through the unified qualitative-quantitative ontological-cosmological triplicity of Surjectivity, Reflexivity, and Projectivity.

2 ONTOMETRICITY: “Ontometric Reality”, Unified Field Theory (Geometrization of Space-Time and Substance, i.e., Fields, Matter, and Motion), and the Ultimate Nature of the Physico-Mathematical Universe

Our fundamental “ontometric picture” of physical reality is embodied in the following purely geometric (and kinematic) equation:

$$(DD - R)U(g, dg) = 0,$$

where DD is a differential wave operator and R is the very peculiar “ontometric spin-curvature” — both are built from the fundamental generalized asymmetric metric tensor (g) and connection form (W), in such a way that there is no point x in our space not dependent on the kinematic pairs (x, dx) and (g, dg) —, and U is the wave function of the Universe — again as a kinematic function of the metric and its differential. This way, there is no geometric point in our space that is merely embedded in it; rather it serves as a fundamental, fully geometric (and fully kinematic) “ontometric meta-point” — constituting already fully geometric and intrinsic charge, mass, magnetic moment, and spin-curvature — for which the space, derived from it, is correspondingly emergent as a meta-space of geometrized fields — the “ontometric meta-space” of geometrically emergent and unified gravity,

electromagnetism, chromodynamics, and superfluidity (matter) along with the fundamental properties of chronometricity, kinematicity, and orthometricity.

This section, just as the above introductory description, is again a condensed form of our peculiar views on the nature of physical reality as outlined in, e.g., “Spin-Curvature and the Unification of Fields in a Twisted Space” and several other unified field theories referred to therein, such as “A Four-Dimensional [Meta-]Continuum Theory of Space-Time and the Classical Physical Fields” — as well as the more recent superfluidity geometrization model “A Hydrodynamical Geometrization of Matter and Chronometricity in [Extended] General Relativity”. These are generally theoretical meta-pictures where I have attempted a theoretical “ontometric” meta-continuum picture of cosmophysical reality aimed at unifying gravitation, electromagnetism, and chromodynamics on one hand, and superfluidity, chirality, spin-curvature, matter, and motion — self-realizably along with Zelmanov’s chronometricity, kinematicity, and orthometricity — on the other, as also independently and quintessentially alluded to in our works cited above. Particularly, we will here outline a fresh summary of the nature of Universe whose ontological and epistemological reality would be most satisfactory to the sense of the profound Zelmanov school of scientific creation. Our common aim, as a scientific group and as a whole — in the tradition of Zelmanov — is not simply to “think differently” (a slogan readily laden with post-modern cliché nowadays), but also to be meta-categorically “different from all differences and similarities, and different still” in the truest and most qualified epistemic sense of science and scientific creation.

As a reminder, a present-day category of approaches to unification (of the physical fields) lacks the ultimate epistemological and scientific characteristics as I have always pointed out elsewhere. This methodological weakness is typical of a lot of post-modern “syllogism physics” (and ultimately the solipsism of such scientism in general). Herein, we shall once again make it clear as to what is meant by a true unified field theory in the furthest epistemological-scientific-dialectical sense, which must inevitably include also the most general (and natural) kinematic unity of the observer and physical observables, i.e., “ontometricity”.

Herein, I shall state my points very succinctly. Apart from the avoidance of absolutely needless verbosity, this is such as to also encompass the scientific spirit of Albert Einstein, who tirelessly and independently pursued a pure kind of geometrization of physics as demanded by the real geometric quintessence of General Relativity, and that of Abraham Zelmanov, who formulated his theory of chronometric invariants and a most all-encompassing classification of inhomogeneous, anisotropic general relativistic cosmological models and who revealed a fundamental preliminary version of the kinematic monad formalism of General Relativity for the unification of the observer and observables in the cosmos.

Thus, we can very empathically state the following:

1. A true unified field theory must not start with an arbitrarily concocted Lagrangian density (with merely the appearance of the metric determinant $\sqrt{-g}$ together with a sum of variables inserted by hand), for this is merely a way to embed — and not construct from first principles — a variational density in an *ad hoc* given space (manifold). In classical General Relativity, the case of pure vacuum, i.e., $R_{\alpha\beta} = 0$, there is indeed a rather unique Lagrangian density: the space-time integral over $R\sqrt{-g}$, the variation of which gives $R_{\alpha\beta} = 0$. Now, precisely because there is only one purely geometric integrand here, namely the Ricci curvature scalar R (apart from the metric volume term $\sqrt{-g}$, this renders itself a valid geometric-variational reconstruction of vacuum General Relativity, and it is a mere tautology: thus it is valid rather in a secondary sense (after the underlying Riemannian geometry of General Relativity is encompassed). Einstein indeed did not primarily construct full General Relativity this way. In the case of classical General Relativity with matter and fields, appended to the pure gravitational Lagrangian density are the matter field and non-geometrized interactions (such as electromagnetism), giving the relevant energy-momentum tensor: this “integralism procedure” (reminiscent of classical Newtonian-Lagrangian dynamics) is again only tautologically valid since classical General Relativity does not geometrize fields other than the gravitational field. Varying such a Lagrangian density sheds no further semantics and information on the deepest nature of the manifold concerned.

2. Post-modern syllogism physics — including string theory and other toy-models (a plethora of “trendy salad approaches”) — relies too heavily on such an arbitrary procedure. Progress associated with such a mere approach — often with big-wig politicized, opportunistic claims —, seems rapid indeed, but it is ultimately a mere facade: something which Einstein himself would scientifically, epistemologically abhor (for him, in both the pure Spinozan and Kantian sense).

3. Thus, a true unified field theory must build the spin-curvature geometry of space-time, matter, and physical fields from scratch (first principles). In other words, it must be constructed from a very fundamental level (say, the differential tetrad and metricity level), i.e., independently of mere embedding and variationalism. When one is able to construct the tetrad and metricity this way, he has a pure theory of kinematicity for the universal manifold M : his generally asymmetric, anholonomic metric $g_{\alpha\beta}$, connection W , and curvature R will depend on not just the coordinates but also on their generally non-integrable (asymmetric) differentials:

$$M(x, dx) \rightarrow M(g, dg) \rightarrow W(g, dg) \rightarrow R(g, dg).$$

In other words, it becomes a multi-fractal first-principle geometric construction, and the geometry is a true chiral meta-continuum. This will then be fully capable of producing the true universal equation of motion of the unified fields

as a whole in a single package (including the electromagnetic Lorentz equation of motion and the chromodynamic Yang-Mills equation of motion) and the nature of pure geometric motion — kinematicity — of the cosmos will be revealed. This, of course, is part of the emergence of a purely geometric energy-momentum tensor as well. The ultimate failure of Einstein’s tireless, beautiful unification efforts in the past was that he could hardly arrive at the correct geometric Lorentz equation of motion and the associated energy-momentum tensor for the electromagnetic field (and this is not as many people, including specialists, would understand it). In my past works (with each of my theories being independent and self-contained), I have shown how all this can be accomplished: one is with the construction of an asymmetric metric tensor whose anti-symmetric part gives pure spin and electromagnetism, and whose differential structure gives an anholonomic, asymmetric connection uniquely dependent on x and dx (and hence x and the world-velocity u , giving a new kind of Finslerian space), which ultimately constructs matter (and motion) from pure kinematic scratch. Such a unified field theory is bound to be scale-independent (and metaphorically saying, “semi-classical”): beyond (i.e., truly independent of) both quantum mechanical and classical methods.

4. Such is the ultimate epistemology — and not just methodology — of a scientific construct with real mindful power (intellection, and not just intellectualism), i.e., with real scientific determination. That is why, the subject of quantum gravity (or quantum cosmology) will look so profoundly different to those rare few who truly understand the full epistemology and the purely geometric method of both our topic (on unification) and General Relativity. These few are the true infinitely self-reserved ones (truly to unbelievable lengths) and cannot at all be said to be products of the age and its trends. Quantizing space-time (even using things like the Feynman path-integrals and such propagators) in (extended) General Relativity means nothing if somewhat alien procedures are merely brought (often in disguise) as part of a mere embedding procedure: space-time is epistemologically and dialectically not exactly on the same footing as quantum and classical fields, matter, and energy (while roughly sharing certain parallelism with these things); rather, it must categorically, axiomatically qualify these things. Even both quantum mechanically and classically it is evident that material things possessed of motion and energy are embedded in a configuration space, but the space-time itself cannot be wholly found in these constituents. In the so-called “standard model”, for example, even when quarks are arrived at as being material constituents “smaller than atoms”, one still has no further (fundamental) information of the profounder things a quark necessarily contains, e.g., electric charge, spin, magnetic moment, and mass. In other words, the nature of both electromagnetism and matter is not yet understood in such a way. At the profoundest level, things cannot merely be embedded in

space-time nor can space-time itself be merely embedded in (and subject to) a known quantum procedure. Geometry is geometry: purer, greater levels of physico-mathematical reality reside therein, within itself, and this is such only with the first-principle construction of a new geometry of spin-curvature purely from scratch — not merely synthetically from without — with the singular purpose to reveal a complete kinematic unity of the geometry itself, which is none other than motion and matter at once. Again, such a geometry is scale-independent, non-simply connected, anholonomic, asymmetric, inhomogeneous: it ultimately has no “inside” nor “outside” (which, however, goes down to saying that there are indeed profound internal geometric symmetries).

5. Thus, the mystery (and complete insightful understanding) of the cosmos lies in certain profound scale-independent, kinematic, internal symmetries of the underlying geometry (i.e., meta-continuum), and not merely in *ad hoc* projective, embedding, and variational procedures (including the popular syllogism of “extra dimensions”).

3 On the Furthest-Qualified Metaphysics, Phenomenology, Ontology, and Cosmology

We have, in our time, very fortunately witnessed the heroic emergence of a class of neutral, vast generalizations (“neutrosophies”, to use the Smarandachean term, after the pioneering logician, mathematician, and polymath F. Smarandache) of logic and dialectics — worked out entirely by very few original, profound minds of genuine universal character — aiming at envisioning a much better future for humanity in the cosmos, e.g., scientific, psychological, social, and economic terms, thus forming an inspirational surge beyond the blatant superficialities and tyranny of certain politically, inter-subjectively established paradigms often masquerading as the “true scientific method” and “objectivity”. The inherently flawed assumptions of these misleading paradigms, as such, can be seen only with clear independent epistemicity (true, objective knowledge, even “un-knowledge”, on the horizon of things), and not in terms of methodology alone (which can often be fabricated and imitated), as to how they are chiefly non-epistemic — thus ultimately pseudo-scientific and pseudo-objective — trends that pretend that certain ontically and epistemically intricate matters are already settled by “consensus” of the majority.

All this is crucially taking place in the incessant, highly nervous background of science and certain peculiar scientific affairs of today (as Thomas Kuhn has indicated just what the “tectonic rims” of science might be), just as it has always appeared historically, and will always appear as such, to rescue the state-of-the-art of science from “usual human tendencies towards promulgating corruption” at very critical epistemological junctions. The common objective of these generalizations is to form a broader window — a truly open window pretty much without cumbersome curtains indeed — for

a more genuine outlook on the landscape of science and humanity.

Having said the above, I hereby applaud any lone epistemic effort — among other such lone efforts — in the direction of a new reality theory and a new semantics theory aimed at, e.g., a new neutral synthesis of ubiquitous doctrines such as substantivalism and occasionalism, as well as absolutism and relativism, for cosmology and cosmogony. Such a work, to the one who knows “how corrugated, discrete, and paradoxical landscapes in the cosmos can be”, is a pure dialectical enjoyment in itself, in the solitary niche where true epistemic minds often hide their solitary effulgence and brilliance. Therein, one is obliged to outline a genuine solution to the persistent, often popularly misunderstood problems and challenges in scientific epistemology from the ancient epochs of the Greeks and the Indians (the Sanskrit/Vedic “Indo-Aryans”), through the medieval ages of the Perso-Arabic — and then pan-Hellenic European — civilization and Renaissance, to the most recent eras of modernism, post-modernism, and scientism.

However, the reader should be aware that behind this simple appraisal a supposedly genuine thought aimed at a conscious stationing (dialectical synthesis) of phenomena constitutes a train of further in-going paradoxical thoughts. Thus, let us do a brief (and yet dense), crucial, signaling surgery on the manifold of thoughts of modernism, post-modernism, and scientism (including critical post-modernism) — as to why such intellectual strands ultimately fail to transcend anything real — and on the dialectical anatomy (“cosmogony”) of the problems of the world in general.

Keep in mind, once and for all, that, despite diverse causes, the root of this meta-situation can be traced back to the cosmic “superset” as to whether the world we inhabit is essentially autonomous in itself or extraneously governed by some kind of intelligence. Further independent epistemic qualifications (including disqualifications) can be applied to these options as new horizons are encompassed. This should suffice to underline what is crucial in any original reality (and linguistics) theory, among other similar and dissimilar epistemically sincere proposals ranging from absolute agnosticism to a further sense of knowing and enlightenment.

I’d like to re-identify, in my own words, the very problem that any genuine reality theory has to deal with in terms of scientific epistemology as follows (as I have stated elsewhere on past occasions, especially in my work on a new kind of Reality theory, namely “The Surjective Monad Theory of Reality” or “Surjective Monism”, and on my seminal address “On Meta-Epistemic Determination of Quality and Reality in Scientific Creation”). Despite many conscious and conspicuous attempts at elevating the use of process-synthetic philosophy and integralism to a “new” key paradigm at the critical crossroads between world affairs and individual well-being, many thinkers have not developed the first-principle logical-dialectical tool needed to solve fundamental existential and

phenomenological problems in modern philosophy (that is to say, since Kant and Copernicus), be it one that directly or indirectly underlies the pure workings of science. This way, the complete surgical tool of meta-logic is still missing from their hands, and so true determination — in the profoundest sense of the word “determination” — is absent. Thus, the purported newness [and trend] of post-modern paradigms do not really constitute a first-principle philosophical newness: it is merely a magnified old-nostalgic trace of process-integralism, an issue contested by the likes of Russell and Whitehead (philosophically, scientifically, and morally) at the critical, dehumanizing, life-shearing onset of last century’s two world-wars as well as the cold war (which continues to prevail under the surface of history, precisely as a dialectical part of epistemicity and historicity, not mere hermeneutics, linguistics, and history).

This is precisely why mere post-modern visions of revisionist holism and inter-subjective facticity (somewhat akin to Gestalt psychology) — both as a natural scientific-revisionist investigation and a purportedly broader philosophical picture — still suffer from the contingency (that is, reflexes, conditions, and associations) of [their] embedding solipsistic sphere, when this on-going contingency ought to be categorically deconstructed in the first place, and not merely highlighted in the light of further arbitrary psychological associationism put forth arbitrarily as “objective science” (such as the “second-hand” inclusion of the convenient psychologism and propaganda that “syntax-only science supersedes semantics”).

Thus, while such an approach may be sufficiently inspirational for a psychological reform within a known, ultimately defective established scientific, political, and cultural system, it is not yet an adequate framework for genuine humanistic revolution and logical determination. A genuine thinker should look for a meta-language, a meta-paradigm for science; one that is free of the usual kinds of pretense and bigotry we encounter from time to time in the history of thought, especially modern thought: a journey from Cartesian dualism to Spinozic monism to Berkeleyan psychologism via the weary intellectual bridges of Hume, Kant, Hegel, Husserl, Heidegger, and Wittgenstein (both the analytic young Wittgenstein and the post-modern old Wittgenstein).

Or else, much of humanity has forgotten — or is simply absolutely, blissfully, complacently ignorant of — the essence of what Max Planck and Ernst Mach — the two pedagogy and epistemology giants (and innovative scientists in their own right) surrounding Albert Einstein in his scientific revolutionary days — once argued about. They argued about the essences, modes, limits, and expansions of science vis-a-vis Reality quite long before Einstein debated Niels Bohr on the nature of the quantum, cosmos, and Reality. And certainly long before Karl Popper outlined his epistemology and ideal criteria for “falsifiable science” against the overly-positivistic Vienna circle led by Moritz Schlick (whose po-

sition is blindly, arbitrarily taken by “thronges of scientists” in the USA and Western hemisphere as of today, whether they know it or not: few are those who are truly conversant with ontology and epistemology, and not just methodology, after all).

At the same time, in fact soon after Mach launched his epistemological program towards “purifying absolutism in science” (especially in Newtonian and celestial mechanics) in Europe, Russia, witnessed heated debates of the nature of science and philosophy vis-a-vis Reality as contested by the likes of Ouspensky (who defended the simultaneously neo-Platonic and neo-Aristotelian traditions of meta-physics), Bogdanov (who tried to generalize Machian thought into a single “empirico-monism”), and those who harshly forced the notion of “materialism over Machianism and all sorts of psychologism and idealism” on scores of Soviet scientists, gaining ultimate support from materialist philosophers and scientists such as the foremost expert on the “reflexes of the higher nervous system”, Ivan Pavlov.

In the sense of critical epistemicity, Einstein, for example, criticized both certain self-assured theists and atheists, among both vocal scientists and vocal lay people concerned about often blurry, oversimplified entities such as “god” and “nature”, as “rogue solipsists”.

4 The Meta-Differential Logic of the Whole, the Word, and the World: Subjective Monism and the “Qualonic Unity” of Sight and Sense

What, then, is a meta-science in our case? It is none other than the great reflex of ontic-epistemic Unity — the Unity of Sight and Sense — in the sense of beholding an object (or phenomenon), while recognizing categorically (up to a point of Absolute Difference) that Existence (Nature, space-time in the most qualified phenomenological sense) is as-it-is a mirror-like apogetic Horizon and Reality is in-itself an eidetic Verizon: one “perigetically” witnesses the object in space (“sight”) and “apogetically” withholds space in the object as “internal time” (“sense”) whereby time here is the sensation (a priori representation) of space by way of the complete dialectical-phenomenological unity of space-time, matter, and motion (in the sense of epistemologically qualified objective events, not arbitrary “frills”). When objectivity is asymmetrically moved along social time-lines and synthetic-paradoxical thinking (“Understanding”, i.e., “thinking about thinking” and “doing about doing”), it becomes “Praxis/Paradigm as it is” — Surdetermination —: a vortex of historicity, capable of creative-reflexive stellar motion at the societal stage, yet whose infinitesimal center of “insight” and “inhering” remains non-integrable and solitary. The highest (eidetic) degree of Quality concerning this, given as a Whole Object (where the Horizon is dialectically part of it, instead of arbitrarily including, eliminating, or excluding it), is none other than the furthest qualification of “noema”, while it shall

be termed “surholding” in the sense of “noesis”: it possesses “Surjective Verizon” as Being and “Reflexive Horizon” as Existence, and not mere inter-subjective projection and inter-objective boundary.

Mere integralism, just like non-epistemic oversimplification and over-generalization, is at best a rhapsodic trend in post-modernism and psychologism (including post-structuralism and neo-psychoanalysis); ultimately, however, it — like the psychologism of Gestalt — is no substitute for a first-principle categorical underpinning of phenomena, that is, the complete dialectical unity — the ontological-epistemological-phenomenological-axiological unicity — between the Real and the Ideal, the material and the mental, the whole and the partial, and all the asymmetric existential-predicative tension between the object and the subject in general. The same defect can be said about the uncritical use of process philosophy without original refined recourse to “noema” (objects-as-they-are) or phenomenology (at least in the sense of Husserl, who was both a mathematician and philosopher, as we need not mention how “phenomenologists” after him have easily misunderstood the fundamentals of Husserlian phenomenology and, thereafter, they have also arbitrarily misunderstood and dismissed each other in the realm of post-modernism).

Again, most post-modern authors of scientism, as well as the majority of so-called “scientists”, do not seem to intuitively emphasize the need for the deconstruction of the ultimately illogical-pathological state of a world much plagued with hypersemiotics, hypernarration, oxymoronism, sycophancy, pseudo-objectivity, pseudo-science, pseudo-philosophy, pseudo-spirituality, pseudo-artistry, solipsism, and ontic-epistemic shallowness.

As easy to see, the prevalent solipsistic type of world-scientism — and, indeed the associated panhandling and psychologism of scientific affairs, coupled with superficial political and economic affairs — is ultimately unscientific and non-logical for not taking into account in the first place the important logico-phenomenological branch of dialectics, let alone of neutrosophy, namely a comprehensive science that attempts to throw light at logic, empiricism, psychologism, existentialism, essentialism, science, philosophy, and history, thereby transforming mere history into dialectical historicity.

Consensus solipsism, no matter how much it is often falsely put forth as “science” and “objectivity” before both the more naive “scientists” and the gullible public, is solely based on a desired paradigm concentrated in, and funded by, corporate and governmental hands by way of visible and invisible “control by proxy” monopoly in many aspects of life, and it attempts to primitively capsize all the rest of scientific existence under its sway by non-dialectically embedding an essentially inhomogeneous, non-simply-connected, variegated world of paradigms and ideas (which it ultimately knows not!) in its own homogenizing pseudo-parametric space, and this, with all the bias, vested political interests, and dupli-

city contained in it, is often neatly disguised — helplessly by way of syllogism and solipsism — as the so-called “scientific method” (thus, some have warned us that there is not a single “scientific method” — just as there is not a single quantum mechanics: there is more than one version of quantum mechanics, than the one following the “Copenhagen interpretation” — and that a scientific economy precept known as “Ockham’s razor” is often misused). Clearly, a “given consensus science” hiding ulterior motives is not the same as science itself, for which new ways of thinking and genuine epistemic objectivity are the primary goals often following long processes of logico-dialectical thinking as well as solitary revolutionary thinking or ideation (alas, as Michael Crichton has pointed out, history has provided us with a set of scoundrels-in-power of mere opportunism when it comes to “consensus science”).

This stuff at the heart of the matter is essentially, intellectually primitive and cumbersome, no matter how much power, psychologism, techno-scientism, and modernity it displays: a set of mere opinions made strong by way of any kind of political favoritism does not solve the age-long problem of syllogistic solipsism and solipsistic syllogism in science and philosophy. Indeed, the world of science — supposedly inherited, both arbitrarily and qualifyingly, from the “ancients” and the more recent “Aufklärung”, just like the world of philosophy — still inherently suffers from mere syllogism and solipsism, albeit in a different intellectual category than other types of solipsism, thereby often resulting in advanced opaque types of dogmatism, absolutism, and relativism, and in the said types of sycophantism and sophism. Note how these are easily interchangeable in each other’s garb and served with fresh inductive duplicity on the daily menu of “loud, bubbly, verbose, trendy, big-wig scientism”.

That is why, a truly qualified science production is always crucial — beyond the said integralism and mere post-modern holism — in all the branches of science, including cosmology, ecological science, and the humanities: it must be based on independent, neutrosophically guided free inquiry, beyond all forms of superficial political control, especially funding systems and political interests. In this scheme, such science production is the first and foremost logical foundation of a revolutionary social-democratic culture, and not capital sums (and so not pretentious scientism — pseudo-intellectual big-otry — with all its hidden subjectivity and opportunism).

Back to the problem of ontology and epistemology as well as cosmology and cosmogony addressed herein, then wholly illuminated, by any genuine reality theory: is the Universe, our home, autonomous or is it dependent (on a supposed “demi-urge” or “creator” — while the word “creation” should in any case be epistemically qualified)? If it is autonomous, is it machine-like and ultimately random, or is it quasi-anthropomorphic and teleological, or is it absolutely autonomous? If it is dependent, what kind of dependency (or creation) is there: epiphanic (as in the neo-Platonic sense), or

theological (as in the Kalam cosmological argument and in the Thomian sense), or none of these? Before answering — or rather, epistemically addressing — such questions, a sense of mindful humility is very important, one akin to Einstein who, as known, did not believe in a personal god, but for whom — like for Spinoza — the word “God” should represent a very broad, genuine sense of Reality and Onto-Realism, namely a non-personal transcendental universal intellect whose attributes and laws are not anthropomorphic and arbitrarily projective but “summa-rational” and “meta-rational”, and whose horizon in the intricate and beautiful cosmos renders “mere reflective human minds” like vanishing dots thereon.

The philosophical propositions for cosmology and cosmogony elaborated upon by such a theory must then transcend the intrinsic self-limitations and extrinsic ex-limitations of both mere dogmatic materialism (solipsistic objectivism) and psychologism (solipsistic subjectivism): a more infinitely reflexive-neutral, let alone “surjective”, realism will be inherently different from mere passive, dogmatic, and biased (thus ultimately solipsistic) “randomness” and “design”, especially when determining a genuine sense of cosmic semi-autonomy as well as both the weak and strong anthropic principles. Such a vein then must be seen as sincere and epistemic enough, and is meant to enrich public understanding of the matter in the very arena of “science and philosophy at a cross-roads”.

Meta-physics is the science dealing not with “non-science”, “non-sense”, or “para-physics”, as many have misinterpreted it, but with the epistemic qualification and entification of the sciences. Ockham’s razor, too, is a meta-physical stance. And so is materialism. As such a “neutrosophist”, in countering the currently prevalent, financially and politically more supported dogma of a self-sufficient material universe emerging by chance and populated by randomness, does not side with creationism, let alone “biblical creationism” or “intelligent design” for he has assuredly maximum epistemic distance from falling solipsistically into this or that (while, like Einstein, considering “religion” only psychologically and historically); rather, like Einstein, he aims to humbly show how the problem is not culturally settled: be it among the Greeks, among medieval thinkers, or among the contemporary minds of today. He, like Einstein, humbly sees a “superior manifestation of intelligence” in Nature and on the horizon of things and, on a psychological and historical note, is merely sympathetic with the minority in this category — and the faintest of voices —, and this is true in any case.

No matter what one’s meta-physical stance is in science and philosophy, the problem presented here is a truly beautiful, profound one. In my view, Reality should be ontologically simple (yet “not that simple”) in the sense of what I term the “Qualic Unity (Unicity) of Sight and Sense”, while being epistemologically so complex (yet “not arbitrarily complex”) at the same time: it is necessarily One-in-itself beyond concrete and abstract, even “noumenal”, count. Metaphorically

speaking of Reality and the Universe, onticity is the whole mountain and ontology is the peak and the verizon; epistemicity is then the quintessential gradient and epistemology is the entire slope: this makes truly qualified knowledge and understanding possible, whether universal or particular, categorical or phenomenal, philosophical or scientific; phenomenology is the mountain’s appearance (verisimilitude) and “stuff” as well as the corresponding horizon and landscape; at last axiology is the rest as concerns judgment and values. This way, there is a profound, four-fold categorical, asymmetric, anholonomic difference between “Being” and “Existence” (as, again, outlined in my own “Surjective Monad Theory of Reality” as a qualified generalization of reflexive monism), just as the meta-categorical, ontic-epistemic, surjective-reflexive distance (“Qualicity”) between Reality and Phenomenality is asymmetric. I will undertake to explain this a little bit, as presented below.

5 The Diffeo-Unitics of Being and Existence in Surjective Monism

Whether one is concerned about the strenuous synthesis between the mundane and the other-worldly, between the economical and the ecological, between the one and the many — that is, basically between a thesis and an anti-thesis in a rather universal sense —, phenomenologically, dialectically speaking, one is essentially referring to Existence as a “negative totality” — instead of both the arbitrary, subjective Unknown of solipsistic mysticism and the equally solipsistic, overly positivistic valence of narrow (non-dialectical) material dogmatism —; that is, Existence is an “inconsistent inner multiplicity in and of itself”: it has parts that do not constitute the Whole by way of simple representation, and yet, unlike mere holism, it is livingly capable of unifying logical synthesis and determination when a portion of humanity is in touch with the said synthesis. The problem here since time immemorial, as renewed by Kantian categorical analysis, overly-symmetrically projected by Hegel, attempted by Husserlian phenomenological analysis, and brought to a further critical stand-still by Heidegger, has been the infinitesimal (essentially surdeterminate) difference between Being and Existence (“Being-as-Being” vis-a-vis “Being-here”) — and also between Idealism and Realism, between noumena and phenomena, as well as between Transcendence and Immanence. Only when this is universally — that is, categorically-eidetically — solved can one truly speak of what is beyond mere essentialism and existentialism, that is, the most qualified Thing-in-itself: the Word and the World, the Whole and the While. That is, in other words, true ontic-epistemic objectivity.

This way, then, Surdetermination (universal determination) of the Whole, the Word, and the World — in the sense of Reality’s Verizon and Horizon — must be aimed at the very Present, more than at the theoretical future.

A logical system is hereby categorical-synthetic-revolutionary (that is, universal) if and only if it encompasses the spiraling interaction between: 1) Existence as the eidetically negative totality and horizon of “non-A and non-non-A” for any entity “A” and the infinitesimality (surdeterminate infinite difference) of “non-A” and the infinity of “non-non-A” — the entirety of possible inter-related, compositional things — and 2) the “twice-aprioristic” (non-arbitrary objective-aprioristic) epistemic set of “A and non-A” representing things-as-they-are (categorically aprioristic-objective existents in pure phenomenological-natural space beyond mere societal conditionings). This, when fully implemented, gives a dialectical “humanity-epistemicity spiral” instead of both the concentrically closed circle of logism (such as dogmatism and monopoly) and the interconnected circles and “biosphere” of post-modernism (especially integralism). Such a fully phenomenological spiral (“connex of causation”) is in the “genes” of Revolution and Praxis without any need to resort to mere idealism and integralism (of the many, especially in the post-modern sense) — other than dealing with noematic object-magnification and object-illumination: not only can an island exist after all in its essentially negative and paradoxical oceanic surroundings, it can also be of the density of a great continent with its spiraling mountain peaks and profound valleys irrespective of its phenomenal size (as perceived by the majority of people).

Having said that, I maintain that “Being-qua-Being” is the “none-of-these” part of the above meta-logic and a most direct Surdetermination (“Surholding”) of Reality, in the subsequent vicinity of the most neutral “non-non-A” determination of Existence whose universal object is a “Qualon”, that is [O]bject = (Surject, Prefect, Abject, Subject, Object) — again, see the work on “Surjective Monism” for the peculiar new-contented glossary of these terms.

6 Epilogue

Such a meta-categorical view on Reality, as presented above, is in eidetic and twice-aprioristic contrast to the pseudo-synthetic, inter-subjective, commutative logism of a thing “A” being arbitrarily, conditionally given as “A and non-A” at the same time by way of a homogenizing, “modernizing”, “newly introduced” human interaction-type superficially (beyond just artificially!) prevalent in today’s society. Consider, for example, both the case of classical Hegelian solipsistic syllogism (in the case of absolutist history and sociology) and the generic example of the one-dimensionality (one-sidedness) between technological gadgets (which can easily be substituted by any given operational post-modern notion) in the “free market” and the majority of their users: a great gap exists between the given (gadgets as conditions) and the conditioned (subjects), that is, unless the subjects are the creators or producers — not mere buyers — of the said gadgets. Here, subjects do not genuinely, aprioristically exist with respect

to Existence (but only with respect to the capriciously conditioning inter-subjective society) and so are devoid of epistemicity; instead, they are conditioned by their whole range of habits determined through the given gadgets and associated contemporary urges.

The full extent of solipsism and syllogism — and the stark absence of true Eidos, Logos, and Eros (of course, not exactly in the Marcusian sense and use of the merely contrasting phrase “Logos and Eros”, rather in a most unified and qualified substantiation of the “Ergo” and not a mere “ego”, being somewhat akin to the very term “ergodicity”) is at the very heart of the problem of contemporary neo-simplistic world at large in relation to puppetry, especially intellectual puppetry: most contemporary people do not touch the ground with their feet (to know the real contour of Existence, and not just the “societal sphere”), and they are unable and not allowed to do so; instead, they are hanging (whether high or low) by conditional proxy and post-modern threads, prodded by ultracapitalistic-ultraconsumerist-hypernarrative rods and sustained daily by superficial image-making tantamount to overall solipsistic-syllogistic defect: that of hypernarration, hyperoxymoronism, hypersemiotics, duplicity, solipsism, and utter ontic-epistemic shallowness. In other words, they are not real, as they do not inhere within Existence (let alone Being!) and its noematic mirror: they are apparitions upon Existence and that mirror. They are not “wrong”: they are “not even wrong” (as a notable mathematician puts it).

The known towering figures of analytic philosophy, who have stood as stern horizons before many, have not been able to completely solve this epistemic problem, owing to the fact that their systems are largely overly-symmetrical, be they empirical, positivistic, or idealistic. Yet the fact remains that the unity referred to as Existence is indeed a negative totality with a positive nescience on the part of multiplicity of most conscious existents: it has an underlying asymmetric connection between things perceived as “parts” and is non-integrable by way of logical representation. Thus, the aim of dialectics is not to “integrate” Existence as such, but to synthesize the given ambiguities in the logical-ideal form of an eidetic-noematic category encompassing object-oriented Praxis/Paradigm, where a priori and posteriori categories are taken as not mere process (a-la Russell and Whitehead), but “surgical modalities” in the face of anti-dogmatism. This, then, would be a positive, dialectical kind of idealism capable of Progress (and real dialectical synthesis) in the real background of the said negative totality — again, akin to constituting a solid island or continent in the greatly paradoxical oceanic surroundings —, in contrast to mere syllogism and solipsism, dogmatism and sophism, absolutivism and relativism.

Except for those who are uncritically conditioned and embedded by it (unfortunately, such sorry individuals account for the majority, as in any age, which is why the superficial world of modernity remains running on misleading wheels

and false horses as it does today), Progress on all fronts of Ideation does not intrinsically belong to non-epistemic solipsism: never it has been so and never it will be. What is often taunted as “scientific progress” (not exactly the same as technological progress, let alone genuine epistemic scientific progress) in the fast linkage of contemporary dehumanization and pseudo-enlightenment (instead of a set of neutral, multi-fractal “micro-paradigms”: a model for an epistemological scientific system incapable of being integrated arbitrarily into an embedding political bastardization of dogmatic scientism and religionism on the large scale) often entails logico-moral duplicity which in turn causes a typical inept individual and stooge to deny any existential footing, almost deliberately mistaking the superficial world (in homogeneous, conforming chains) for the real, paradoxical, non-dogmatic terrain of Existence: the weight, the feet, and the ground of Existence he never realizes and touches, for he is ineptly hoisted high by the external manipulative world upon superficial hooks, hangers, and logisms (seeming situational logical thoughts that are ultimately, on the edge of the world, “not even wrong”), and still it is somewhat guaranteed by the collective solipsism of the majority that such one is able to derive his happiness — if not his entire absurd situation and way of being — from subconscious folly and conceit often arising merely from shallow international conformity and hidden feudalism based on common image-making (indeed, instead of common good and true democracy); in other words, from internal incapacity and inconsistency as to what really transpires on the small and large scales of the cosmos and the world of human activities and considerations.

In short, solipsistic logism, including both the schemers and the blind workers, suffers from all kinds of pseudo-objectivity, especially on the horizon of things. The penultimate revolutionary-intellectual human, however, firmly touches the ground with his own feet, and is capable of the paradoxical contour of Existence — by way of encompassing the four categorical, meta-epistemic “a priori’s” and “a posteriori’s”: ontic-eidetic-noetic, synthetic-apogetic-a priori, synthetic-peripheral-a posteriori, and subjective-psychological — leading all the way from the abyss to the summit, as Revolution in the sciences is always ardently wholly needed, not a mere reform: a new Word for the World, and a new World for the Word.

Submitted on: May 25, 2014 / Accepted on: May 30, 2014

A Closed Universe Expanding Forever

Nilton Penha Silva

Departamento de Física (Retired Professor), Universidade Federal de Minas Gerais, Belo Horizonte, MG, Brazil
 Email: nilton.penha@gmail.com

In a recent paper, the expression $a(t) = e^{\frac{H_0 T_0}{\beta} \left[\left(\frac{t}{T_0} \right)^\beta - 1 \right]}$ where $\beta = 0.5804$, was proposed for the expansion factor of our Universe. According to it, gravity dominates the expansion (*matter era*) until the age of $T_\star = 3.214$ Gyr and, after that, dark energy dominates (*dark energy era*) leading to an eternal expansion, no matter if the Universe is closed, flat or open. In this paper we consider only the closed version and show that there is an upper limit for the size of the radial comoving coordinate, beyond which nothing is observed by our fundamental observer, on Earth. Our observable Universe may be only a tiny portion of a much bigger Universe most of it unobservable to us. This leads to the idea that an endless number of other fundamental observers may live on equal number of Universes similar to ours. Either we talk about many Universes — Multiverse — or about an unique Universe, only part of it observable to us.

1 Introduction

The Cosmological Principle states that the Universe is spatially homogeneous and isotropic on a sufficiently large scale [1–7]. This is expressed by the Friedmann spacetime metric:

$$ds^2 = \mathfrak{R}^2(T_0) a^2(t) (d\psi^2 + f_k^2(\psi) (d\theta^2 + \sin^2 \theta d\phi^2)) - c^2 dt^2, \quad (1)$$

where ψ , θ and ϕ are comoving space coordinates ($0 \leq \psi \leq \pi$, for closed Universe, $0 \leq \psi \leq \infty$, for open and flat Universe, $0 \leq \theta \leq \pi$, $0 \leq \phi \leq 2\pi$), t is the proper time shown by any observer clock in the comoving system. $\mathfrak{R}(t)$ is the scale factor in units of distance; actually it is the modulus of the *radius of curvature* of the Universe. The proper time t may be identified as the cosmic time. The function $a(t)$ is the usual expansion factor

$$a(t) = \frac{\mathfrak{R}(t)}{\mathfrak{R}(T_0)}, \quad (2)$$

being T_0 the current age of the Universe. The term $f_k^2(\psi)$ assumes the following expressions:

$$f_k^2(\psi) \begin{cases} f_1^2(\psi) = \sin^2 \psi & (\text{closed Universe}) \\ f_0^2(\psi) = \psi^2 & (\text{flat Universe}) \\ f_{-1}^2(\psi) = \sinh^2 \psi & (\text{open Universe}) \end{cases} \quad (3)$$

In a previous paper [8], we have succeeded in obtaining an expression for the expansion factor

$$a(t) = e^{\frac{H_0 T_0}{\beta} \left[\left(\frac{t}{T_0} \right)^\beta - 1 \right]}, \quad (4)$$

where $\beta = 0.5804$ and H_0 is the so called Hubble constant, the value of the Hubble parameter $H(t)$ at $t = T_0$, the current age of the Universe. Expression (4) is supposed to be describing the expansion of the Universe from the beginning of the so called *matter era* ($t \approx 1.3 \times 10^{-5}$ Gyr, after the Big Bang).

Right before that the Universe went through the so called *radiation era*. In reference [8] we consider only the role of the matter (baryonic and non-baryonic) and the dark energy.

In Figure 1 the behaviour of the expansion acceleration, $\ddot{a}(t)$, is reproduced [8]. Before $t = T_\star = 3.214$ Gyr, acceleration is negative, and after that, acceleration is positive. To perform the numerical calculations we have used the following values: $H_0 = 69.32 \text{ km} \cdot \text{s}^{-1} \cdot \text{Mpc}^{-1} = 0.0709 \text{ Gyr}^{-1}$, $T_0 = 13.772 \text{ Gyr}$ [9].

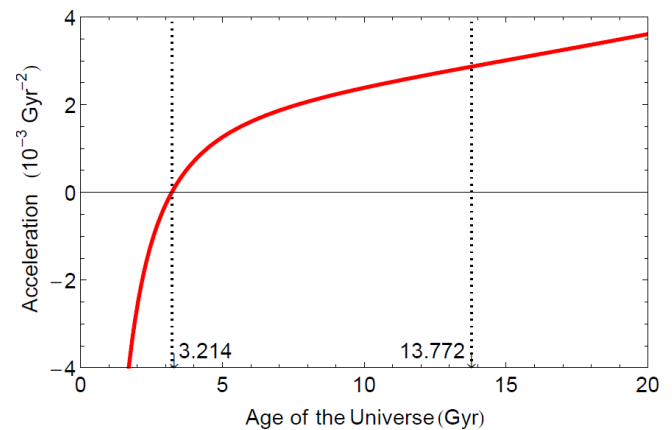


Fig. 1: $\ddot{a}(t) = a(t) \left(H_0 \left(\frac{t}{T_0} \right)^\beta - (1 - \beta) \frac{1}{t} \right) H_0 \left(\frac{t}{T_0} \right)^{\beta-1}$.

2 The closed Universe

In reference [8], some properties such as Gaussian curvature $K(t)$, Ricci scalar curvature $R(t)$, matter and dark energy density parameters (Ω_m, Ω_λ), matter and dark energy densities (ρ_m, ρ_λ), were calculated and plotted against the age of the Universe, for $k = 1, 0, -1$. It was found that the current curvature radius $\mathfrak{R}(T_0)$ has to be larger than 100 Gly. So, arbitrarily, we have chosen $\mathfrak{R}(T_0) = 102 \text{ Gly}$. None of the results

were sufficient to decide which value of k is more appropriate for the Universe. The bigger the radius of curvature, the less we can distinguish which should be the right k .

In this paper we explore only the $k = 1$ case (closed Universe). First, we feel it is appropriate to make the following consideration. At time $t \approx 3.8 \times 10^{-4}$ Gyr, after the Big Bang, the temperature of the universe fell to the point where nuclei could combine with electrons to create neutral atoms and photons no longer interacted with much frequency with matter. The universe became transparent, the cosmic microwave background radiation (*CMB*) erupted and the structure formation took place [10]. The occurrence of such *CMB* and the beginning of the matter era happen at different times, but, for our purpose here, we can assume that they occurred approximately at the same time $t \approx 0$, since we will be dealing with very large numbers (billion of years). We have to set that our fundamental observer (Earth) occupies the $\psi = 0$ position in the comoving reference system. To reach him(her) at cosmic time T , the *CMB* photons spend time T since their emission at time $t \approx 0$, at a specific value of the comoving coordinate ψ . Let us call ψ_T this specific value of ψ . We are admitting that the emission of the *CMB* photons occurred simultaneously ($t \approx 0$) for all possible values of ψ .

Having said that, we can write, for the trajectory followed by a *CMB* photon ($ds^2 = 0, d\phi = d\theta = 0$), the following:

$$-\frac{cdt}{\mathfrak{R}(t)} = d\psi, \tag{5}$$

$$-\int_0^T \frac{c}{\mathfrak{R}(t)} dt = \int_{\psi_T}^0 d\psi, \tag{6}$$

$$\psi_T = \frac{c}{\mathfrak{R}(T_0)} \int_0^T \frac{1}{a(t)} dt. \tag{7}$$

The events ($\psi = 0, t = T$) and ($\psi = \psi_T, t = 0$) are connected by a null geodesics. ψ gets bigger out along the radial direction and has the unit of angle.

The comoving coordinate which corresponds to the current "edge" (particle horizon) of our visible (observable) Universe is

$$\begin{aligned} \psi_{T_0} &= \frac{c}{\mathfrak{R}(T_0)} \int_0^{T_0} \frac{1}{a(t)} dt \\ &= \frac{c}{\mathfrak{R}(T_0)} \int_0^{T_0} e^{\frac{H_0 T_0}{\beta} \left(1 - \left(\frac{t}{T_0}\right)^\beta\right)} dt \\ &= 0.275 \text{ Radians} = 15.7 \text{ Degrees.} \end{aligned} \tag{8}$$

So *CMB* photons emitted at ψ_{T_0} and $t = 0$ arrive at $\psi = 0$ and $t = T_0$, the current age. Along their whole trajectory, other photons emitted, at later times, by astronomical objects that lie on the way, join the troop before reaching the fundamental observer. So he(he) while looking outwards deep into the sky, may see all the information "collected" along the trajectory of primordial *CMB* photons. Other photons emitted at the same time $t = 0$, at a comoving position $\psi > \psi_{T_0}$

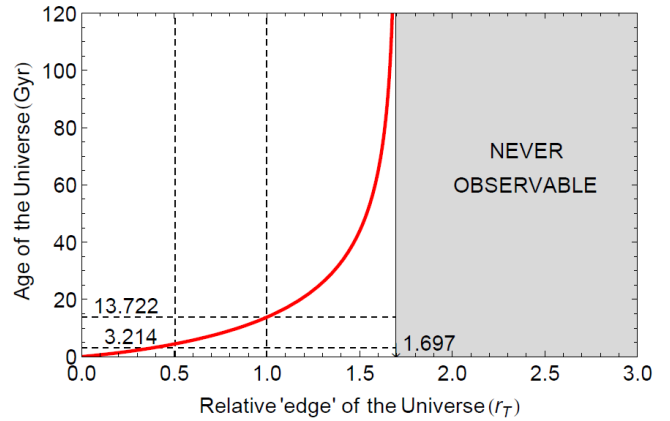


Fig. 2: $r_T = \int_0^T \frac{1}{a(t)} dt / \int_0^{T_0} \frac{1}{a(t)} dt$. The relative comoving coordinate r_T , from which *CMB* photons leave, at $t \approx 0$, and reach relative comoving coordinate $r = 0$ at age $t = T$ gives the relative position of the "edge" of the Universe ($r_{T \rightarrow \infty} \rightarrow 1.697$). (Axes were switched.)

will reach $\psi = 0$ at $t > T_0$, together with the other photons provenient from astronomical objects along the way. As the Universe gets older, its "edge" becomes more distant and its size gets bigger.

The value of ψ depends on $\mathfrak{R}(T_0)$, the curvature radius. According to reference [8], it is important to recall that the current radius of curvature should be greater than 100 Gly and, in order to perform our numerical calculations, we choose $\mathfrak{R}(T_0) = 102$ Gly. The actual value for ψ_{T_0} should be, consequently, less than that above (equation (8)).

To get rid of such dependence on $\mathfrak{R}(T_0)$, we find convenient to work with the ratio r

$$r \equiv \frac{\psi}{\psi_{T_0}}, \tag{9}$$

which we shall call the relative comoving coordinate.

Obviously, at the age T , r_T is a relative measure of "edge" position with respect to the fundamental observer. For a plot of r_T see Figure 2.

3 Universe or Multiverse?

One question that should come out of the mind of the fundamental observer is: "Is there a maximum value for the relative comoving coordinate r ?" What would be the value of r_∞ ?

By calculating r_∞ , we get

$$r_\infty = \frac{\int_0^\infty \frac{1}{a(t)} dt}{\int_0^{T_0} \frac{1}{a(t)} dt} = \frac{47.558}{28.024} = 1.697. \tag{10}$$

To our fundamental observer (Earth), there is an upper limit for the relative comoving coordinate $r = r_\infty = 1.697$, beyond that no astronomical object can ever be seen. This should raise a very interesting point under consideration.

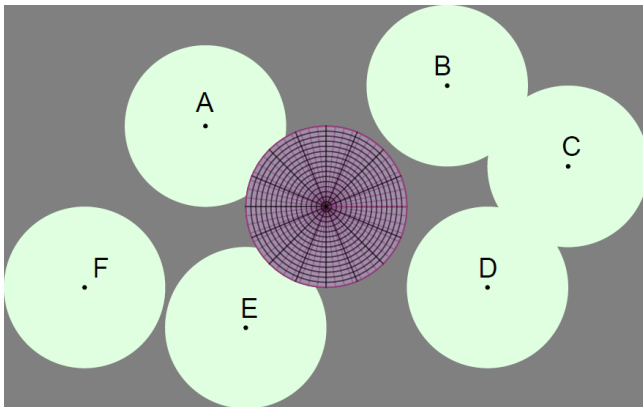


Fig. 3: This illustration tries to show schematically a hypersurface at time T with our Universe surrounded by other similar Universes, arbitrarily positioned, some of them overlapping.

Any other fundamental observer placed at a relative comoving coordinate $r > 2r_\infty$ ($\psi > 2\psi_\infty$), with respect to ours, will never be able to see what is meant to be our observable Universe. He (she) will be in the middle of another visible portion of a same whole Universe; He (she) will be thinking that he (she) lives in an observable Universe, just like ours. Everything we have been debating here should equally be applicable to such an “other” Universe.

The maximum possible value of ψ is π (equation (1)), then the maximum value of r should be at least 11.43. Just recall that $r = 1$ when $\psi = \psi_{T_0}$. This ψ_{T_0} was overevaluated as being 0.275 Radians = 15.7 Degrees, in equation (8) when considering the current radius of curvature as $\mathfrak{R}(T_0) = 102$ Gly. As found in reference [8] $\mathfrak{R}(T_0)$ should be bigger than that, not smaller. Consequently the real ψ_{T_0} should be smaller than 0.275 Radians = 15.7 Degrees. One direct consequence of this is that there is room for the occurrence of a large number of isolated similar *observable Universes* just like ours.

We may say that the Big Bang gave birth to a large Universe, of which our current observable Universe is part, perhaps a tiny part. The rest is unobservable to us and an endless number of portions just the size of our visible Universe certainly exist, each one with their fundamental observer, very much probable discussing the same Physics as us.

Of course, we have to consider also the cases of overlapping Universes.

The important thing is that we are talking about one Universe, originated from one Big Bang, and that, contains many other Universes similar to ours. Would it be a *multiverse*? See Figure 3.

4 Proper distance, volume, recession speed and redshift

When referring to the relative coordinate r_T we are not properly saying it is a function of time. Actually r_T is the value of the relative comoving coordinate r from which the *CMB*

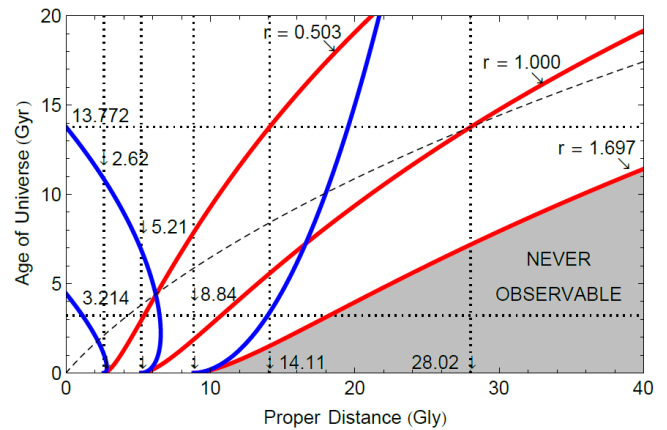


Fig. 4: Proper distances for $r = (0.503, 1.000, 1.697)$.

$d^{(r)}(T) = a(T)r d(T_0)$ (red curves),
 $d(T) = a(T)r_T d(T_0)$ (dashed curve),
 $d^{(r)}(T) - d(T) = a(T)(r - r_T)d(T_0)$ (blue curves).
 Axes were switched for convenience.

photons leave, at $t \approx 0$, to reach our fundamental observer at cosmic time T . Because of the expansion of the Universe, the proper distance from our observer ($r = 0$) and a given point at $r > 0$, at the age t , is

$$d(t) = \mathfrak{R}(t)r\psi_{T_0} = a(t)cr \int_0^{T_0} \frac{1}{a(t')} dt'. \quad (11)$$

The proper distance from our observer ($r = 0$) to the farthest observable point ($r = r_T$), at the age T , is known as horizon distance:

$$d(T) = \mathfrak{R}(T) \int_0^T \frac{1}{\mathfrak{R}(t)} dt = a(T)cr_T \int_0^{T_0} \frac{1}{a(t)} dt. \quad (12)$$

Besides defining the “edge” of the observable Universe at age T , it is also a measure of its proper radius and does not depend on the radius of curvature. In Figure 4 it is the dashed curve. Its current value is

$$d(T_0) = c \int_0^{T_0} \frac{1}{a(t)} dt = 28.02 \text{ Gly}. \quad (13)$$

It will become $d(T \rightarrow \infty) \rightarrow \infty$. Although there is an upper value for r (or ψ), the proper radius of the Universe is not limited because of the continuous expansion (equation 1).

The proper distance from the observer to the position of arbitrarily fixed value of r is

$$d^{(r)}(T) = a(T)r d(T_0). \quad (14)$$

where $d(T_0)$ is given in equation (13). In Figure (4) we plot the age of the Universe as function of the proper distance, for three values of the relative comoving coordinate r (0.503, 1.000, 1.697) – red curves. Blue curves refer to null geodesics

$$d^{(r)}(T) - d(T) = a(T)(r - r_T)d(T_0) \quad (15)$$

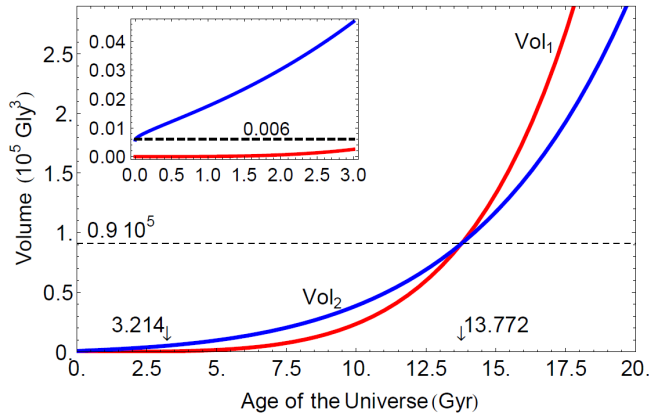


Fig. 5: Two evaluations of the volume of the Universe:
 $Vol_1(T) = 2\pi\mathfrak{R}^3(T_0)a^3(T)(r_T\psi_{T_0} - \frac{1}{2}\sin 2r_T\psi_{T_0})$,
 $Vol_2(T) = 2\pi\mathfrak{R}^3(T_0)a^3(T)(\psi_{T_0} - \frac{1}{2}\sin 2\psi_{T_0})$.

for fixed values of $r \neq 0$. (The axes in Figure 4 are switched, for convenience.)

Consider the volume of our observable Universe. The general expression is

$$Vol(t) = \mathfrak{R}^3(T_0)a^3(t) \int_0^\psi \sin^2 \psi d\psi \int_0^\pi \sin \theta d\theta \int_0^{2\pi} d\phi \quad (16)$$

$$= 2\pi\mathfrak{R}^3(T_0)a^3(t) \left(\psi - \frac{1}{2}\sin 2\psi \right).$$

Our fundamental observer may ask about two volumes:

First, the volume of the allways visible (observable) part since the beginning - such volume should be approximately zero for $t \approx 0$; Second, the volume of what became later the current visible part and that was not visible in its integrity in the past since $t \approx 0$. They are respectively,

$$Vol_1(T) = 2\pi\mathfrak{R}^3(T_0)a^3(T) \left(\psi - \frac{1}{2}\sin 2\psi \right) \quad (17)$$

$$= 2\pi\mathfrak{R}^3(T_0)a^3(T) \left(r_T\psi_{T_0} - \frac{1}{2}\sin 2r_T\psi_{T_0} \right).$$

$$Vol_2(T) = 2\pi\mathfrak{R}^3(T_0)a^3(T) \left(\psi_{T_0} - \frac{1}{2}\sin 2\psi_{T_0} \right). \quad (18)$$

By evaluating equations (17 – 18) with $T = 0$, we get

$$Vol_1(0) = 0 \quad (19)$$

$$Vol_2(0) = 0.006 \times 10^5 Gly^3.$$

These results are not surprising. To our observer, located at $r = 0$, at $t \approx 0$, the visible Universe is approximately zero, just because all the *CMB* photons are “born” at the same moment ($T = 0$); He (she) sees first the closest photons and then, in the sequence, the others as time goes on.

On the other hand,

$$Vol_2(T_0) = Vol_1(T_0) = 0.9 \times 10^5 Gly^3, \quad (20)$$

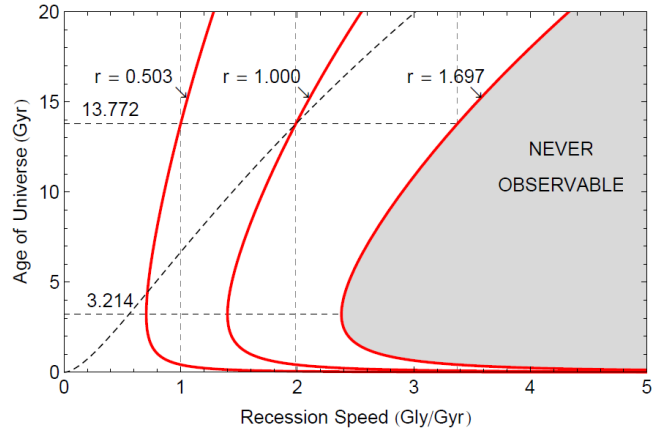


Fig. 6: $v(T) = a(T)H(T)rd(T_0)$. Recession speed is calculated for three values of the relative comoving coordinate r , as function of the age T of the Universe. For convenience the axes were switched.

which is the volume of current observable Universe. See Figure 4. It is only about 150 times bigger than it was at $t = 0$.

Just one comment: If the reader wants to calculate the volume using the classical euclidean expression for the sphere $((4\pi/3)\mathfrak{R}^3(T_0)a^3(t)\psi^3)$, he (she) will get practically the same result. So here, as in reference [8], no distinction between $k = 0$ and $k = 1$.

The recession speed of a point of the Universe at a given relative comoving coordinate r , at cosmic time t , is

$$v(t) = a(t)H(t)rd(T_0), \quad (21)$$

where $\dot{a}(t)$ was replaced by

$$\dot{a}(t) = a(t)H(t), \quad (22)$$

and the Hubble parameter $H(t)$ is given by [8]

$$H(t) = H_0 \left(\frac{t}{T_0} \right)^{\beta-1}. \quad (23)$$

The cosmological redshift is defined as

$$z = \frac{\Delta\lambda}{\lambda_e} = \frac{a(t_o)}{a(t_e)} - 1, \quad (24)$$

where λ_e and λ_o are, respectively, the photon wavelength at the source ($t = t_e$) and at the observer ($r = 0, t = t_o$). Due to expansion of the Universe, these two wavelengths are different. The redshift to be detected by the observer at $r = 0$, at current age should be

$$z = \frac{1}{a(t_e)} - 1 = e^{\frac{H_0 T_0}{\beta} \left(1 - \frac{t_e}{T_0} \right)^\beta} - 1. \quad (25)$$

The recession speed at coordinate r at time ($t = t_e$) is

$$v(t_e) = a(t_e)H(t_e)rd(T_0). \quad (26)$$

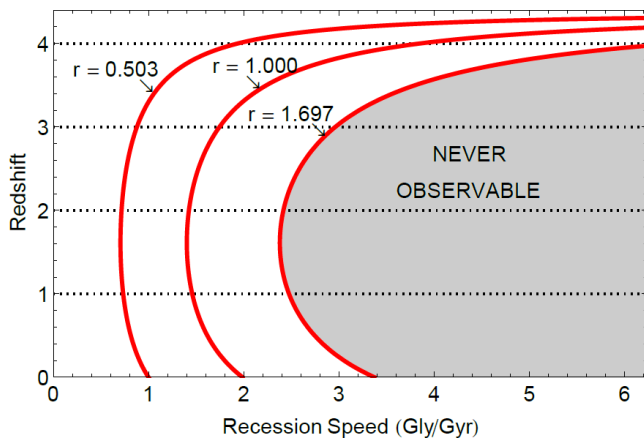


Fig. 7: $v(z) = \left(1 - \frac{\beta}{H_0 T_0} \text{Log}(1+z)\right)^{\beta - \frac{1}{\beta}} \frac{H_0 r}{1+z} d(T_0)$. Recession speeds calculated as function of the cosmological redshift and plotted with switched axes, for convenience.

From equation (25) we obtain

$$t_e = T_0 \left(1 - \frac{\beta}{H_0 T_0} \text{Log}(1+z)\right)^{\frac{1}{\beta}}, \tag{27}$$

which inserted into equation (24) gives

$$v(z) = \left(1 - \frac{\beta}{H_0 T_0} \text{Log}(1+z)\right)^{\beta - \frac{1}{\beta}} \frac{H_0 r}{1+z} d(T_0). \tag{28}$$

Because of the transition from negative to positive expansion acceleration phenomenon, we have, in many situations, two equal recession speeds separated in time leading to two different redshifts. See Figure 7.

5 Conclusion

The expansion factor $a(t) = e^{\frac{H_0 T_0}{\beta} \left(\left(\frac{t}{T_0}\right)^\beta - 1\right)}$, where $\beta = 0.5804$ [8], is applied to our Universe, here treated as being closed ($k = 1$). We investigate properties of comoving coordinates, proper distances, volume and redshift under the mentioned expansion factor. Some very interesting conclusions were drawn. One of them is that the radial relative comoving coordinate r , measured from the fundamental observer, $r = 0$ (on Earth), to the "edge" (horizon) of our observable Universe has an upper limit. We found that $r \rightarrow 1.697$ when $T \rightarrow \infty$. Therefore all astronomical objects which lie beyond such limit would never be observed by our fundamental observer ($r = 0$). On the other hand any other fundamental observer that might exist at $r > 2 \times 1.697$ would be in the middle of another Universe, just like ours; he/she would never be able to observe our Universe. Perhaps he/she might be thinking that his/her Universe is the only one to exist. An endless number of other fundamental observers and an equal number of Universes similar to ours may clearly exist. Situations in which overlapping Universes should exist too. See Figure 3.

The fact is that the Big Bang originated a big Universe. A small portion of that is what we call our observable Universe. The rest is unobservable to our fundamental observer. Equal portions of the rest may be called also Universe by their fundamental observers if they exist. So we may speak about many Universes - a Multiverse - or about only one Universe, a small part of it is observable to our fundamental observer.

Acknowledgements

We wish to thank our friends Dr. Alencastro V. De Carvalho, Dr. Paulo R. Silva and Dr. Rodrigo D. Társia, for reading the manuscript and for stimulating discussions.

Submitted on June 14, 2014 / Accepted on June 17, 2014

References

1. Raine D. An Introduction to the Science Of Cosmology. Institute of Physics Publishing Ltd, 2001.
2. Peacock J.A. Cosmological Physics. Cambridge University Press, 1999.
3. Harrison E.R. Cosmology: The Science of the Universe. Cambridge University Press, 2nd ed. 2000.
4. Islam J.N. An Introduction to Mathematical Cosmology. Cambridge University Press. 2002.
5. Ellis G.F.R. et al. Relativistic Cosmology. Cambridge University Press, 2012.
6. Springel V., Frenk C. S., and White S. D. (2006). The large-scale structure of the Universe. *Nature*, 440(7088), 1137–1144.
7. Luminet J.P. Cosmic topology: twenty years after. *Gravitation and Cosmology*, 2014, v. 20, 1, 15–20
8. Silva N.P. A model for the expansion of the Universe. *Progress in Physics*, 2014, v. 10, 93–97.
9. Bennett C.L. et al. Nine-year Wilkinson Microwave Anisotropy Probe (WMAP) observations: final maps and results. arXiv: astro-ph.CO, 2013.
10. Peebles P.J.E. The Large-scale Structure of the Universe. Princeton University Press, Princeton, 1980.

New Possible Physical Evidence of the Homogeneous Electromagnetic Vector Potential for Quantum Theory.

Idea of a Test Based on a G. P. Thomson-like Arrangement

Spiridon Dumitru

(Retired) Department of Physics, "Transilvania" University, B-dul Eroilor 29, 500036 Brasov, Romania
Email: s.dumitru42@unitbv.ro

It is suggested herein a test able to reveal the physical evidence of the homogeneous electromagnetic vector potential field in relation to quantum theory. We take into consideration three reliable entities as main pieces of the test: (i) influence of a potential vector of the de Broglie wavelength (ii) a G. P. Thomson-like experimental arrangement and (iii) a special coil designed to create a homogeneous vector potential. The alluded evidence is not connected with magnetic fluxes surrounded by the vector potential field lines, rather it depends on the fluxes which are outside of the respective lines. Also the same evidence shows that the tested vector potential field is a uniquely defined physical quantity, free of any adjusting gauge. So the phenomenology of the suggested quantum test differs from that of the macroscopic theory where the vector potential is not uniquely defined and allows a gauge adjustment. Of course, we contend that this proposal has to be subsequently subjected to adequate experimental validation.

1 Introduction

The physical evidence of the vector potential \vec{A} field, distinctly of electric and/or magnetic local actions, is known as Aharonov-Bohm-effect (A-B-eff). It aroused scientific discussions for more than half a century (see [1–8] and references). As a rule in the A-B-eff context, the vector potential is curl-free field, but it is non-homogeneous ($\mathbf{n-h}$) i.e. spatially non-uniform. In the same context, the alluded evidence is connected quantitatively with magnetic fluxes surrounded by the lines of \vec{A} field. In the present paper we try to suggest a test intended to reveal the possible physical evidence of a homogeneous (\mathbf{h}) \vec{A} field. Note that in both $\mathbf{n-h}$ and \mathbf{h} cases herein, we take into consideration only fields which are constant in time.

The announced test has as constitutive pieces three reliable entities (\mathbf{E}) namely:

- \mathbf{E}_1 : The fact that a vector potential \vec{A} field changes the values of the de Broglie wavelength λ^{dB} for electrons. ■
- \mathbf{E}_2 : An experimental arrangement of the G. P. Thomson type, able to monitor the mentioned λ^{dB} values. ■
- \mathbf{E}_3 : A feasible special coil designed so as to create a $\mathbf{h-A}$ field. ■

Accordingly, on the whole, the test has to put together the mentioned entities and, consequently, to synthesize a clear verdict regarding the alluded evidence of a $\mathbf{h-A}$ field.

Experimental setup of the suggested test is detailed in the next Section 2. Essential theoretical considerations concerning the action of a $\mathbf{h-A}$ field are given in Section 3. The above-noted considerations are fortified in Section 4 by a set of numerical estimations for the quantities aimed to be measured through the test. Some concluding thoughts regarding a pos-

sible positive result of the suggested test close the main body of the paper in Section 5. Constructive and computational details regarding the special coil designed to generate a $\mathbf{h-A}$ field are presented in the Appendix.

2 Setup details of the experimental arrangement

The setup of the suggested experimental test is pictured and detailed below in Fig. 1. It consists primarily of a G. P. Thomson-like arrangement partially located in an area with a $\mathbf{h-A}$ field. The alluded arrangement is inspired by some illustrative images [9, 10] about G. P. Thomson's original experiment and it disposes in a straight line of the following elements: electron source, electron beam, crystalline grating, and detecting screen. An area with a $\mathbf{h-A}$ field can be obtained through a certain special coil whose constructive and computational details are given in the above-mentioned Appendix at the end of this paper.

The following notes have to be added to the explanatory records accompanying Fig. 1.

Note 1: If in Fig. 1 the elements 7 and 8 are omitted (i.e. the sections in special coil and the lines of $\mathbf{h-A}$ field) one obtains a G. P. Thomson-like arrangement as it is illustrated in the said references [9, 10]. ■

Note 2: Surely the above mentioned G. P. Thomson-like arrangement is so designed and constructed that it can be placed inside of a vacuum glass container. The respective container is not shown in Fig. 1 and it will leave out the special coil. ■

Note 3: When incident on the crystalline foil, the electron beam must ensure a coherent and plane front of de Broglie waves. Similar ensuring is required [11] for

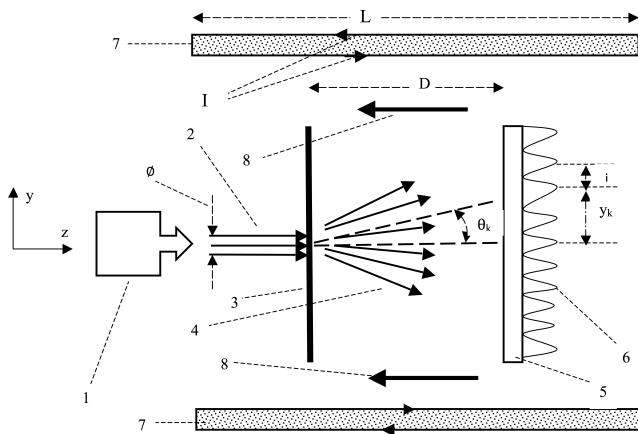


Fig. 1: Plane section in the image of suggested experimental setup, accompanied by the following explanatory records. 1 – Source for a beam of mono-energetic and parallel moving electrons; 2 – Beam of electrons in parallel movements; 3 – Thin crystalline foil as diffraction grating; 4 – Diffracted electrons; 5 – Detecting screen; 6 – Fringes in the plane section of the diffraction pattern; 7 – Sections in the special coil able to create a $\mathbf{h}\text{-}\vec{A}$ field; 8 – $\mathbf{h}\text{-}\vec{A}$ field; ϕ = the width of the electron beam with $\phi \gg a$ (a = interatomic spacing in the crystal lattice of the foil -3); θ_k = diffraction angle for the k -th order fringe ($k = 0, 1, 2, 3, \dots$); y_k = displacement from the center line of the k -th order fringe; i = interfringe width = $y_{k+1} - y_k$; D = distance between crystalline foil and screen ($D \gg \phi$); L = length of the special coil ($L \gg D$); I = intensity of current in wires of the coil.

optical diffracting waves at a classical diffraction grating. ■

Note 4: In Fig. 1 the detail 6 displays only the linear projections of the fringes from the diffraction pattern. On the whole, the respective pattern consists in a set of concentric circular fringes (diffraction rings). ■

3 Theoretical considerations concerning action of a $\mathbf{h}\text{-}\vec{A}$ field

The leading idea of the above-suggested test is to search for possible changes caused by a $\mathbf{h}\text{-}\vec{A}$ field in the diffraction of quantum (de Broglie) electronic waves. That is why we begin by recalling some quantitative characteristics of the diffraction phenomenon.

The most known scientific domain wherein the respective phenomenon is studied regards optical light waves [11]. In the respective domain, one uses as the main element the so-called *diffraction grating* i.e. a piece with a periodic structure having slits separated each by a distance a and which diffracts the light into beams in different directions. For a light normally incident on such an element, the grating equation (condition for intensity maximums) has the form: $a \cdot \sin \theta_k = k\lambda$, where $k = 0, 1, 2, \dots$. In the respective equation, λ denotes the light's wavelength and θ_k is the angle at which the diffracted

light has the k -th order maximum. If the diffraction pattern is received on a detecting screen, the k -th order maximum appears on the screen in the position y_k given by the relation $\tan \theta_k = (y_k/D)$, where D denotes the distance between the screen and the grating. For the distant screen assumption, when $D \gg y_k$, the following relation holds: $\sin \theta_k \approx \tan \theta_k \approx (y_k/D)$. Then, with regard to the mentioned assumption, one observes that the diffraction pattern on the screen is characterized by an interfringe distance $i = y_{k+1} - y_k$ given through the relation

$$i = \lambda \frac{D}{a}. \quad (1)$$

Note the fact that the above quantitative aspects of diffraction have a generic character, i.e. they are valid for all kinds of waves including de Broglie ones. The respective fact is presumed as a main element of the experimental test suggested in the previous section. Another main element of the alluded test is the largely agreed upon idea [1–8] that the de Broglie electronic wavelength λ^{dB} is influenced by the presence of a \vec{A} field. Based on the two afore-mentioned main elements the considered test can be detailed as follows.

In the experimental setup depicted in Fig. 1 the crystalline foil 3 having interatomic spacing a plays the role of a diffraction grating. In the same experiment, on the detecting screen 5 it is expected to appear a diffraction pattern of the electrons. The respective pattern would be characterized by an interfringe distance i^{dB} definable through the formula $i^{dB} = \lambda^{dB} \cdot (D/a)$. In that formula, D denotes the distance between the crystalline foil and the screen, supposed to satisfy the condition $D \gg \phi$, where ϕ represents the width of the incident electron beam. In the absence of a $\mathbf{h}\text{-}\vec{A}$ field, the λ^{dB} of a non-relativistic electron is known to satisfy the following expression:

$$\lambda^{dB} = \frac{h}{p_{kin}} = \frac{h}{mv} = \frac{h}{\sqrt{2m\mathcal{E}}}. \quad (2)$$

In the above expression, h is Planck's constant while p_{kin} , m , v and \mathcal{E} denote respectively the kinetic momentum, mass, velocity, and kinetic energy of the electron. If the alluded energy is obtained in the source of the electron beam (i.e. piece 1 in Fig. 1) under the influence of an accelerating voltage U , one can write $\mathcal{E} = e \cdot U$ and $p_{kin} = mv = \sqrt{2meU}$.

Now, in connection with the situation depicted in Fig. 1, let us look for the expression of the electrons' characteristic λ^{dB} and respectively of $i^{dB} = \lambda^{dB} \cdot (D/a)$ in the presence of a $\mathbf{h}\text{-}\vec{A}$ field. Firstly, we note the known fact [6] that a particle with the electric charge q and the kinetic momentum $\vec{p}_{kin} = m\vec{v}$ in a potential vector \vec{A} field acquires an additional (*add*) momentum, $\vec{p}_{add} = q\vec{A}$, so that its *effective* (eff) momentum is $\vec{P}_{eff} = \vec{p}_{kin} + \vec{p}_{add} = m\vec{v} + q\vec{A}$. Then for the electrons (with $q = -e$) supposed to be implied in the experiment depicted in Fig. 1, one obtains the effective (eff) quantities

$$\lambda_{eff}^{dB}(A) = \frac{h}{mv + eA}; \quad i_{eff}^{dB}(A) = \frac{hD}{a(mv + eA)}. \quad (3)$$

Further on, we have to take into account the fact that the $\mathbf{h}\vec{A}$ field acting in the experiment presented before is generated by a special coil whose plane section is depicted by the elements 7 from Fig. 1. Then from the relation (10) established in the Appendix, we have $A = \mathcal{K} \cdot I$, where $\mathcal{K} = \frac{\mu_0 N}{2\pi} \cdot \ln\left(\frac{R_2}{R_1}\right)$. Add here the fact that in this experiment $mv = \sqrt{2meU}$. Then for the effective interfringe distance i_{eff}^{dB} of the diffracted electrons, one finds

$$i_{eff}^{dB}(A) = i_{eff}^{dB}(U, I) = \frac{hD}{a(\sqrt{2meU} + e\mathcal{K}I)}, \quad (4)$$

respectively

$$\frac{1}{i_{eff}^{dB}(U, I)} = f(U, I) = \frac{a\sqrt{2me}}{hD}\sqrt{U} + \frac{ae\mathcal{K}}{hD}I. \quad (5)$$

4 A set of numerical estimations

The verisimilitude of the above-suggested test can be fortified to some extent by transposing several of the previous formulas into their corresponding numerical values. For such a transposing, we firstly will appeal to numerical values known from G. P. Thomson-like experiments. So, as regarding the elements from Fig. 1, we quote the values $a = 2.55 \times 10^{-10}$ m (for a crystalline foil of copper) and $D = 0.1$ m. As regarding U , we take the often quoted value: $U = 30$ kV. Then the kinetic momentum of the electrons will be $p_{kin} = mv = \sqrt{2meU} = 9.351 \times 10^{-23}$ kg m/s. The additional (add) momentum of the electron, induced by the special coil, is of the form $p_{add} = e\mathcal{K} \times I$ where $\mathcal{K} = \frac{\mu_0 N}{2\pi} \times \ln\left(\frac{R_2}{R_1}\right)$. In order to estimate the value of \mathcal{K} , we propose the following practically workable values: $R_1 = 0.1$ m, $R_2 = 0.12$ m, $N = 2\pi R_1 \times n$ with $n = 2 \times 10^3$ m $^{-1}$ = number of wires (of 1 mm in diameter) per unit length, arranged into two layers. With the well known values for e and μ_0 one obtains $p_{add} = 7.331 \times 10^{-24}$ (kg m C $^{-1}$) $\cdot I$ (with C = Coulomb).

For wires of 1 mm in diameter, by changing the polarity of the voltage powering the coil, the current I can be adjusted in the range $I \in (-10 \text{ to } +10)A$. Then the effective momentum $\vec{P}_{eff} = \vec{p}_{kin} + \vec{p}_{add}$ of the electrons shall have the values within the interval $(2.040 \text{ to } 16.662) \times 10^{-23}$ kg m/s. Consequently, due to the above mentioned values of a and D , the effective interfringe distance i_{eff}^{dB} defined in (4) changes in the range (1.558 to 12.725) mm, respectively its inverse from (5) has values within the interval (78.58 to 641.84) m $^{-1}$. Then it results that in this test the $\mathbf{h}\vec{A}$ field takes its magnitude within the interval $A \in (-4.5, +4.5) \times 10^{-4}$ kg m C $^{-1}$, (C = Coulomb).

Now note that in the absence of the $\mathbf{h}\vec{A}$ field (i.e. when $I = 0$) the interfrange distance i^{dB} specific to a simple G. P. Thomson experiment has the value $i^{dB} = \frac{hD}{a\sqrt{2meU}} = 2.776$ mm. Such a value is within the range of values of i_{eff}^{dB}

characterizing the presence of the $\mathbf{h}\vec{A}$ field. This means that the quantitative evaluation of the mutual relationship of i_{eff}^{dB} versus I , and therefore the testing evidence of a $\mathbf{h}\vec{A}$ field can be done with techniques and accuracies similar to those of the G. P. Thomson experiment.

5 Some concluding remarks

The aim of the experimental test suggested above is to verify a possible physical evidence for the $\mathbf{h}\vec{A}$ field. Such a test can be done by comparative measurements of the interfringe distance i_{eff}^{dB} and of the current I . Additionally it must examine whether the results of the mentioned measurements verify the relations (4) and (5) (particularly according to (5) the quantity $(i_{eff}^{dB})^{-1}$ is expected to show a linear dependence of I). If the above outcomes are positive, one can notice the fact that a $\mathbf{h}\vec{A}$ field has its own characteristics of physical evidence. Such a fact leads in one way or another to the following remarks (**R**):

R₁: The physical evidence of the $\mathbf{h}\vec{A}$ field differs from the one of the $\mathbf{n}\mathbf{h}\vec{A}$ field which appears in the A-B-eff. This happens because, by comparison to the illustrations from [12], one can see that: (i) by changing the values of $\mathbf{n}\mathbf{h}\vec{A}$, the diffraction pattern undergoes a simple translation on the screen, without any modification of interfringe distance, while (ii) according to the relations (4) and (5) a change of $\mathbf{h}\vec{A}$ (by means of current I) does not translate the diffraction pattern but varies the value of associated interfringe distance i_{eff}^{dB} . The mentioned variation is similar to that induced [12] by changing (through accelerating the voltage U) the values of kinetic momentum $\vec{p}_{kin} = m\vec{v}$ for electrons. ■

R₂: There is a difference between the physical evidence (objectification) of the $\mathbf{h}\vec{A}$ and the $\mathbf{n}\mathbf{h}\vec{A}$ fields in relation with the magnetic fluxes surrounded or not by the field lines. The difference is pointed out by the following subsequent aspects:

(i) On the one hand, as it is known from the A-B-eff, in case of the $\mathbf{n}\mathbf{h}\vec{A}$ field, the corresponding evidence depends directly on magnetic fluxes surrounded by the \vec{A} field lines.

(ii) On the other hand, the physical evidence of the $\mathbf{h}\vec{A}$ field is not connected to magnetic fluxes surrounded by the field lines. But note that due to the relations (4) and (5), the respective evidence appears to be dependent (through the current I) on magnetic fluxes not surrounded by the field lines of the $\mathbf{h}\vec{A}$. ■

R₃: A particular characteristic of the physical evidence forecasted above for the $\mathbf{h}\vec{A}$ regards the macroscopic versus quantum difference concerning the uniqueness (gauge freedom) of the vector potential field. As is known, in macroscopic situations [13, 14] the vector potential \vec{A} field is not uniquely defined (i.e. it has a gauge freedom). In such situations, an arbitrary \vec{A} field

allows a gauge fixing (adjustment), without any alteration of macroscopic relevant variables/equations (particularly of those involving the magnetic field \vec{B}). So two distinct vector potential fields \vec{A} and \vec{A}^1 have the same macroscopic actions (effects) if $\vec{A}^1 = \vec{A} + \nabla f$, where f is an arbitrary gauge functions. On the other hand, in a quantum context, a $\mathbf{h}\text{-}\vec{A}$ has not any gauge freedom. This is because if this test has positive results, two fields like $\mathbf{h} - \vec{A} = A \cdot \vec{k}$ and $\mathbf{h} - \vec{A}^1 = \mathbf{h} - \vec{A} + \nabla f$ are completely distinct if $f = (-z \cdot A \cdot \vec{k})$, where \vec{k} denotes the unit vector of the Oz axis. So we can conclude that, with respect to the $\mathbf{h}\text{-}\vec{A}$ field, the quantum aspects differ fundamentally from those aspects originating in a macroscopic consideration. Surely, such a fact (difference) and its profound implications have to be approached in subsequently more elaborated studies. ■

Postscript

As presented above, the suggested test and its positive results appear as purely hypothetical things, despite the fact that they are based on essentially reliable entities (constitutive pieces) presented in the Introduction. Of course, we hold that a true confirmation of the alluded results can be done by the action of putting in practice the whole test. Unfortunately, at the moment I do not have access to material logistics able to allow me an effective practical approach of the test in question. Thus I warmly appeal to the concerned experimentalists and researchers who have adequate logistics to put in practice the suggested test and to verify its validity.

Appendix: Constructive and computational details for a special coil able to create a $\mathbf{h}\text{-}\vec{A}$ field

The case of an ideal coil

An experimental area of macroscopic size with the $\mathbf{h}\text{-}\vec{A}$ field can be realized with the aid of a special coil whose constructive and computational details are presented below. The announced details are improvements of the ideas promoted by us in an early preprint [15].

The basic element in designing the mentioned coil is the $\mathbf{h}\text{-}\vec{A}$ field generated by a rectilinear infinite conductor carrying a direct current. If the conductor is located along the axis Oz and the current has the intensity I, the Cartesian components (written in SI units) of the mentioned $\mathbf{h}\text{-}\vec{A}$ field are given [16] by the following formulas:

$$A_x(1) = 0, \quad A_y(1) = 0, \quad A_z(1) = -\mu_0 \frac{I}{2\pi} \ln r. \quad (6)$$

Here r denotes the distance from the conductor of the point where the $\mathbf{h}\text{-}\vec{A}$ is evaluated and where μ_0 is the vacuum permeability.

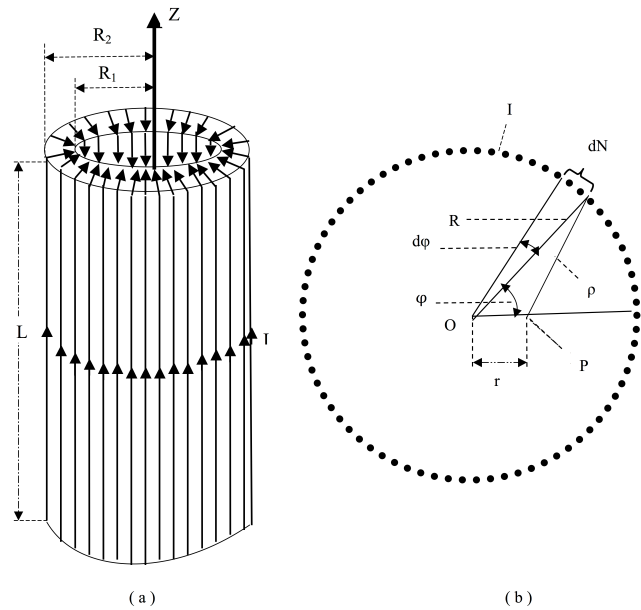


Fig. 2: Schemes for an annular special coil.

Note that formulas (6) are of ideal essence because they describe the $\mathbf{h}\text{-}\vec{A}$ field generated by an infinite (ideal) rectilinear conductor. Further onwards, we firstly use the respective formulas in order to obtain the $\mathbf{h}\text{-}\vec{A}$ field generated by an ideal annular coil. Later on we will specify the conditions in which the results obtained for the ideal coil can be used with fairly good approximation in the characterization of a real (non-ideal) coil of practical interest for the experimental test suggested and detailed in Sections 2,3 and 4.

The mentioned special coil has the shape depicted in Fig. 2-(a) (i.e. it is a toroidal coil with a rectangular cross section). In the respective figure the finite quantities R_1 and R_2 represent the inside and outside finite radii of the coil while $L \rightarrow \infty$ is the length of the coil. For evaluation of the $\mathbf{h}\text{-}\vec{A}$ generated inside of the mentioned coil let us now consider an array of infinite rectilinear conductors carrying direct currents of the same intensity I. The conductors are mutually parallel and uniformly disposed on the circular cylindrical surface with the radius R. The conductors are also parallel with Oz as the symmetry axis. In a cross section, the considered array is disposed on a circle of radius R as can be seen in Fig. 2b. On the respective circle, the azimuthal angle φ locates the infinitesimal arc element whose length is $Rd\varphi$. On the respective arc there was placed a set of conductors whose number is $dN = \left(\frac{N}{2\pi}\right) d\varphi$, where N represents the total number of conductors in the whole considered array. Let there be an observation point P situated at distances r and ρ from the center O of the circle respectively from the infinitesimal arc (see the Fig. 2b). Then, by taking into account (6), the z-component of the $\mathbf{h}\text{-}\vec{A}$ field generated in P by the dN conductors is given

by relation

$$A_z(dN) = A_z(1)dN = -\mu_0 \frac{NI}{4\pi^2} \ln \rho \cdot d\varphi, \quad (7)$$

where $\rho = \sqrt{(R^2 + r^2 - 2Rr \cos \varphi)}$. Then all N conductors will generate in the point P a $\mathbf{h}\text{-}\vec{A}$ field whose value A is

$$A = A_z(N) = -\mu_0 \frac{NI}{8\pi^2} \int_0^{2\pi} \ln(R^2 + r^2 - 2Rr \cos \varphi) \cdot d\varphi. \quad (8)$$

In calculating the above integral, the formula (4.224-14) from [17] can be used. So, one obtains

$$A = -\mu_0 \frac{NI}{2\pi} \ln R. \quad (9)$$

This relation shows that the value of A does not depend on r , i.e. on the position of P inside the circle of radius R . Accordingly this means that inside the respective circle, the potential vector is homogeneous. Then starting from (9), one obtains that the inside space of an ideal annular coil depicted in Fig. 2a is characterized by the $\mathbf{h}\text{-}\vec{A}$ field whose value is

$$A = \mu_0 \frac{NI}{2\pi} \ln \left(\frac{R_2}{R_1} \right). \quad (10)$$

From the ideal coil to a real one

The above-presented coil is of ideal essence because their characteristics were evaluated on the basis of an ideal formula (6). But in practical matters, such as the experimental test proposed in Sections 2 and 3, one requires a real coil which may be effectively constructed in a laboratory. That is why it is important to specify the main conditions in which the above ideal results can be used in real situations. The mentioned conditions are displayed here below.

On the geometrical sizes: In a laboratory, it is not possible to operate with objects of infinite size. Thus we must take into account the restrictive conditions so that the characteristics of the ideal coil discussed above to remain as good approximations for a real coil of similar geometric form. In the case of a finite coil having the form depicted in the Fig. 2a, the alluded restrictive conditions impose the relations $L \gg R_1$, $L \gg R_2$ and $L \gg (R_2 - R_1)$. If the respective coil is regarded as a piece in the test experiment from Fig. 1, indispensable are the relations $L \gg D$ and $L \gg \phi$.

About the marginal fragments: On the whole, the marginal fragments of coil (of width $(R_2 - R_1)$) can have disturbing effects on the Cartesian components of \vec{A} inside the the space of practical interest. Note that, on the one hand, in the above-mentioned conditions $L \gg R_1$, $L \gg R_2$ and $L \gg (R_2 - R_1)$ the alluded effects can be neglected in general practical affairs. On the other hand,

in the particular case of the proposed coil the alluded effects are also diminished by the symmetrical flows of currents in the respective marginal fragments.

As concerns the helicity: The discussed annular coil is supposed to be realized by winding a single piece of wire. The spirals of the respective wire are not strictly parallel to the symmetry axis of the coil (the Oz axis) but they have a certain helicity (corkscrew-like path). Of course, the alluded helicity has disturbing effects on the components of \vec{A} inside the coils. Note that the mentioned helicity-effects can be diminished (and practically eliminated) by using an idea noted in another context in [18]. The respective idea proposes to arrange the spirals of the coil in an even number of layers, with the spirals from adjacent layers having equal helicity but of opposite sense.

Submitted on May 6, 2014 / Accepted on May 30, 2014

References

- Aharonov Y., Bohm D., Significance of electromagnetic potentials in the quantum theory. *Phys. Rev.*, 1959, v. 115, 485–491.
- Aharonov Y., Bohm D. Further considerations on electromagnetic potentials in the quantum theory. *Phys. Rev.*, 1961, v. 123 1511–1524.
- Olariu S., Popescu I.I. The quantum effects of electromagnetic fluxes. *Rev. Mod. Phys.*, 1985, v. 57, 339–436.
- Peshkin M., Tonomura A. The Aharonov-Bohm Effect. *Lecture Notes in Physics*, Springer, v. 340, 1989, 1–152.
- Dennis M., Popescu S., Vaidman L., Quantum phases: 50 years of the Aharonov-Bohm effect and 25 years of the Berry phase. *J. Phys. A: Math. Theor.*, 2010, v. 43, 350301.
- Ershkovich A. Electromagnetic potentials and Aharonov-Bohm effect. arXiv: 1209.1078
- Leus V.A., Smith R.T., Maher S. The physical entity of vector potential in electromagnetism. *Applied Physics Research*, 2013, v. 5, 56–68.
- Hiley B.J. The early history of the Aharonov-Bohm effect. arXiv: 1304.4736.
- Images for G.P. Thomson experiment at <http://www.google.com>
- Arias T.A. G.P. Thomson Experiment. <http://muchomas.lassp.cornell.edu/8.04/1997/quiz1/node4.html>
- Born M., Wolf E. Principle of Optics, Electromagnetic Theory of Propagation, Interference and Diffraction of Light. Seventh (expanded) edition, Cambridge University Press, 2003.
- Blinder S.M. Aharonov-Bohm Effect, from the Wolfram Demonstrations Project. <http://www.youtube.com>
- Jackson J.D. Classical Electrodynamics. John Wiley, N.Y., 1962.
- Landau L., Lifchitz E. Theorie des Champs. Ed. Mir, Moscou, 1970.
- Dumitru S., Dumitru M. Are there observable effects of the vector potential? A suggestion for probative experiments of a new type (different from the proposed Aharonov-Bohm one). CERN Central Library PRE 24618, Barcode 38490000001, Jan 1981, 20 pages.
- Feynman R.P., Leighton R.B., Sands M. The Feynman Lectures on Physics, vol. II. Addison-Wesley, Reading (Mass.), 1964.
- Gradshteyn I.S., Ryzhik I.M. Table of Integrals, Series, and Products. Seventh Edition, Elsevier, 2007.
- Costa de Beauregard O., Vigoureux J.M. Flux quantization in “autistic” magnets. *Phys. Rev. D*, 1974, v. 9, 1626–1632.

Progress in Physics is an American scientific journal on advanced studies in physics, registered with the Library of Congress (DC, USA): ISSN 1555-5534 (print version) and ISSN 1555-5615 (online version). The journal is peer reviewed and listed in the abstracting and indexing coverage of: Mathematical Reviews of the AMS (USA), DOAJ of Lund University (Sweden), Zentralblatt MATH (Germany), Scientific Commons of the University of St.Gallen (Switzerland), Open-J-Gate (India), Referential Journal of VINITI (Russia), etc. **Progress in Physics** is an open-access journal published and distributed in accordance with the Budapest Open Initiative: this means that the electronic copies of both full-size version of the journal and the individual papers published therein will always be accessed for reading, download, and copying for any user free of charge. The journal is issued quarterly (four volumes per year).

Electronic version of this journal: <http://www.ptep-online.com>

Editorial board:

Dmitri Rabounski (Editor-in-Chief), Florentin Smarandache, Larissa Borissova

Editorial team:

Gunn Quznetsov, Andreas Ries, Ebenezer Chifu, Felix Scholkmann, Pierre Millette

Postal address:

Department of Mathematics and Science, University of New Mexico,
705 Gurley Avenue, Gallup, NM 87301, USA

Printed in the United States of America
